

Supplementary Figures for Chapter 4 of Thesis “Ocean Biogeochemical Optimisation in Earth System Models”

Sophy Oliver

November 25, 2021

Contents

1	Summary	1
2	Parameter <code>r0</code> : the CaCO_3 : POC: export rain ratio scalar.	2
3	Parameter <code>vsed</code> : the detritus gravitational sinking rate.	7
4	Parameter <code>xald</code> : the diatom chl-specific initial slope of P-I curve.	12
5	Parameter <code>xaln</code> : the non-diatom chl-specific initial slope of P-I curve.	17
6	Parameter <code>xfastc</code> : the excess organic carbon dissolution length scale.	22
7	Parameter <code>xfastca</code> : the calcium carbonate dissolution length scale.	27
8	Parameter <code>xfastsi</code> : the biogenic silicon dissolution length scale.	32
9	Parameter <code>xfrac1</code> : the fast-sinking fraction of diatom natural mortality losses.	37
10	Parameter <code>xfrac2</code> : the fast-sinking fraction of meso-zooplankton mortality losses.	42
11	Parameter <code>xfrac3</code> : the fast-sinking fraction of diatom silicon grazing losses.	47

12	Parameter xfld: the diatom iron nutrient uptake half-saturation constant.	52
13	Parameter xfln: the non-diatom iron nutrient uptake half-saturation constant.	57
14	Parameter xgme: the maximum meso-zooplankton grazing rate.	62
15	Parameter xgmi: the maximum micro-zooplankton grazing rate.	67
16	Parameter xmd: the detrital nitrogen remineralisation rate.	72
17	Parameter xmdc: the detrital carbon remineralisation rate.	77
18	Parameter xmzme: the meso-zooplankton maximum loss rate.	82
19	Parameter xmzmi: the micro-zooplankton maximum loss rate.	87
20	Parameter xnld: the diatom nitrogen nutrient uptake half-saturation constant.	92
21	Parameter xnln: the non-diatom nitrogen nutrient uptake half-saturation constant.	97
22	Parameter xsld: the diatom silicon nutrient uptake half-saturation constant.	102
23	Parameter xthetanit: the oxygen consumption by nitrogen remineralisation.	107
24	Parameter xthetarem: the oxygen consumption by carbon remineralisation.	112
25	Parameter xvpd: the maximum growth rate for diatoms.	117
26	Parameter xvpn: the maximum growth rate for non-diatoms.	122

List of Figures

1	r0: Change in column inventory of DIN, OXY, ALK, SIL,NPP.	3
2	r0: Change in zonally averaged DIN, OXY, ALK, SIL.	3
3	r0: Change in column inventory of DET, DIC, DTC, FER.	4
4	r0: Change in zonally averaged DET, DIC, DTC, FER.	4
5	r0: Change in column inventory of CHN, CHD, PHN, PHD.	5
6	r0: Change in zonally averaged CHN, CHD, PHN, PHD.	5
7	r0: Change in column inventory of PDS, ZMI, ZME.	6
8	r0: Change in zonally averaged PDS, ZMI, ZME.	6
9	vsed: Change in column inventory of DIN, OXY, ALK, SIL,NPP.	8
10	vsed: Change in zonally averaged DIN, OXY, ALK, SIL.	8
11	vsed: Change in column inventory of DET, DIC, DTC, FER.	9
12	vsed: Change in zonally averaged DET, DIC, DTC, FER.	9
13	vsed: Change in column inventory of CHN, CHD, PHN, PHD.	10
14	vsed: Change in zonally averaged CHN, CHD, PHN, PHD.	10
15	vsed: Change in column inventory of PDS, ZMI, ZME.	11
16	vsed: Change in zonally averaged PDS, ZMI, ZME.	11
17	xald: Change in column inventory of DIN, OXY, ALK, SIL,NPP.	13
18	xald: Change in zonally averaged DIN, OXY, ALK, SIL.	13
19	xald: Change in column inventory of DET, DIC, DTC, FER.	14
20	xald: Change in zonally averaged DET, DIC, DTC, FER.	14
21	xald: Change in column inventory of CHN, CHD, PHN, PHD.	15
22	xald: Change in zonally averaged CHN, CHD, PHN, PHD.	15
23	xald: Change in column inventory of PDS, ZMI, ZME.	16
24	xald: Change in zonally averaged PDS, ZMI, ZME.	16
25	xaln: Change in column inventory of DIN, OXY, ALK, SIL,NPP.	18
26	xaln: Change in zonally averaged DIN, OXY, ALK, SIL.	18

27	xaln: Change in column inventory of DET, DIC, DTC, FER.	19
28	xaln: Change in zonally averaged DET, DIC, DTC, FER.	19
29	xaln: Change in column inventory of CHN, CHD, PHN, PHD.	20
30	xaln: Change in zonally averaged CHN, CHD, PHN, PHD.	20
31	xaln: Change in column inventory of PDS, ZMI, ZME.	21
32	xaln: Change in zonally averaged PDS, ZMI, ZME.	21
33	xfastc: Change in column inventory of DIN, OXY, ALK, SIL,NPP.	23
34	xfastc: Change in zonally averaged DIN, OXY, ALK, SIL.	23
35	xfastc: Change in column inventory of DET, DIC, DTC, FER.	24
36	xfastc: Change in zonally averaged DET, DIC, DTC, FER.	24
37	xfastc: Change in column inventory of CHN, CHD, PHN, PHD.	25
38	xfastc: Change in zonally averaged CHN, CHD, PHN, PHD.	25
39	xfastc: Change in column inventory of PDS, ZMI, ZME.	26
40	xfastc: Change in zonally averaged PDS, ZMI, ZME.	26
41	xfastca: Change in column inventory of DIN, OXY, ALK, SIL,NPP.	28
42	xfastca: Change in zonally averaged DIN, OXY, ALK, SIL.	28
43	xfastca: Change in column inventory of DET, DIC, DTC, FER.	29
44	xfastca: Change in zonally averaged DET, DIC, DTC, FER.	29
45	xfastca: Change in column inventory of CHN, CHD, PHN, PHD.	30
46	xfastca: Change in zonally averaged CHN, CHD, PHN, PHD.	30
47	xfastca: Change in column inventory of PDS, ZMI, ZME.	31
48	xfastca: Change in zonally averaged PDS, ZMI, ZME.	31
49	xfasts: Change in column inventory of DIN, OXY, ALK, SIL,NPP.	33
50	xfasts: Change in zonally averaged DIN, OXY, ALK, SIL.	33
51	xfasts: Change in column inventory of DET, DIC, DTC, FER.	34
52	xfasts: Change in zonally averaged DET, DIC, DTC, FER.	34
53	xfasts: Change in column inventory of CHN, CHD, PHN, PHD.	35
54	xfasts: Change in zonally averaged CHN, CHD, PHN, PHD.	35

55	xfastsi: Change in column inventory of PDS, ZMI, ZME.	36
56	xfastsi: Change in zonally averaged PDS, ZMI, ZME.	36
57	xfdffrac1: Change in column inventory of DIN, OXY, ALK, SIL,NPP.	38
58	xfdffrac1: Change in zonally averaged DIN, OXY, ALK, SIL.	38
59	xfdffrac1: Change in column inventory of DET, DIC, DTC, FER.	39
60	xfdffrac1: Change in zonally averaged DET, DIC, DTC, FER.	39
61	xfdffrac1: Change in column inventory of CHN, CHD, PHN, PHD.	40
62	xfdffrac1: Change in zonally averaged CHN, CHD, PHN, PHD.	40
63	xfdffrac1: Change in column inventory of PDS, ZMI, ZME.	41
64	xfdffrac1: Change in zonally averaged PDS, ZMI, ZME.	41
65	xfdffrac2: Change in column inventory of DIN, OXY, ALK, SIL,NPP.	43
66	xfdffrac2: Change in zonally averaged DIN, OXY, ALK, SIL.	43
67	xfdffrac2: Change in column inventory of DET, DIC, DTC, FER.	44
68	xfdffrac2: Change in zonally averaged DET, DIC, DTC, FER.	44
69	xfdffrac2: Change in column inventory of CHN, CHD, PHN, PHD.	45
70	xfdffrac2: Change in zonally averaged CHN, CHD, PHN, PHD.	45
71	xfdffrac2: Change in column inventory of PDS, ZMI, ZME.	46
72	xfdffrac2: Change in zonally averaged PDS, ZMI, ZME.	46
73	xfdffrac3: Change in column inventory of DIN, OXY, ALK, SIL,NPP.	48
74	xfdffrac3: Change in zonally averaged DIN, OXY, ALK, SIL.	48
75	xfdffrac3: Change in column inventory of DET, DIC, DTC, FER.	49
76	xfdffrac3: Change in zonally averaged DET, DIC, DTC, FER.	49
77	xfdffrac3: Change in column inventory of CHN, CHD, PHN, PHD.	50
78	xfdffrac3: Change in zonally averaged CHN, CHD, PHN, PHD.	50
79	xfdffrac3: Change in column inventory of PDS, ZMI, ZME.	51
80	xfdffrac3: Change in zonally averaged PDS, ZMI, ZME.	51
81	xfld: Change in column inventory of DIN, OXY, ALK, SIL,NPP.	53
82	xfld: Change in zonally averaged DIN, OXY, ALK, SIL.	53

83	xfld: Change in column inventory of DET, DIC, DTC, FER.	54
84	xfld: Change in zonally averaged DET, DIC, DTC, FER.	54
85	xfld: Change in column inventory of CHN, CHD, PHN, PHD.	55
86	xfld: Change in zonally averaged CHN, CHD, PHN, PHD.	55
87	xfld: Change in column inventory of PDS, ZMI, ZME.	56
88	xfld: Change in zonally averaged PDS, ZMI, ZME.	56
89	xfln: Change in column inventory of DIN, OXY, ALK, SIL,NPP.	58
90	xfln: Change in zonally averaged DIN, OXY, ALK, SIL.	58
91	xfln: Change in column inventory of DET, DIC, DTC, FER.	59
92	xfln: Change in zonally averaged DET, DIC, DTC, FER.	59
93	xfln: Change in column inventory of CHN, CHD, PHN, PHD.	60
94	xfln: Change in zonally averaged CHN, CHD, PHN, PHD.	60
95	xfln: Change in column inventory of PDS, ZMI, ZME.	61
96	xfln: Change in zonally averaged PDS, ZMI, ZME.	61
97	xgme: Change in column inventory of DIN, OXY, ALK, SIL,NPP.	63
98	xgme: Change in zonally averaged DIN, OXY, ALK, SIL.	63
99	xgme: Change in column inventory of DET, DIC, DTC, FER.	64
100	xgme: Change in zonally averaged DET, DIC, DTC, FER.	64
101	xgme: Change in column inventory of CHN, CHD, PHN, PHD.	65
102	xgme: Change in zonally averaged CHN, CHD, PHN, PHD.	65
103	xgme: Change in column inventory of PDS, ZMI, ZME.	66
104	xgme: Change in zonally averaged PDS, ZMI, ZME.	66
105	xgmi: Change in column inventory of DIN, OXY, ALK, SIL,NPP.	68
106	xgmi: Change in zonally averaged DIN, OXY, ALK, SIL.	68
107	xgmi: Change in column inventory of DET, DIC, DTC, FER.	69
108	xgmi: Change in zonally averaged DET, DIC, DTC, FER.	69
109	xgmi: Change in column inventory of CHN, CHD, PHN, PHD.	70
110	xgmi: Change in zonally averaged CHN, CHD, PHN, PHD.	70

111	xgmi: Change in column inventory of PDS, ZMI, ZME.	71
112	xgmi: Change in zonally averaged PDS, ZMI, ZME.	71
113	xmd: Change in column inventory of DIN, OXY, ALK, SIL,NPP.	73
114	xmd: Change in zonally averaged DIN, OXY, ALK, SIL.	73
115	xmd: Change in column inventory of DET, DIC, DTC, FER.	74
116	xmd: Change in zonally averaged DET, DIC, DTC, FER.	74
117	xmd: Change in column inventory of CHN, CHD, PHN, PHD.	75
118	xmd: Change in zonally averaged CHN, CHD, PHN, PHD.	75
119	xmd: Change in column inventory of PDS, ZMI, ZME.	76
120	xmd: Change in zonally averaged PDS, ZMI, ZME.	76
121	xmdc: Change in column inventory of DIN, OXY, ALK, SIL,NPP.	78
122	xmdc: Change in zonally averaged DIN, OXY, ALK, SIL.	78
123	xmdc: Change in column inventory of DET, DIC, DTC, FER.	79
124	xmdc: Change in zonally averaged DET, DIC, DTC, FER.	79
125	xmdc: Change in column inventory of CHN, CHD, PHN, PHD.	80
126	xmdc: Change in zonally averaged CHN, CHD, PHN, PHD.	80
127	xmdc: Change in column inventory of PDS, ZMI, ZME.	81
128	xmdc: Change in zonally averaged PDS, ZMI, ZME.	81
129	xmzme: Change in column inventory of DIN, OXY, ALK, SIL,NPP.	83
130	xmzme: Change in zonally averaged DIN, OXY, ALK, SIL.	83
131	xmzme: Change in column inventory of DET, DIC, DTC, FER.	84
132	xmzme: Change in zonally averaged DET, DIC, DTC, FER.	84
133	xmzme: Change in column inventory of CHN, CHD, PHN, PHD.	85
134	xmzme: Change in zonally averaged CHN, CHD, PHN, PHD.	85
135	xmzme: Change in column inventory of PDS, ZMI, ZME.	86
136	xmzme: Change in zonally averaged PDS, ZMI, ZME.	86
137	xmzmi: Change in column inventory of DIN, OXY, ALK, SIL,NPP.	88
138	xmzmi: Change in zonally averaged DIN, OXY, ALK, SIL.	88

139	xmzmi: Change in column inventory of DET, DIC, DTC, FER.	89
140	xmzmi: Change in zonally averaged DET, DIC, DTC, FER.	89
141	xmzmi: Change in column inventory of CHN, CHD, PHN, PHD.	90
142	xmzmi: Change in zonally averaged CHN, CHD, PHN, PHD.	90
143	xmzmi: Change in column inventory of PDS, ZMI, ZME.	91
144	xmzmi: Change in zonally averaged PDS, ZMI, ZME.	91
145	xnld: Change in column inventory of DIN, OXY, ALK, SIL,NPP.	93
146	xnld: Change in zonally averaged DIN, OXY, ALK, SIL.	93
147	xnld: Change in column inventory of DET, DIC, DTC, FER.	94
148	xnld: Change in zonally averaged DET, DIC, DTC, FER.	94
149	xnld: Change in column inventory of CHN, CHD, PHN, PHD.	95
150	xnld: Change in zonally averaged CHN, CHD, PHN, PHD.	95
151	xnld: Change in column inventory of PDS, ZMI, ZME.	96
152	xnld: Change in zonally averaged PDS, ZMI, ZME.	96
153	xnlnd: Change in column inventory of DIN, OXY, ALK, SIL,NPP.	98
154	xnlnd: Change in zonally averaged DIN, OXY, ALK, SIL.	98
155	xnlnd: Change in column inventory of DET, DIC, DTC, FER.	99
156	xnlnd: Change in zonally averaged DET, DIC, DTC, FER.	99
157	xnlnd: Change in column inventory of CHN, CHD, PHN, PHD.	100
158	xnlnd: Change in zonally averaged CHN, CHD, PHN, PHD.	100
159	xnlnd: Change in column inventory of PDS, ZMI, ZME.	101
160	xnlnd: Change in zonally averaged PDS, ZMI, ZME.	101
161	xsld: Change in column inventory of DIN, OXY, ALK, SIL,NPP.	103
162	xsld: Change in zonally averaged DIN, OXY, ALK, SIL.	103
163	xsld: Change in column inventory of DET, DIC, DTC, FER.	104
164	xsld: Change in zonally averaged DET, DIC, DTC, FER.	104
165	xsld: Change in column inventory of CHN, CHD, PHN, PHD.	105
166	xsld: Change in zonally averaged CHN, CHD, PHN, PHD.	105

167	xsld: Change in column inventory of PDS, ZMI, ZME.	106
168	xsld: Change in zonally averaged PDS, ZMI, ZME.	106
169	xthetanit: Change in column inventory of DIN, OXY, ALK, SIL,NPP. . . .	108
170	xthetanit: Change in zonally averaged DIN, OXY, ALK, SIL.	108
171	xthetanit: Change in column inventory of DET, DIC, DTC, FER.	109
172	xthetanit: Change in zonally averaged DET, DIC, DTC, FER.	109
173	xthetanit: Change in column inventory of CHN, CHD, PHN, PHD.	110
174	xthetanit: Change in zonally averaged CHN, CHD, PHN, PHD.	110
175	xthetanit: Change in column inventory of PDS, ZMI, ZME.	111
176	xthetanit: Change in zonally averaged PDS, ZMI, ZME.	111
177	xthetarem: Change in column inventory of DIN, OXY, ALK, SIL,NPP. . .	113
178	xthetarem: Change in zonally averaged DIN, OXY, ALK, SIL.	113
179	xthetarem: Change in column inventory of DET, DIC, DTC, FER.	114
180	xthetarem: Change in zonally averaged DET, DIC, DTC, FER.	114
181	xthetarem: Change in column inventory of CHN, CHD, PHN, PHD.	115
182	xthetarem: Change in zonally averaged CHN, CHD, PHN, PHD.	115
183	xthetarem: Change in column inventory of PDS, ZMI, ZME.	116
184	xthetarem: Change in zonally averaged PDS, ZMI, ZME.	116
185	xvpd: Change in column inventory of DIN, OXY, ALK, SIL,NPP.	118
186	xvpd: Change in zonally averaged DIN, OXY, ALK, SIL.	118
187	xvpd: Change in column inventory of DET, DIC, DTC, FER.	119
188	xvpd: Change in zonally averaged DET, DIC, DTC, FER.	119
189	xvpd: Change in column inventory of CHN, CHD, PHN, PHD.	120
190	xvpd: Change in zonally averaged CHN, CHD, PHN, PHD.	120
191	xvpd: Change in column inventory of PDS, ZMI, ZME.	121
192	xvpd: Change in zonally averaged PDS, ZMI, ZME.	121
193	xvpn: Change in column inventory of DIN, OXY, ALK, SIL,NPP.	123
194	xvpn: Change in zonally averaged DIN, OXY, ALK, SIL.	123

195	xvpn: Change in column inventory of DET, DIC, DTC, FER.	124
196	xvpn: Change in zonally averaged DET, DIC, DTC, FER.	124
197	xvpn: Change in column inventory of CHN, CHD, PHN, PHD.	125
198	xvpn: Change in zonally averaged CHN, CHD, PHN, PHD.	125
199	xvpn: Change in column inventory of PDS, ZMI, ZME.	126
200	xvpn: Change in zonally averaged PDS, ZMI, ZME.	126

1 Summary

Here below are the supplementary figures for Chapter 4 of the PhD thesis titled “Ocean Biogeochemical Optimisation in Earth System Models”, by Sophy Oliver, University of Oxford. In this chapter a simple parameter perturbation study on 25 biogeochemical parameters was carried out within the global ocean biogeochemical model MEDUSA-2.0 (Yool et. al. 2013). Each of the 25 parameters was individually perturbed by +10% of their feasible range and their influence on 16 model output distributions (see Table 1) was assessed relative to the default simulation. The figures below are to be read in conjunction with Chapter 4, which describes and analyses the figures.

Abbreviation	Description	Units
OXY	Dissolved oxygen	mmol O ₂ /m ³
ALK	Alkalinity	meq/m ³
SIL	Silicate	mmol Si/m ³
DIN	Dissolved inorganic nitrogen	mmol N/m ³
DET	Detrital nitrogen	mmol N/m ³
FER	Dissolved iron	mmol Fe/m ³
DTC	Detrital carbon	mmol C/m ³
DIC	Dissolved inorganic carbon	mmol C/m ³
CHN	Chl-a concentration in non-diatom phytoplankton	mg Chl/m ³
CHD	Chl-a concentration in diatom phytoplankton	mg Chl/m ³
PHN	Non-diatom phytoplankton	mmol N/m ³
PHD	Diatom phytoplankton	mmol N/m ³
PDS	Biogenic silicon in diatom phytoplankton	mmol Si/m ³
ZMI	Micro zooplankton	mmol N/m ³
ZME	Meso zooplankton	mmol N/m ³
NPP	Non-diatom and diatom primary production	mmol N/m ² /d

Table 1: The 16 annually-averaged variables output by MEDUSA used for analysis. MEDUSA models 15 tracers, however NPP was then also calculated from output diagnostic variables.

- 2 Parameter r_0 : the CaCO_3 : POC: export rain ratio scalar.

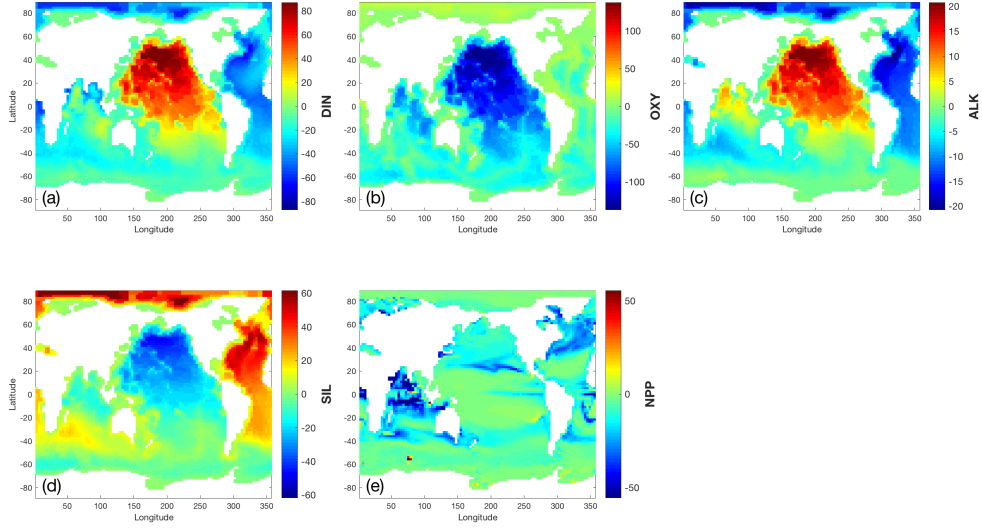


Figure 1: Change in column inventory of (a) DIN, (b) OXY, (c) ALK, (d) SIL, and (e) NPP after a +10% perturbation in r_0 , the CaCO_3 : POC: export rain ratio scalar.

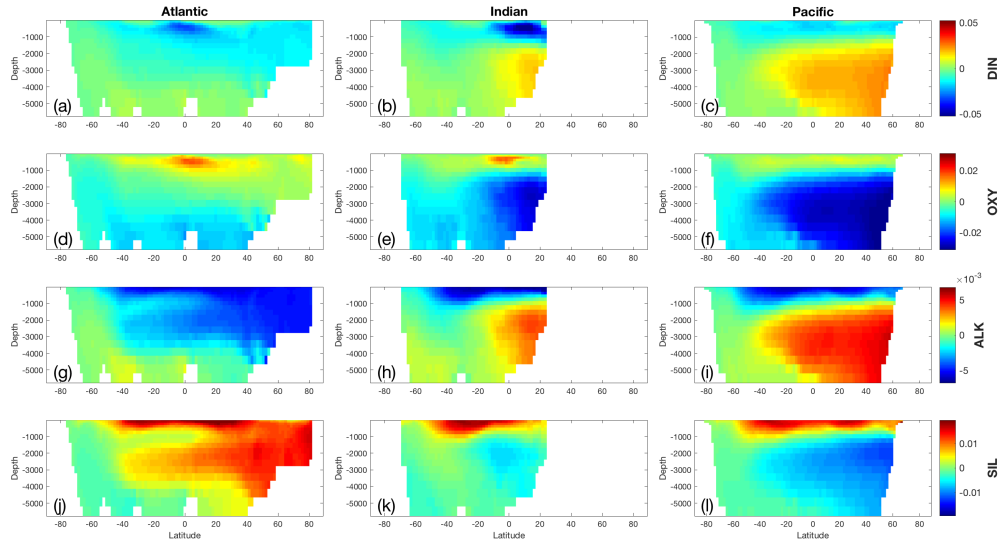


Figure 2: Change in volume-weighted zonally averaged (a-c) DIN, (d-f) OXY, (g-i) ALK, and (j-l) SIL after a +10% perturbation in r_0 , the CaCO_3 : POC: export rain ratio scalar, for the (left) Atlantic, (middle) Indian, and (right) Pacific Oceans.

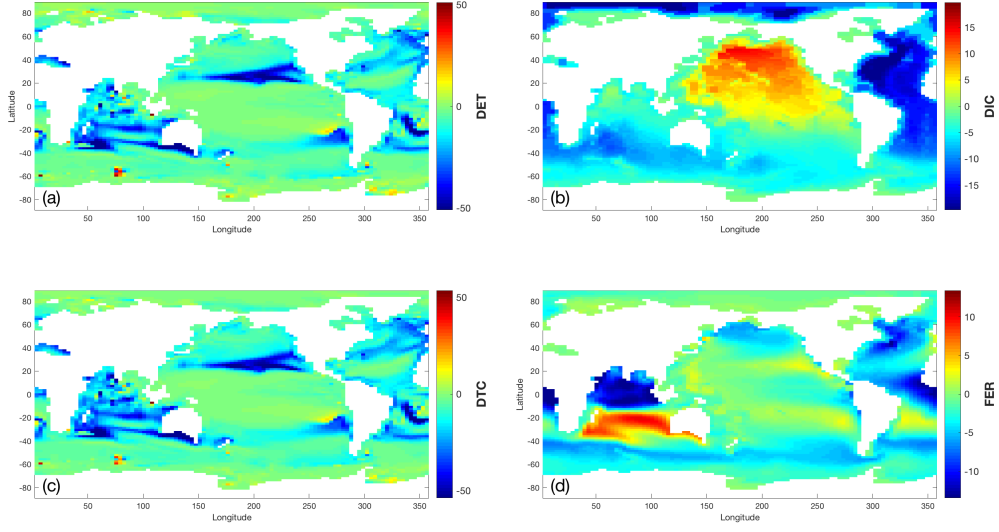


Figure 3: Change in column inventory of (a) DET, (b) DIC, (c) DTC, and (d) FER after a +10% perturbation in r_0 , the CaCO_3 : POC: export rain ratio scalar.

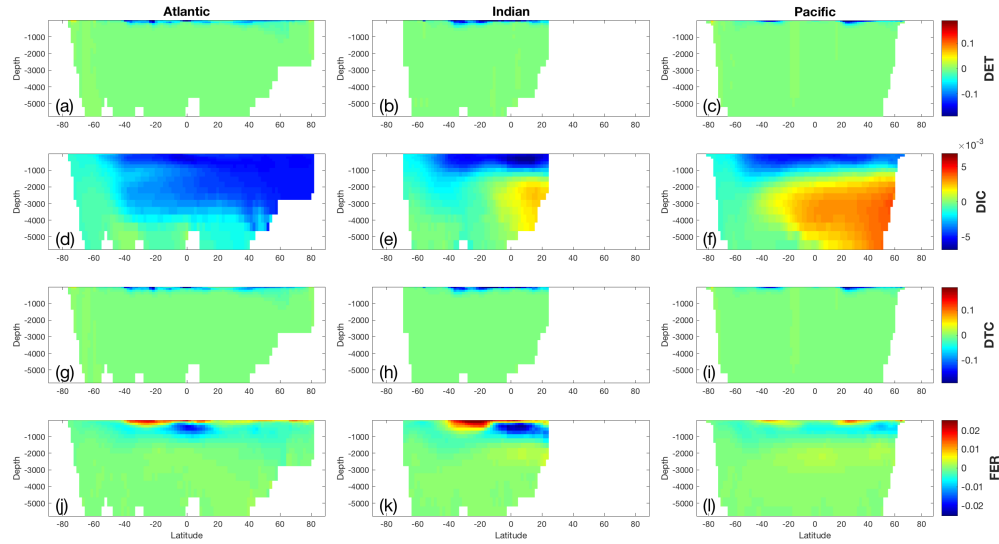


Figure 4: Change in volume-weighted zonally averaged (a-c) DET, (d-f) DIC, (g-i) DTC, and (j-l) FER after a +10% perturbation in r_0 , the CaCO_3 : POC: export rain ratio scalar, for the (left) Atlantic, (middle) Indian, and (right) Pacific Oceans.

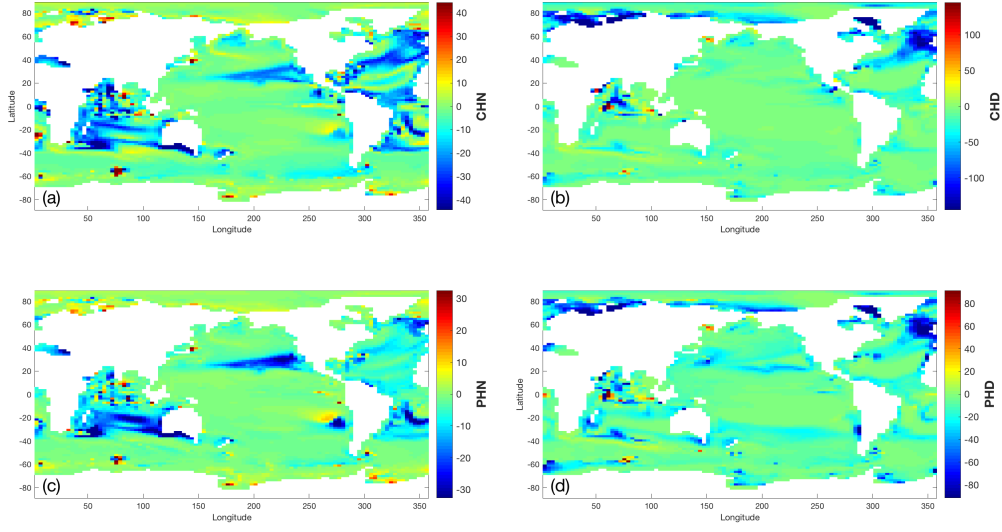


Figure 5: Change in column inventory of (a) CHN, (b) CHD, (c) PHN, and (d) PHD. after a +10% perturbation in r_0 , the CaCO_3 : POC: export rain ratio scalar.

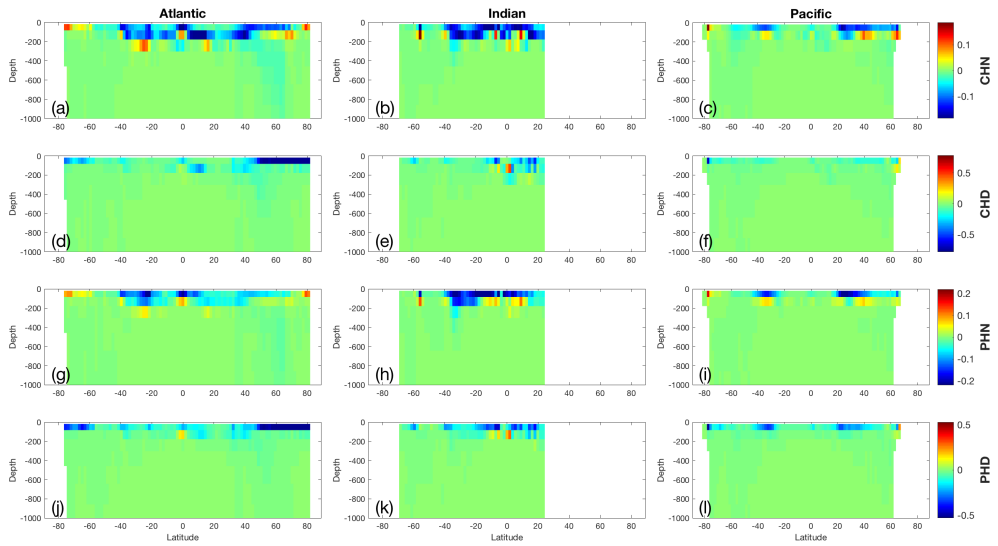


Figure 6: Change in volume-weighted zonally averaged (a-c) CHN, (d-f) CHD, (g-i) PHN, and (j-l) PHD after a +10% perturbation in r_0 , the CaCO_3 : POC: export rain ratio scalar, for the (left) Atlantic, (middle) Indian, and (right) Pacific Oceans.

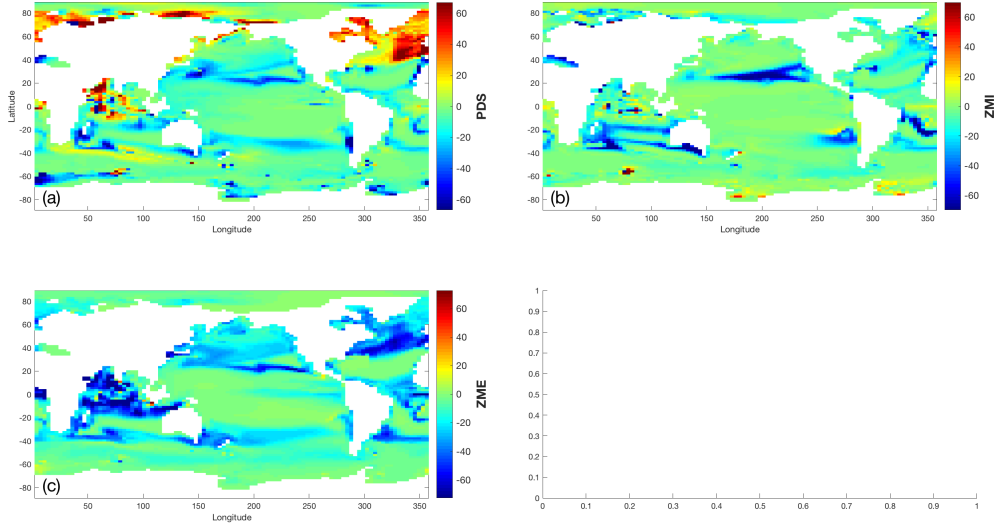


Figure 7: Change in column inventory of (a) PDS, (b) ZMI, and (c) ZME, after a +10% perturbation in r_0 , the CaCO_3 : POC: export rain ratio scalar.

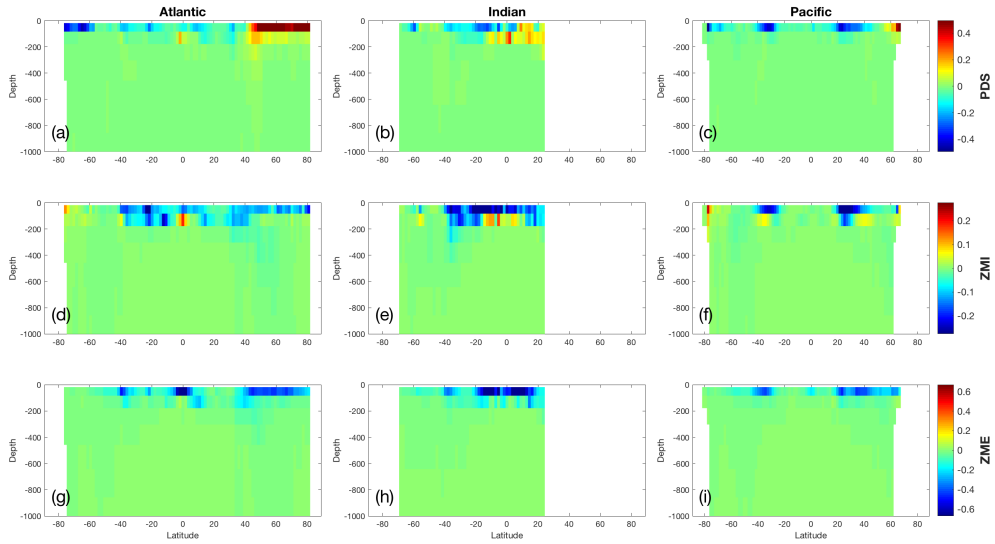


Figure 8: Change in volume-weighted zonally averaged (a-c) PDS, (d-f) ZMI, and (g-i) ZME after a +10% perturbation in r_0 , the CaCO_3 : POC: export rain ratio scalar, for the (left) Atlantic, (middle) Indian, and (right) Pacific Oceans.

3 Parameter used: the detritus gravitational sinking rate.

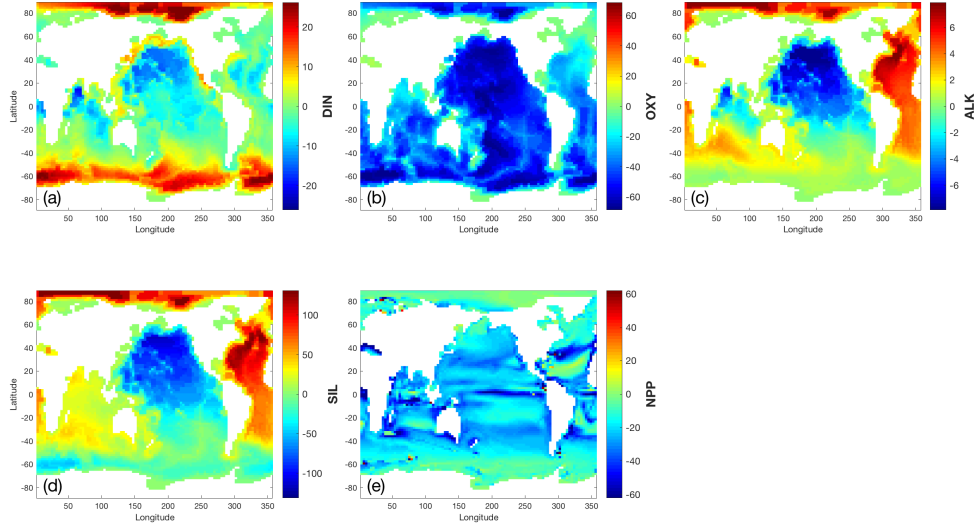


Figure 9: Change in column inventory of (a) DIN, (b) OXY, (c) ALK, (d) SIL, and (e) NPP after a +10% perturbation in v_{sed} , the detritus gravitational sinking rate.

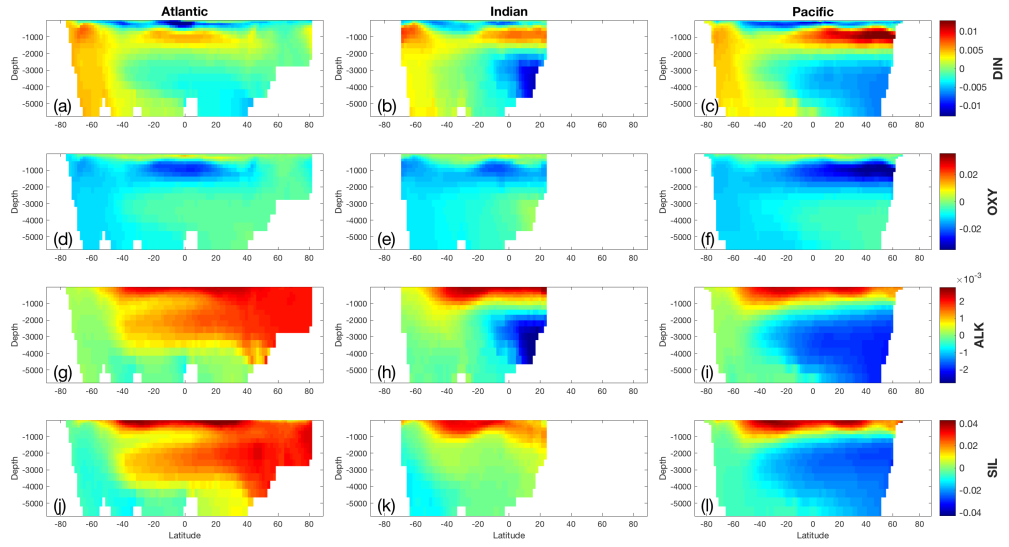


Figure 10: Change in volume-weighted zonally averaged (a-c) DIN, (d-f) OXY, (g-i) ALK, and (j-l) SIL after a +10% perturbation in v_{sed} , the detritus gravitational sinking rate, for the (left) Atlantic, (middle) Indian, and (right) Pacific Oceans.

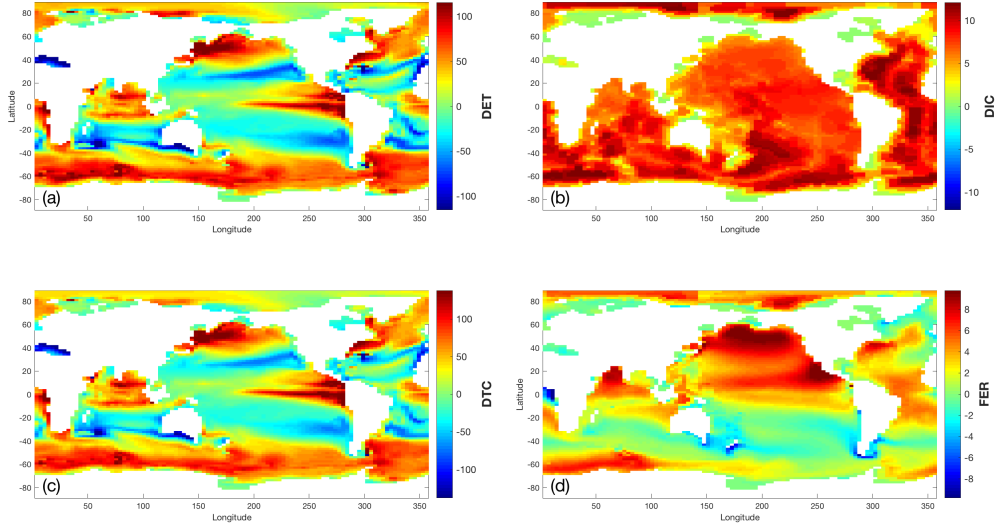


Figure 11: Change in column inventory of (a) DET, (b) DIC, (c) DTC, and (d) FER after a +10% perturbation in v_{sed} , the detritus gravitational sinking rate.

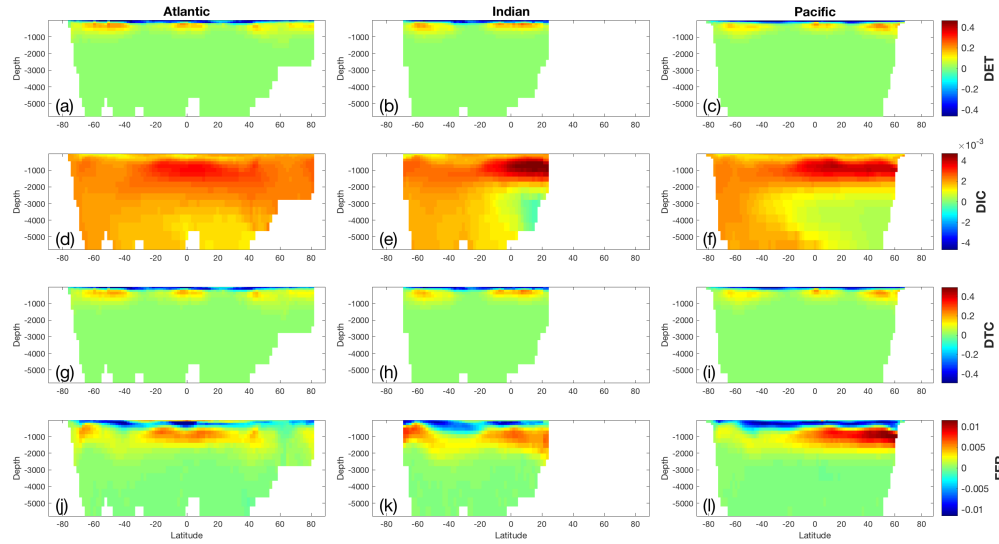


Figure 12: Change in volume-weighted zonally averaged (a-c) DET, (d-f) DIC, (g-i) DTC, and (j-l) FER after a +10% perturbation in v_{sed} , the detritus gravitational sinking rate, for the (left) Atlantic, (middle) Indian, and (right) Pacific Oceans.

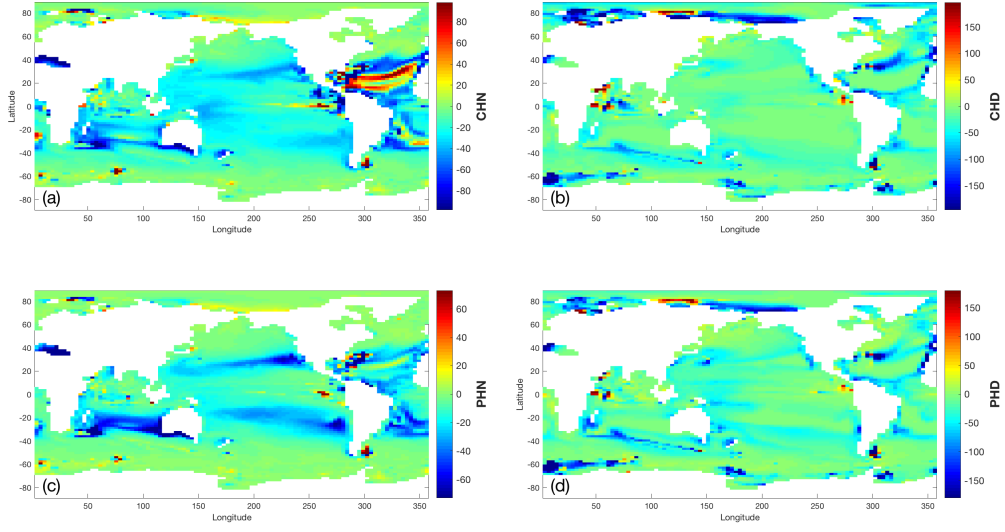


Figure 13: Change in column inventory of (a) CHN, (b) CHD, (c) PHN, and (d) PHD. after a +10% perturbation in v_{sed} , the detritus gravitational sinking rate.

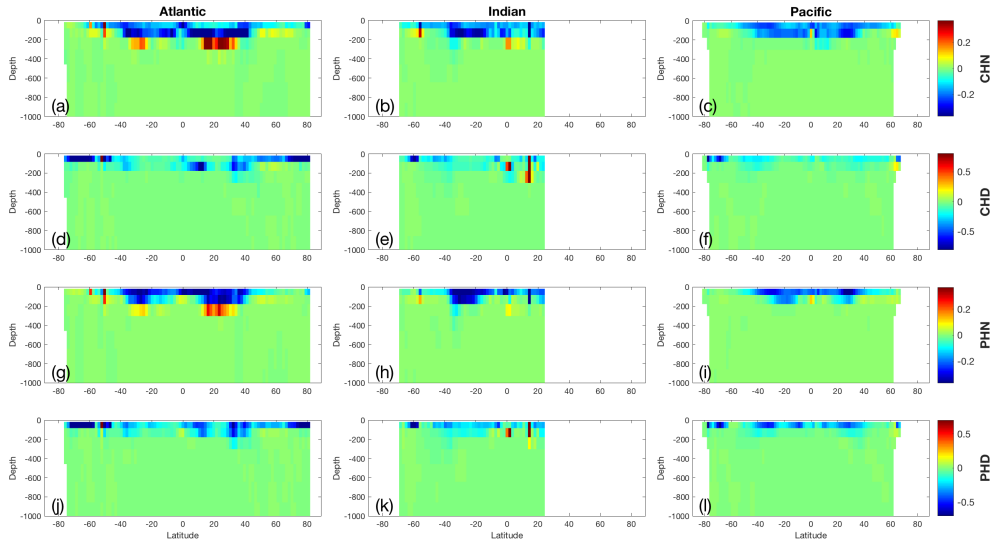


Figure 14: Change in volume-weighted zonally averaged (a-c) CHN, (d-f) CHD, (g-i) PHN, and (j-l) PHD after a +10% perturbation in v_{sed} , the detritus gravitational sinking rate, for the (left) Atlantic, (middle) Indian, and (right) Pacific Oceans.

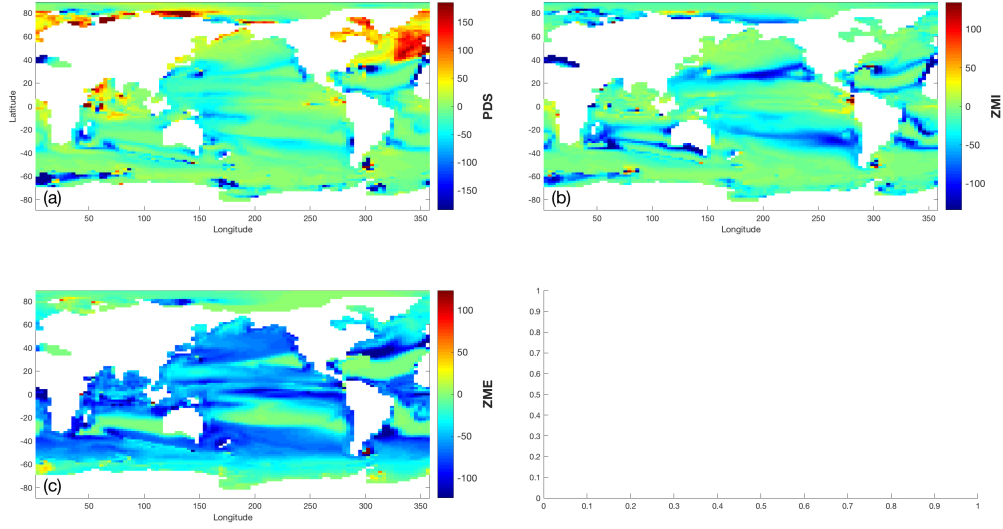


Figure 15: Change in column inventory of (a) PDS, (b) ZMI, and (c) ZME, after a +10% perturbation in v_{sed} , the detritus gravitational sinking rate.

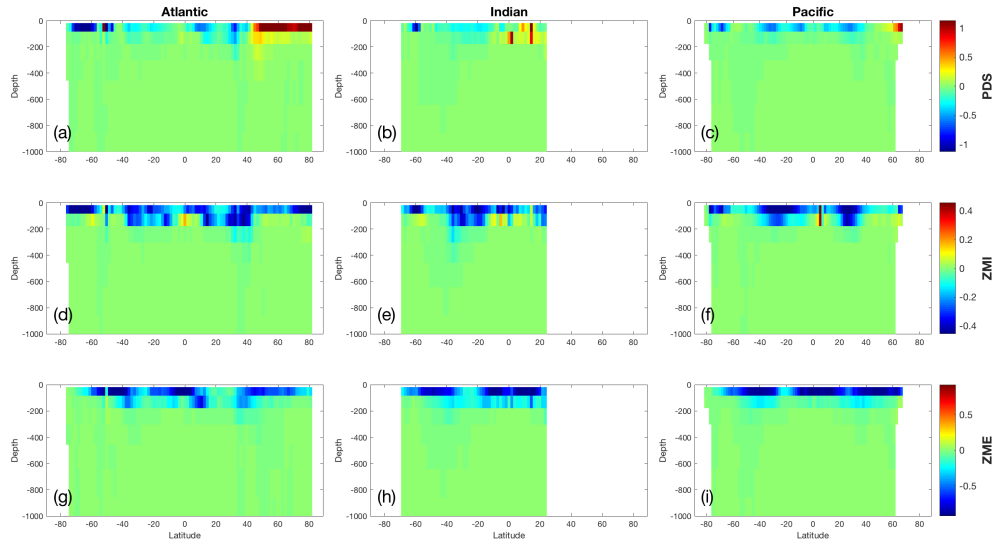


Figure 16: Change in volume-weighted zonally averaged (a-c) PDS, (d-f) ZMI, and (g-i) ZME after a +10% perturbation in v_{sed} , the detritus gravitational sinking rate, for the (left) Atlantic, (middle) Indian, and (right) Pacific Oceans.

- 4 Parameter `xald`: the diatom chl-specific initial slope of P-I curve.

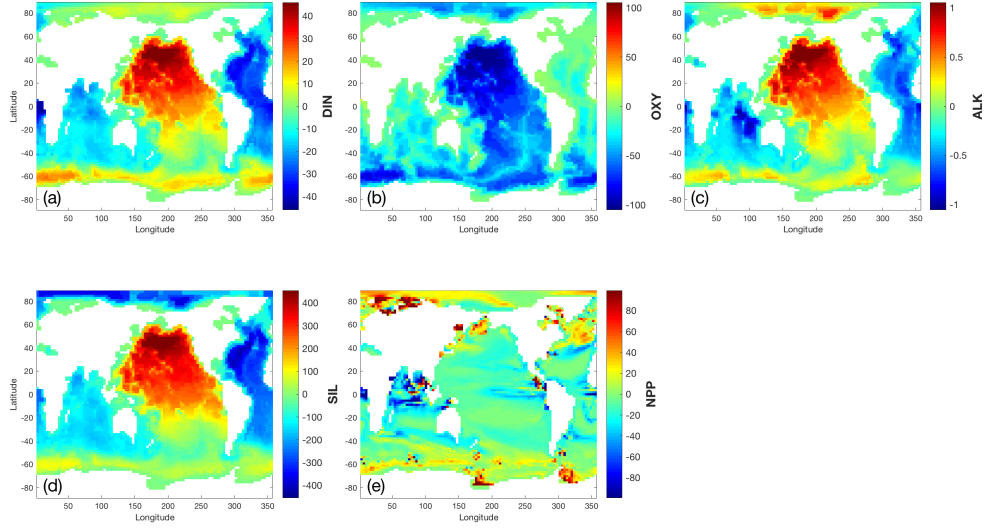


Figure 17: Change in column inventory of (a) DIN, (b) OXY, (c) ALK, (d) SIL, and (e) NPP after a +10% perturbation in x_{ald} , the diatom chl-specific initial slope of P-I curve.

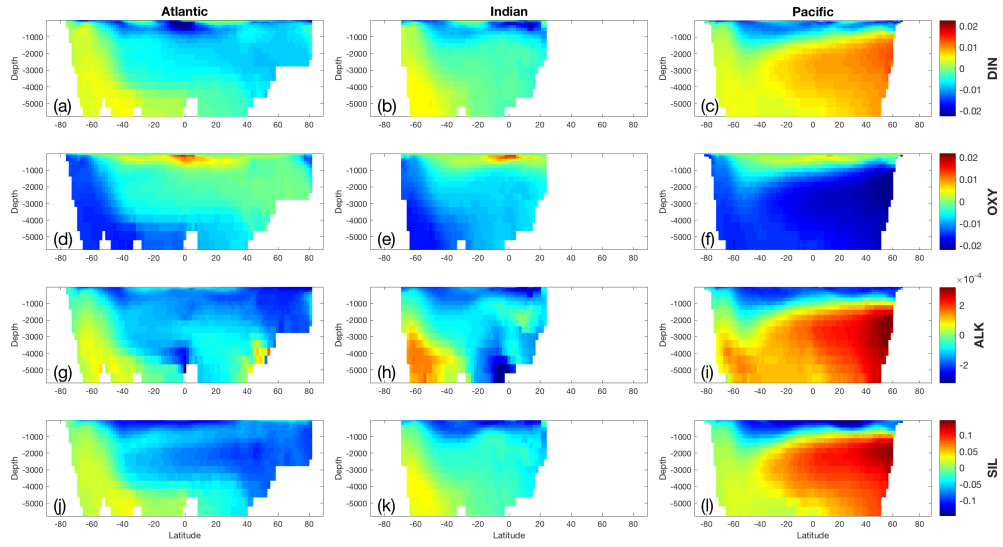


Figure 18: Change in volume-weighted zonally averaged (a-c) DIN, (d-f) OXY, (g-i) ALK, and (j-l) SIL after a +10% perturbation in x_{ald} , the diatom chl-specific initial slope of P-I curve, for the (left) Atlantic, (middle) Indian, and (right) Pacific Oceans.

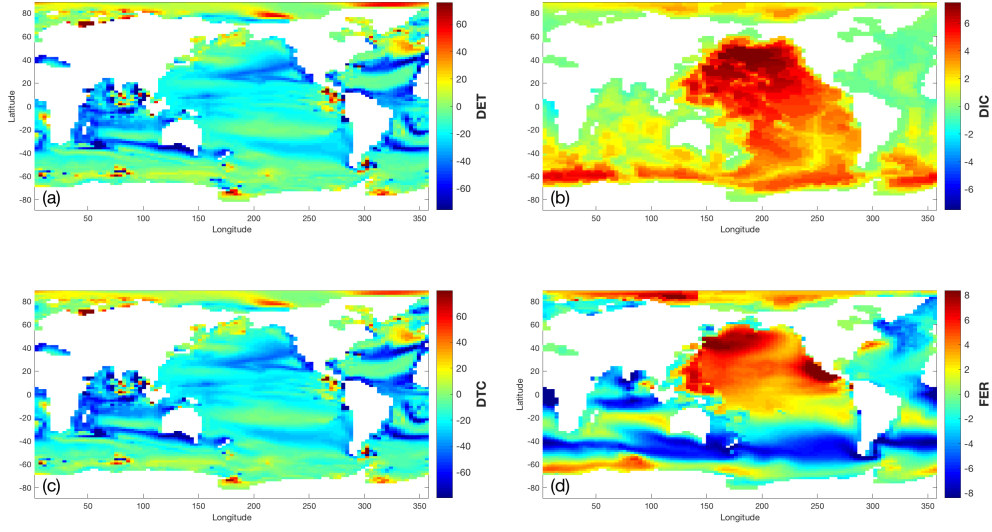


Figure 19: Change in column inventory of (a) DET, (b) DIC, (c) DTC, and (d) FER after a +10% perturbation in xald, the diatom chl-specific initial slope of P-I curve.

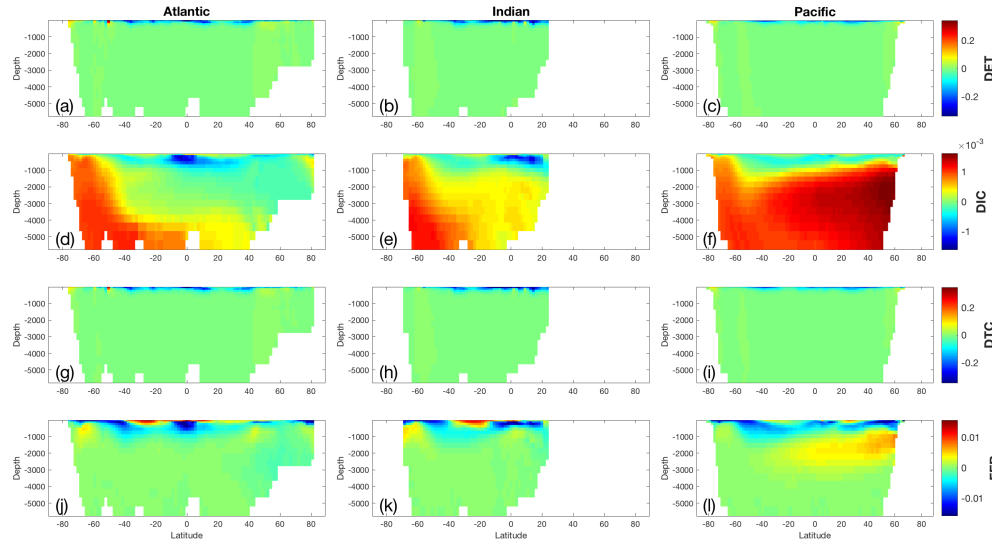


Figure 20: Change in volume-weighted zonally averaged (a-c) DET, (d-f) DIC, (g-i) DTC, and (j-l) FER after a +10% perturbation in xald, the diatom chl-specific initial slope of P-I curve, for the (left) Atlantic, (middle) Indian, and (right) Pacific Oceans.

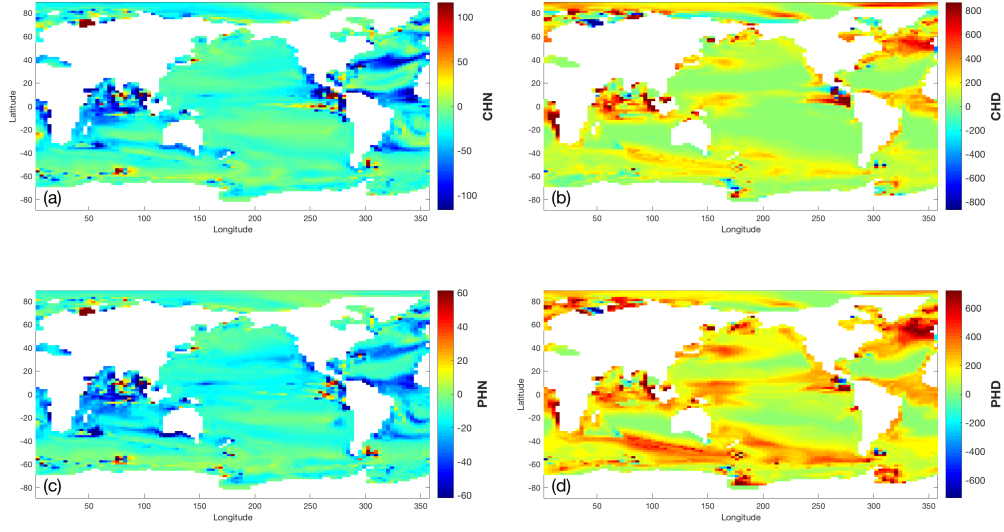


Figure 21: Change in column inventory of (a) CHN, (b) CHD, (c) PHN, and (d) PHD. after a +10% perturbation in xald, the diatom chl-specific initial slope of P-I curve.

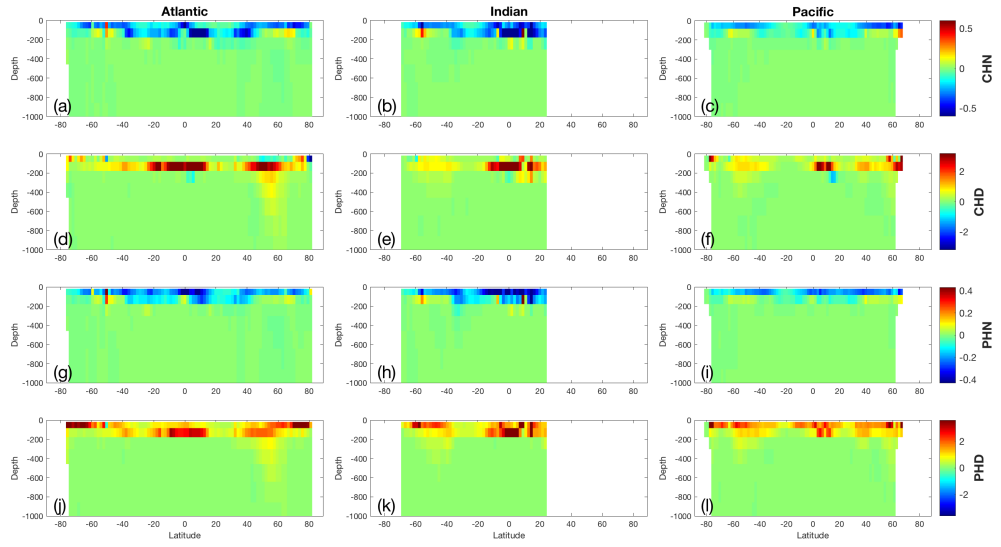


Figure 22: Change in volume-weighted zonally averaged (a-c) CHN, (d-f) CHD, (g-i) PHN, and (j-l) PHD after a +10% perturbation in xald, the diatom chl-specific initial slope of P-I curve, for the (left) Atlantic, (middle) Indian, and (right) Pacific Oceans.

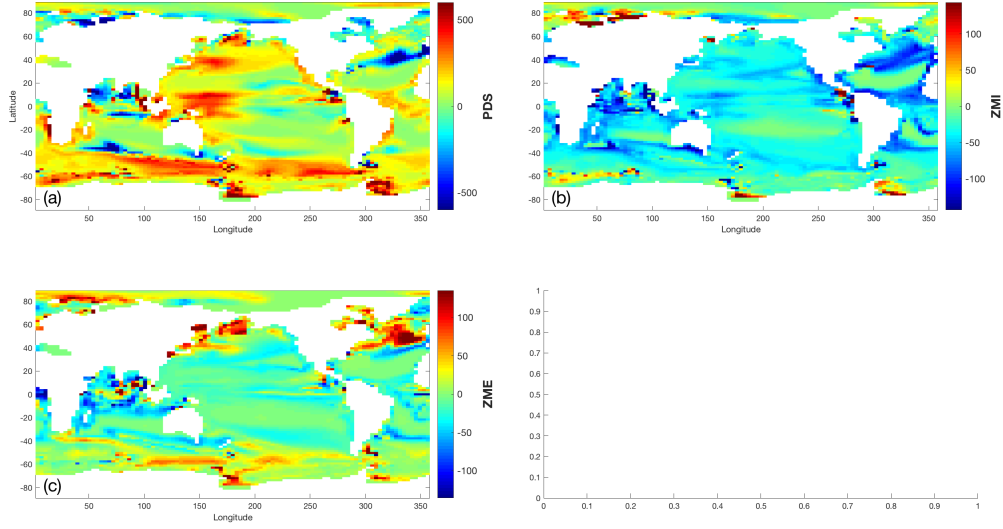


Figure 23: Change in column inventory of (a) PDS, (b) ZMI, and (c) ZME, after a +10% perturbation in x_{ald} , the diatom chl-specific initial slope of P-I curve.

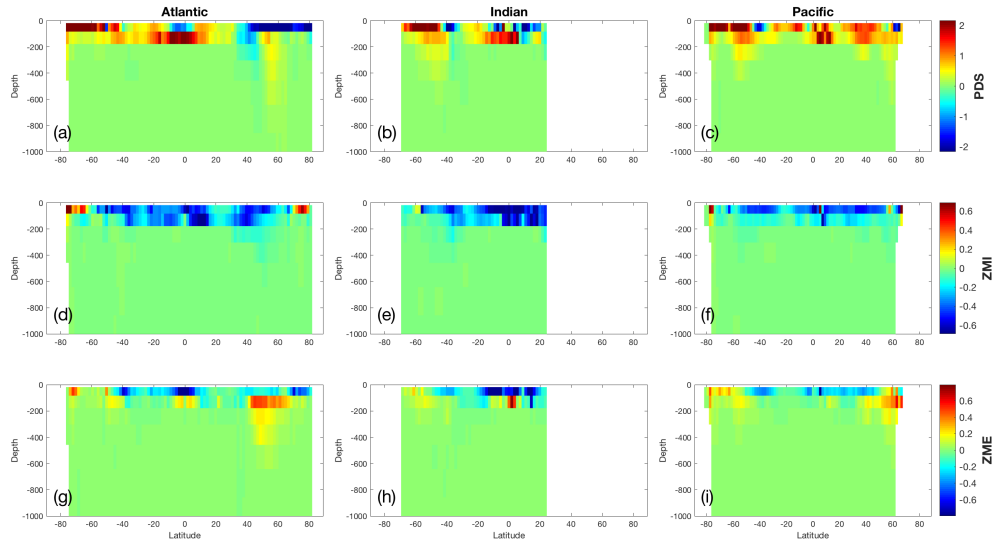


Figure 24: Change in volume-weighted zonally averaged (a-c) PDS, (d-f) ZMI, and (g-i) ZME after a +10% perturbation in x_{ald} , the diatom chl-specific initial slope of P-I curve, for the (left) Atlantic, (middle) Indian, and (right) Pacific Oceans.

- 5 Parameter `xaln`: the non-diatom chl-specific initial slope of P-I curve.

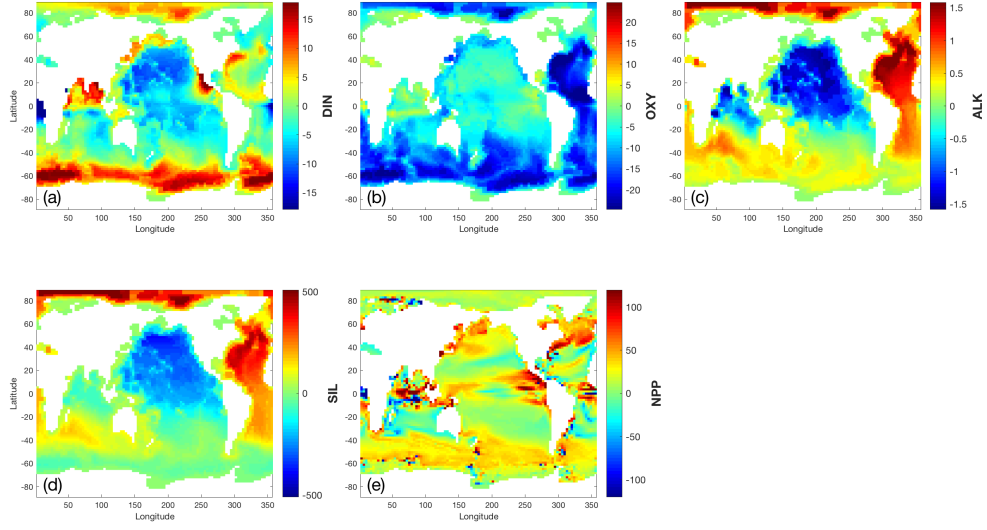


Figure 25: Change in column inventory of (a) DIN, (b) OXY, (c) ALK, (d) SIL, and (e) NPP after a +10% perturbation in x_{aln} , the non-diatom chl-specific initial slope of P-I curve.

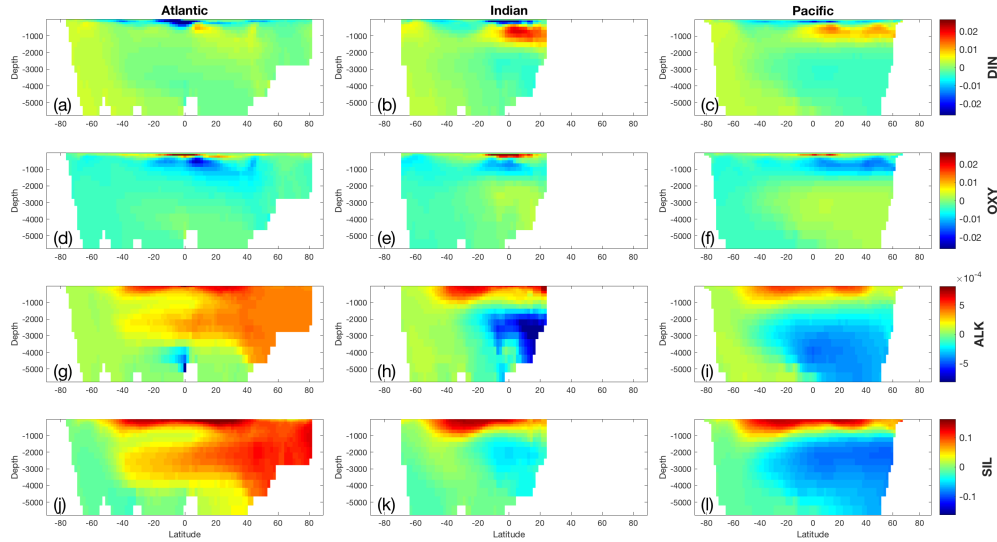


Figure 26: Change in volume-weighted zonally averaged (a-c) DIN, (d-f) OXY, (g-i) ALK, and (j-l) SIL after a +10% perturbation in x_{aln} , the non-diatom chl-specific initial slope of P-I curve, for the (left) Atlantic, (middle) Indian, and (right) Pacific Oceans.

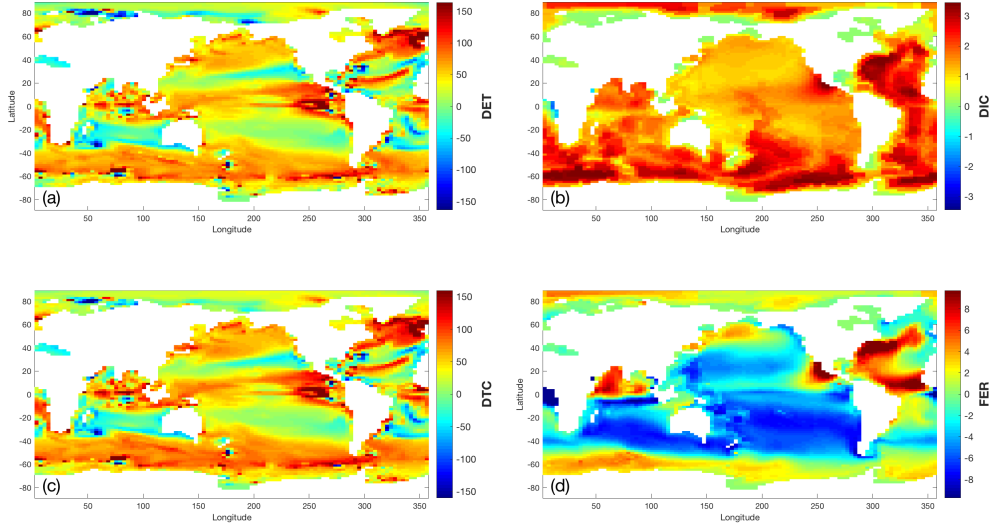


Figure 27: Change in column inventory of (a) DET, (b) DIC, (c) DTC, and (d) FER after a +10% perturbation in xaln, the non-diatom chl-specific initial slope of P-I curve.

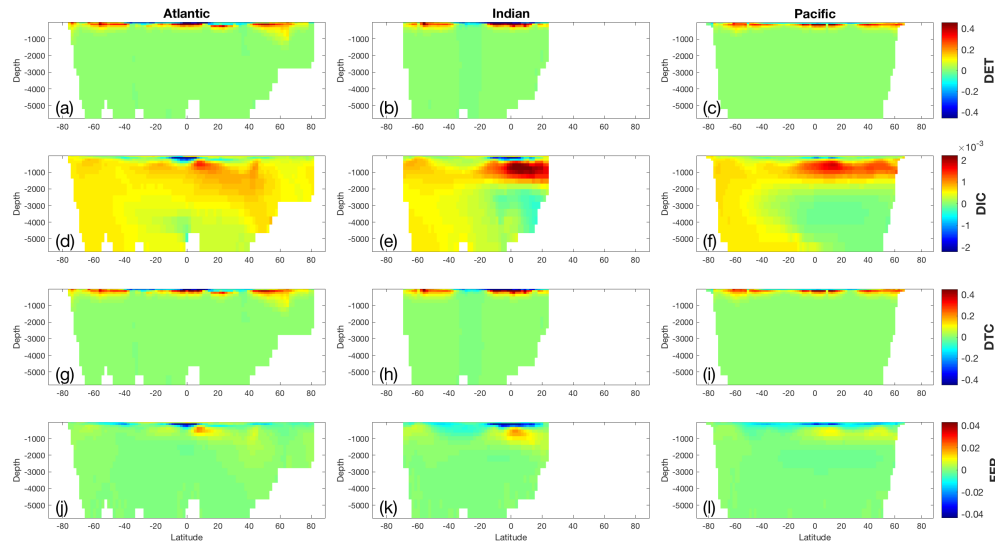


Figure 28: Change in volume-weighted zonally averaged (a-c) DET, (d-f) DIC, (g-i) DTC, and (j-l) FER after a +10% perturbation in xaln, the non-diatom chl-specific initial slope of P-I curve, for the (left) Atlantic, (middle) Indian, and (right) Pacific Oceans.

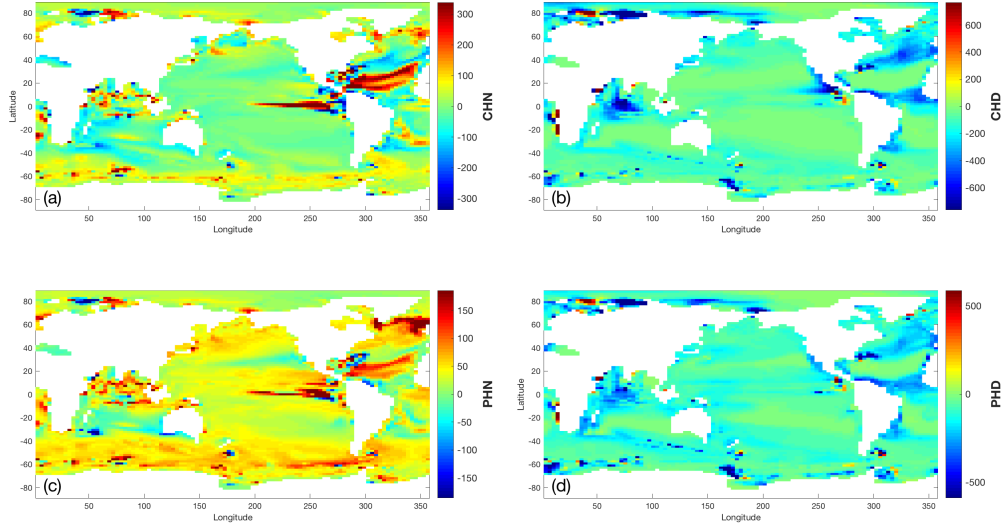


Figure 29: Change in column inventory of (a) CHN, (b) CHD, (c) PHN, and (d) PHD. after a +10% perturbation in xaln, the non-diatom chl-specific initial slope of P-I curve.

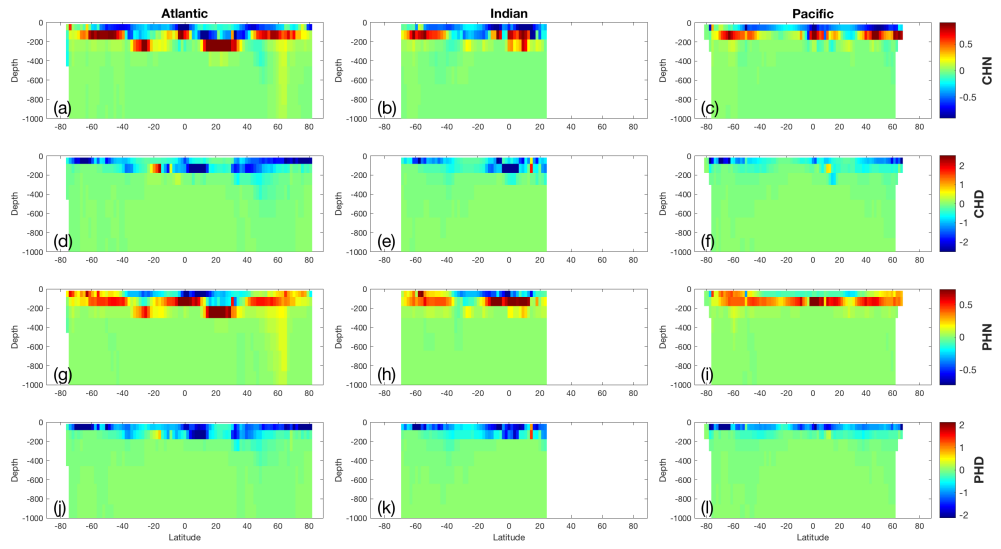


Figure 30: Change in volume-weighted zonally averaged (a-c) CHN, (d-f) CHD, (g-i) PHN, and (j-l) PHD after a +10% perturbation in xaln, the non-diatom chl-specific initial slope of P-I curve, for the (left) Atlantic, (middle) Indian, and (right) Pacific Oceans.

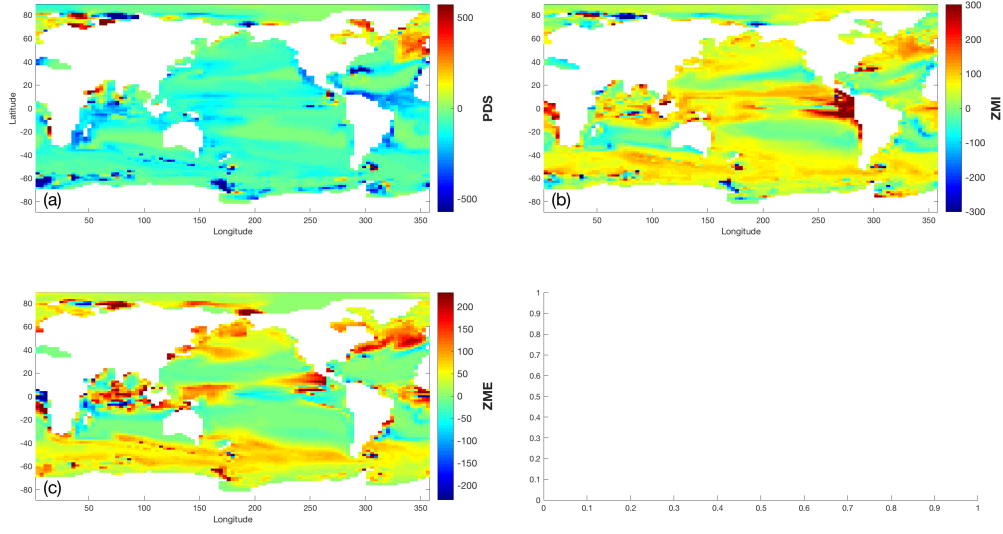


Figure 31: Change in column inventory of (a) PDS, (b) ZMI, and (c) ZME, after a +10% perturbation in x_{aln} , the non-diatom chl-specific initial slope of P-I curve.

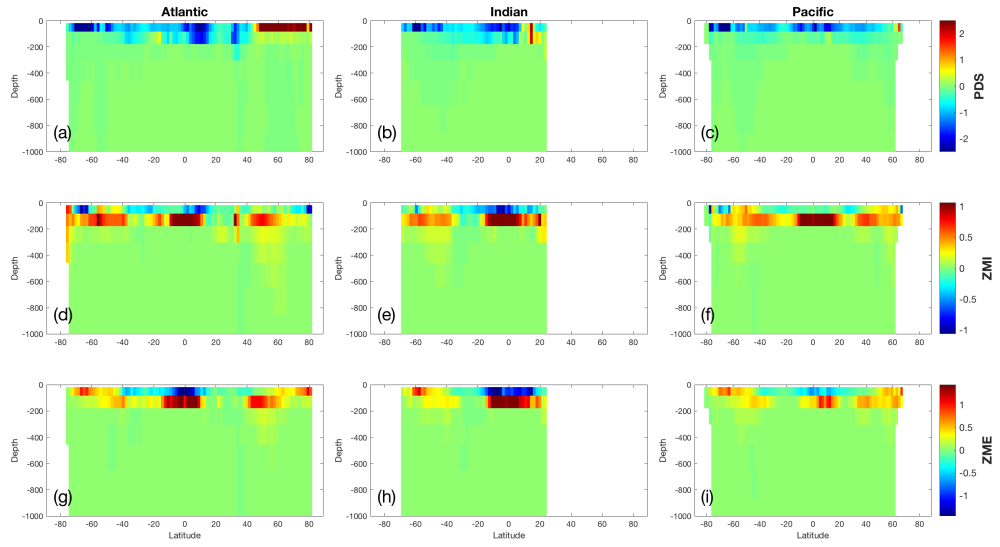


Figure 32: Change in volume-weighted zonally averaged (a-c) PDS, (d-f) ZMI, and (g-i) ZME after a +10% perturbation in x_{aln} , the non-diatom chl-specific initial slope of P-I curve, for the (left) Atlantic, (middle) Indian, and (right) Pacific Oceans.

- 6 Parameter `xfastc`: the excess organic carbon dissolution length scale.

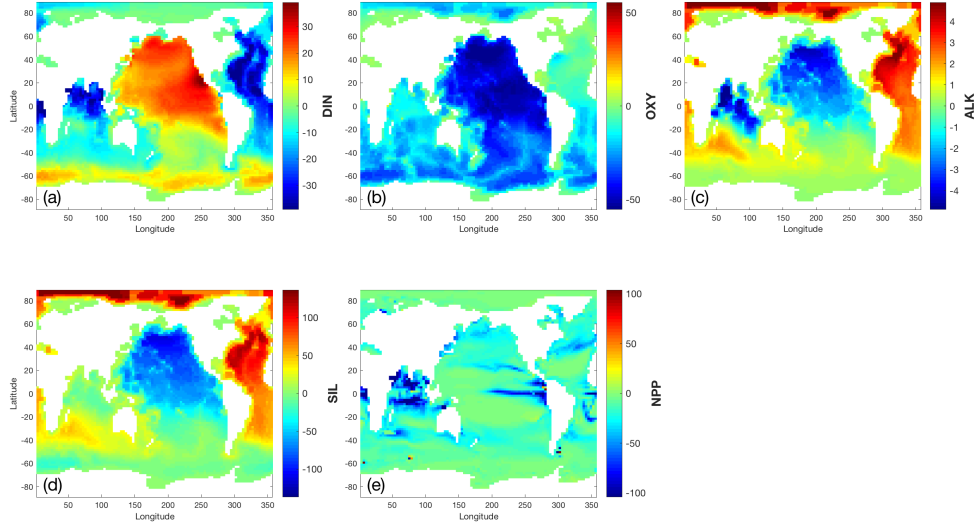


Figure 33: Change in column inventory of (a) DIN, (b) OXY, (c) ALK, (d) SIL, and (e) NPP after a +10% perturbation in x_{fastc} , the excess organic carbon dissolution length scale.

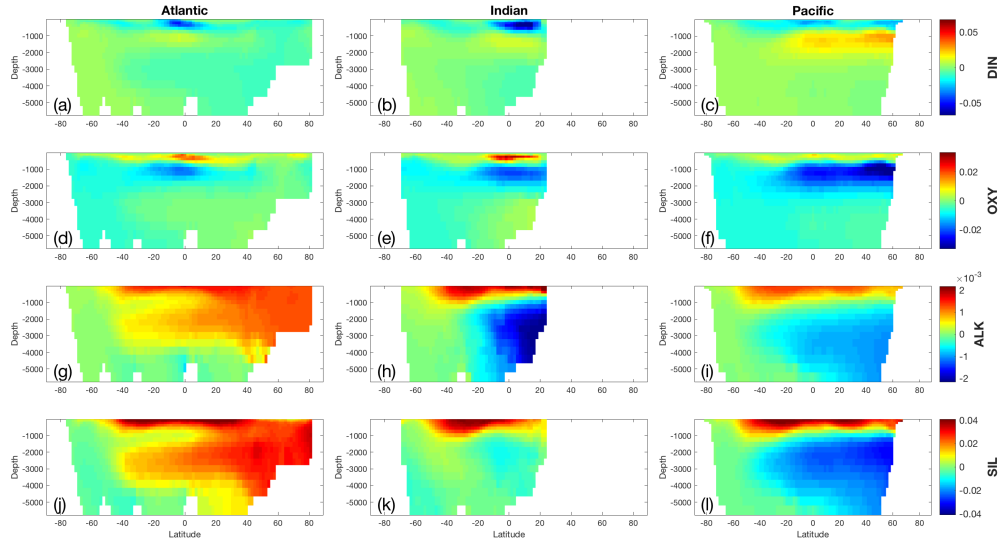


Figure 34: Change in volume-weighted zonally averaged (a-c) DIN, (d-f) OXY, (g-i) ALK, and (j-l) SIL after a +10% perturbation in x_{fastc} , the excess organic carbon dissolution length scale, for the (left) Atlantic, (middle) Indian, and (right) Pacific Oceans.

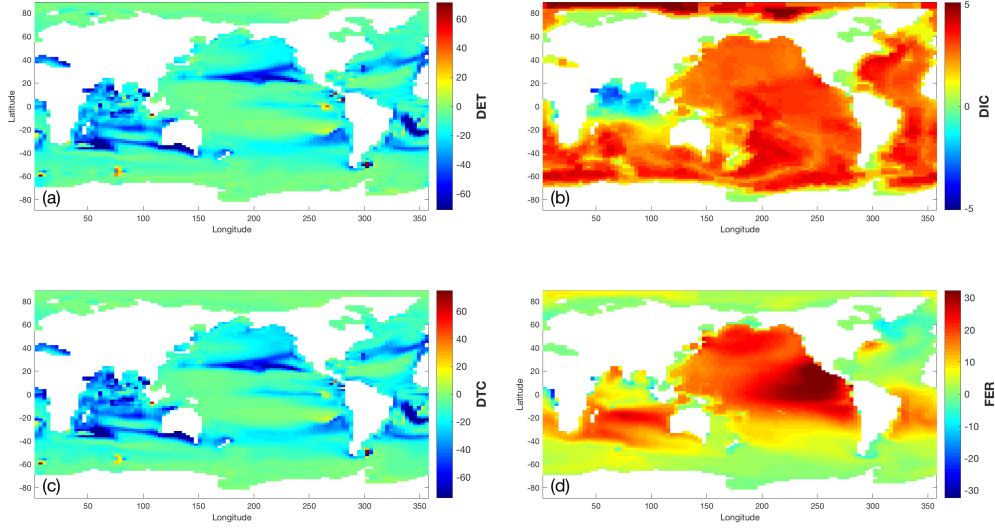


Figure 35: Change in column inventory of (a) DET, (b) DIC, (c) DTC, and (d) FER after a +10% perturbation in xfastc, the excess organic carbon dissolution length scale.

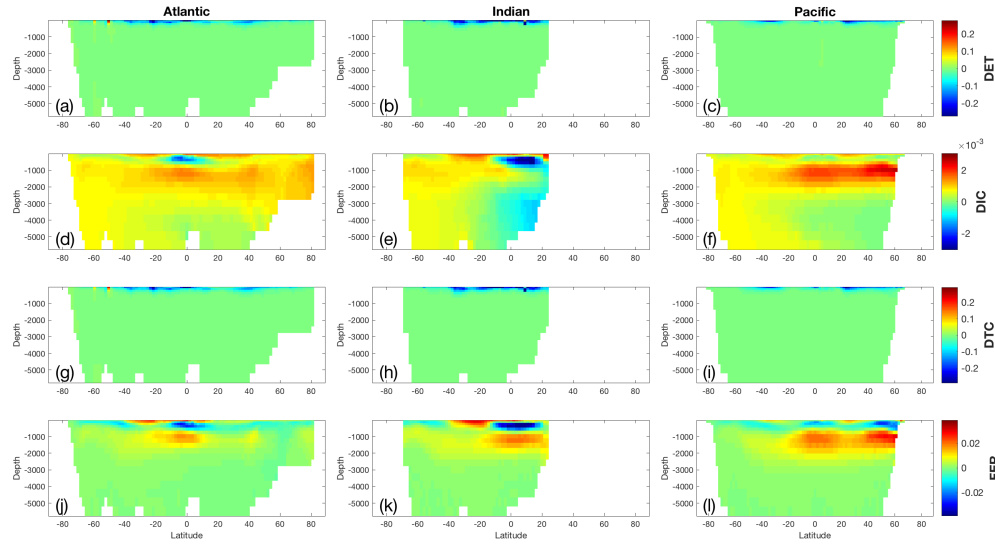


Figure 36: Change in volume-weighted zonally averaged (a-c) DET, (d-f) DIC, (g-i) DTC, and (j-l) FER after a +10% perturbation in xfastc, the excess organic carbon dissolution length scale, for the (left) Atlantic, (middle) Indian, and (right) Pacific Oceans.

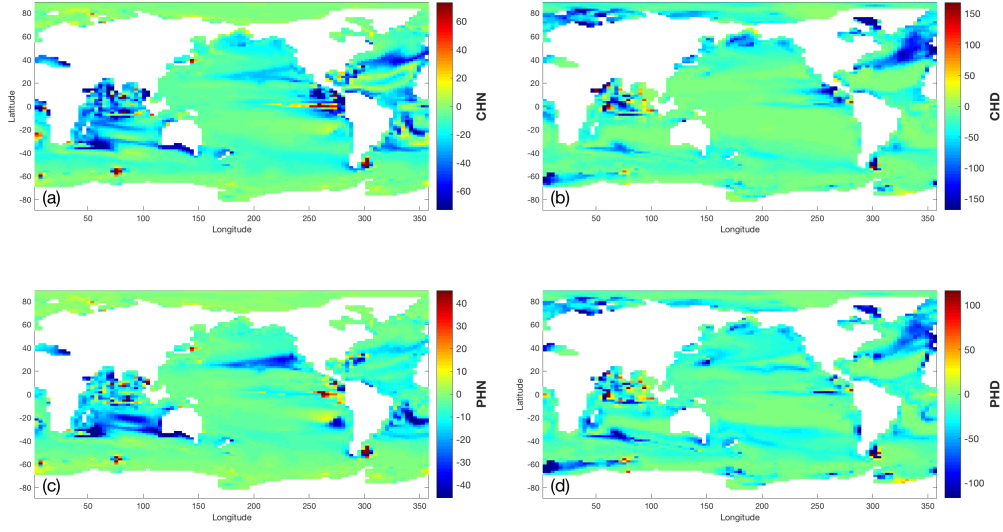


Figure 37: Change in column inventory of (a) CHN, (b) CHD, (c) PHN, and (d) PHD. after a +10% perturbation in xfastc, the excess organic carbon dissolution length scale.

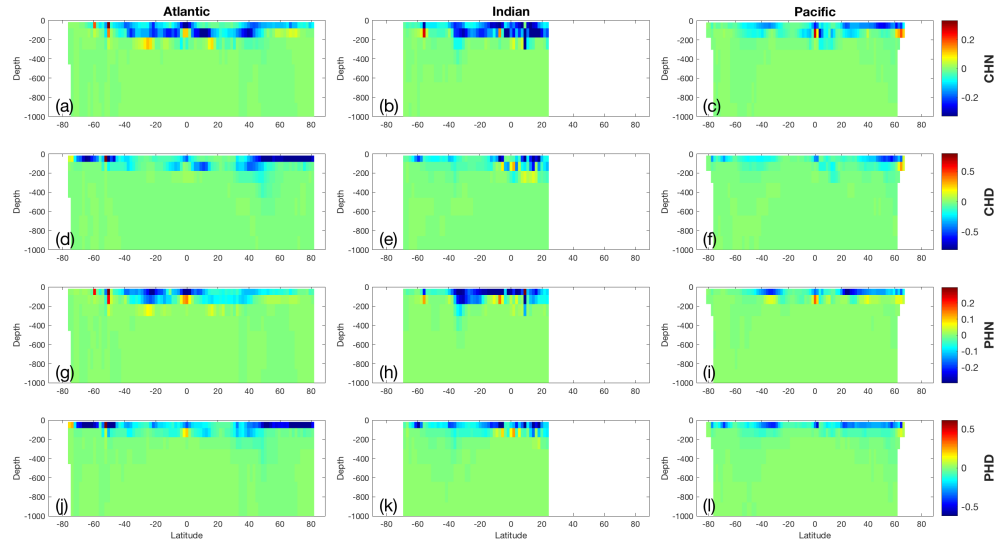


Figure 38: Change in volume-weighted zonally averaged (a-c) CHN, (d-f) CHD, (g-i) PHN, and (j-l) PHD after a +10% perturbation in xfastc, the excess organic carbon dissolution length scale, for the (left) Atlantic, (middle) Indian, and (right) Pacific Oceans.

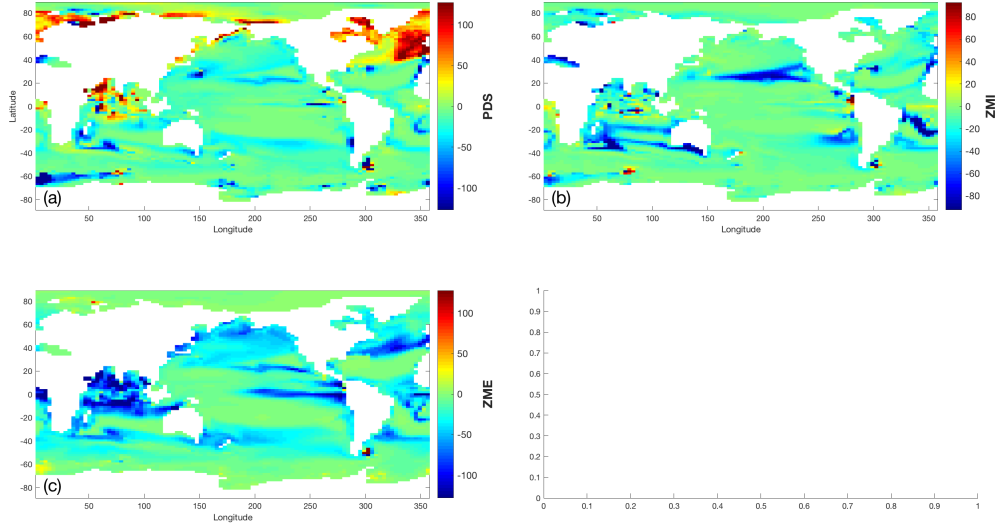


Figure 39: Change in column inventory of (a) PDS, (b) ZMI, and (c) ZME, after a +10% perturbation in xfastc, the excess organic carbon dissolution length scale.

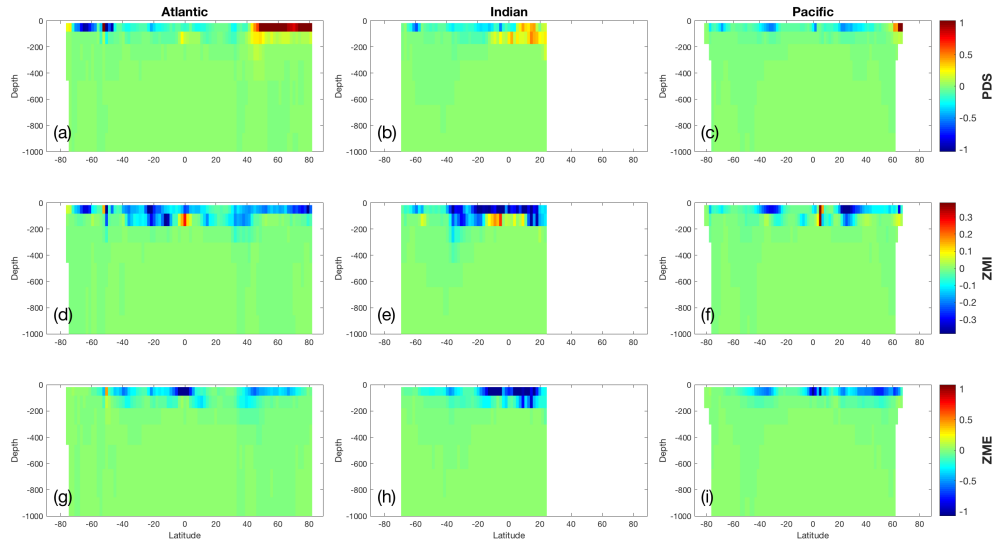


Figure 40: Change in volume-weighted zonally averaged (a-c) PDS, (d-f) ZMI, and (g-i) ZME after a +10% perturbation in xfastc, the excess organic carbon dissolution length scale, for the (left) Atlantic, (middle) Indian, and (right) Pacific Oceans.

- 7 Parameter `xfastca`: the calcium carbonate dissolution length scale.

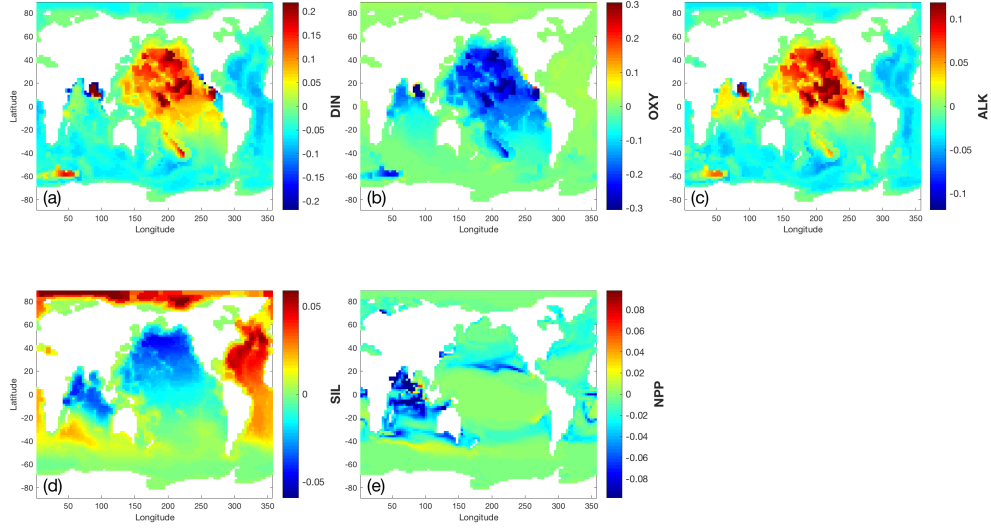


Figure 41: Change in column inventory of (a) DIN, (b) OXY, (c) ALK, (d) SIL, and (e) NPP after a +10% perturbation in x_{fastca} , the calcium carbonate dissolution length scale.

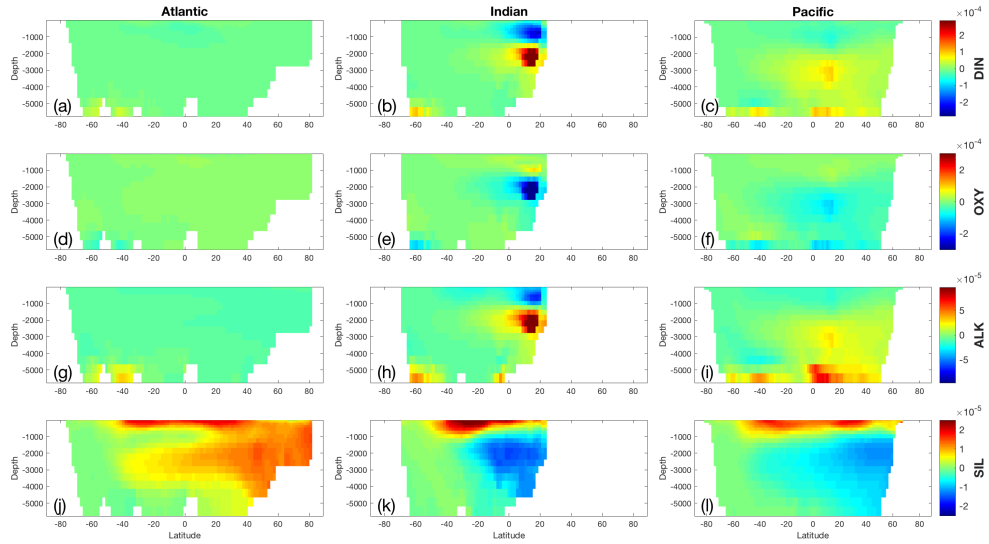


Figure 42: Change in volume-weighted zonally averaged (a-c) DIN, (d-f) OXY, (g-i) ALK, and (j-l) SIL after a +10% perturbation in x_{fastca} , the calcium carbonate dissolution length scale, for the (left) Atlantic, (middle) Indian, and (right) Pacific Oceans.

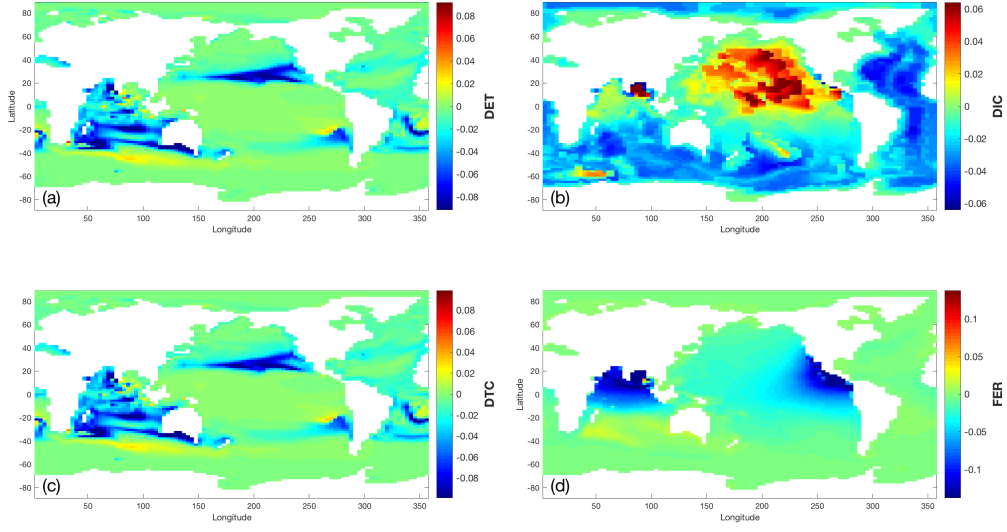


Figure 43: Change in column inventory of (a) DET, (b) DIC, (c) DTC, and (d) FER after a +10% perturbation in xfastca, the calcium carbonate dissolution length scale.

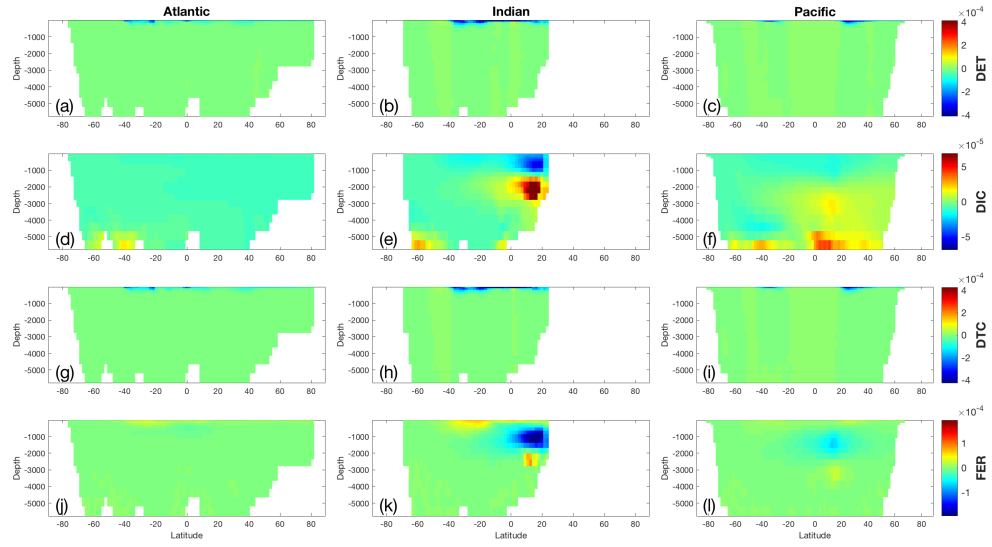


Figure 44: Change in volume-weighted zonally averaged (a-c) DET, (d-f) DIC, (g-i) DTC, and (j-l) FER after a +10% perturbation in xfastca, the calcium carbonate dissolution length scale, for the (left) Atlantic, (middle) Indian, and (right) Pacific Oceans.

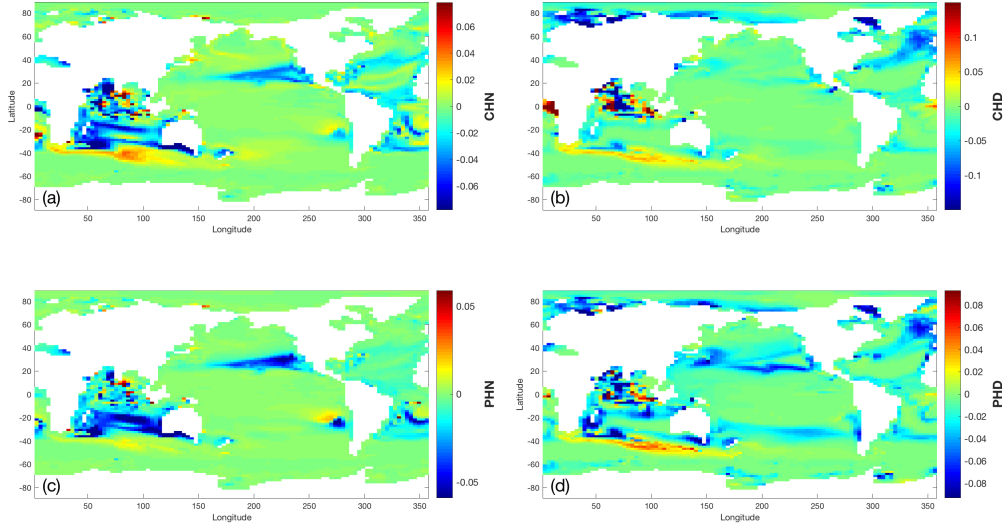


Figure 45: Change in column inventory of (a) CHN, (b) CHD, (c) PHN, and (d) PHD. after a +10% perturbation in x_{fastca} , the calcium carbonate dissolution length scale.

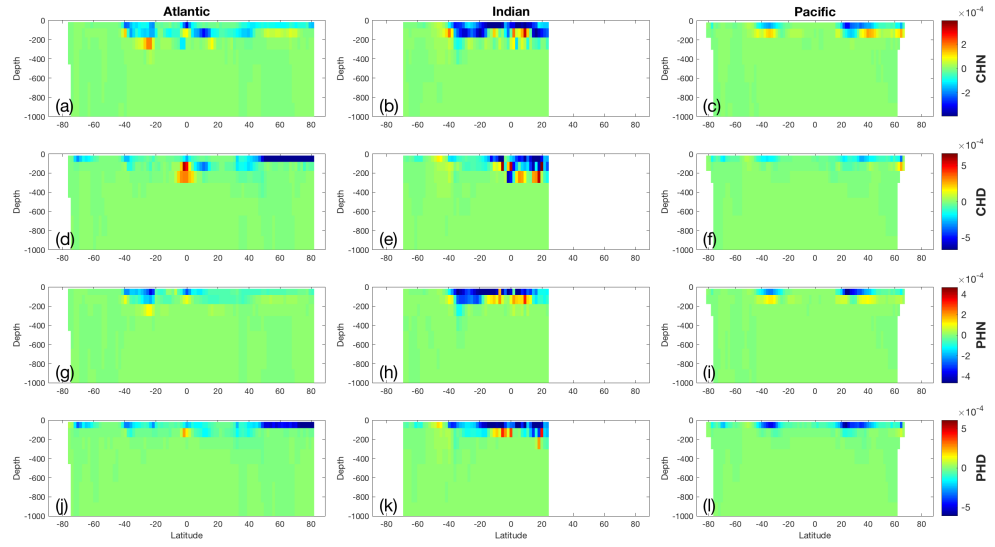


Figure 46: Change in volume-weighted zonally averaged (a-c) CHN, (d-f) CHD, (g-i) PHN, and (j-l) PHD after a +10% perturbation in x_{fastca} , the calcium carbonate dissolution length scale, for the (left) Atlantic, (middle) Indian, and (right) Pacific Oceans.

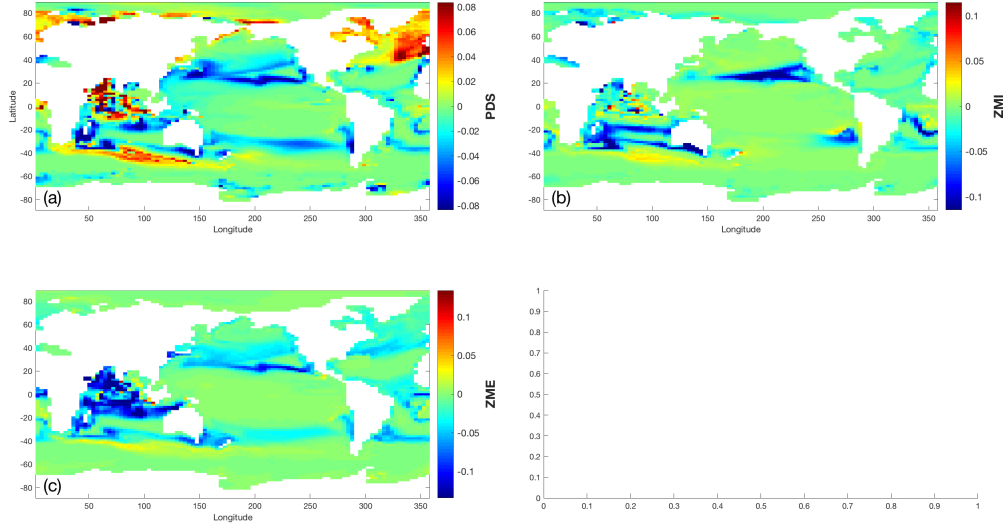


Figure 47: Change in column inventory of (a) PDS, (b) ZMI, and (c) ZME, after a +10% perturbation in *xfastca*, the calcium carbonate dissolution length scale.

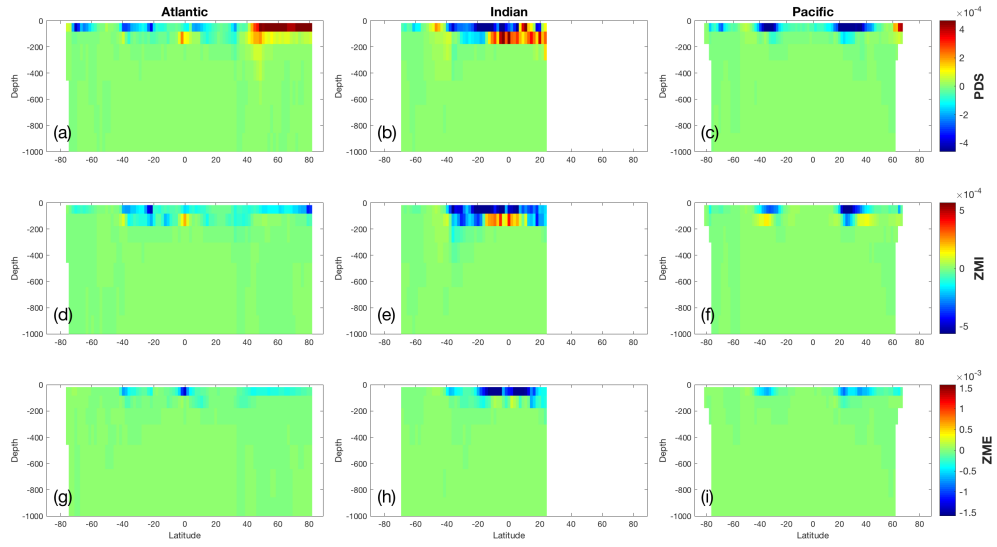


Figure 48: Change in volume-weighted zonally averaged (a-c) PDS, (d-f) ZMI, and (g-i) ZME after a +10% perturbation in *xfastca*, the calcium carbonate dissolution length scale, for the (left) Atlantic, (middle) Indian, and (right) Pacific Oceans.

- 8 Parameter `xfastsi`: the biogenic silicon dissolution length scale.

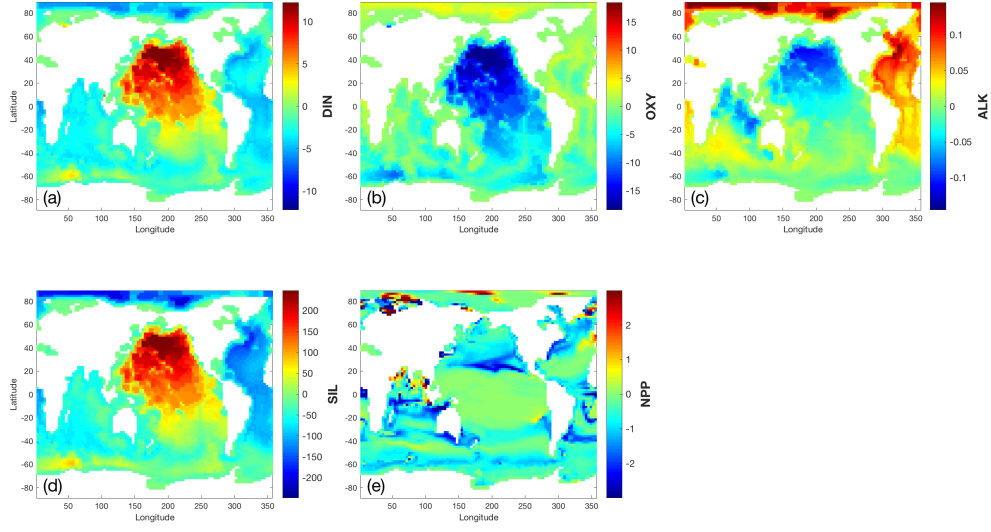


Figure 49: Change in column inventory of (a) DIN, (b) OXY, (c) ALK, (d) SIL, and (e) NPP after a +10% perturbation in x_{fastsi} , the biogenic silicon dissolution length scale.

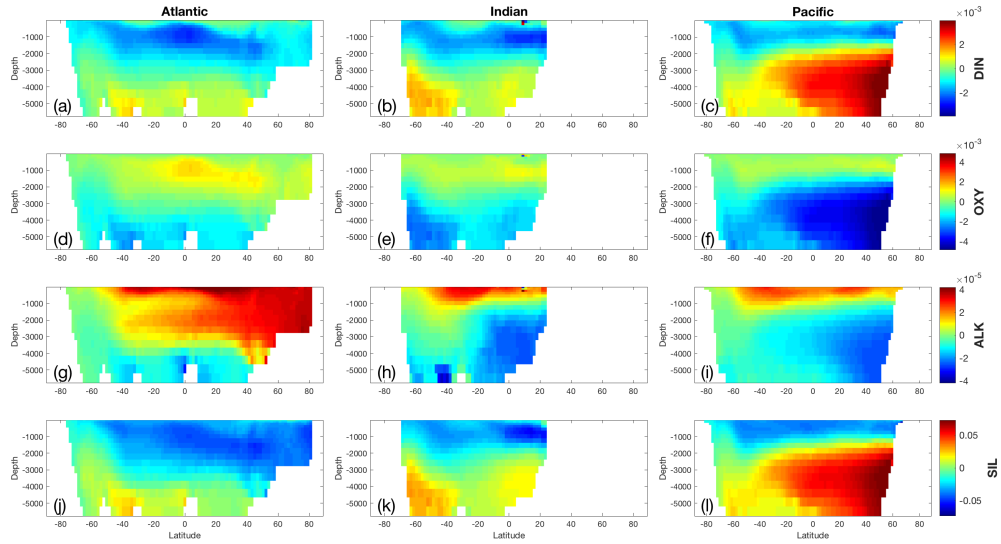


Figure 50: Change in volume-weighted zonally averaged (a-c) DIN, (d-f) OXY, (g-i) ALK, and (j-l) SIL after a +10% perturbation in x_{fastsi} , the biogenic silicon dissolution length scale, for the (left) Atlantic, (middle) Indian, and (right) Pacific Oceans.

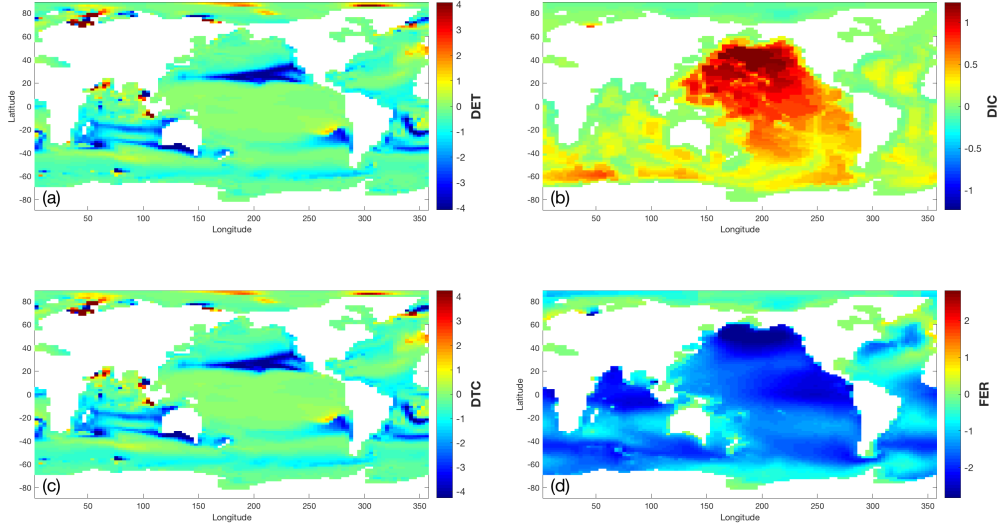


Figure 51: Change in column inventory of (a) DET, (b) DIC, (c) DTC, and (d) FER after a +10% perturbation in x_{fastsi} , the biogenic silicon dissolution length scale.

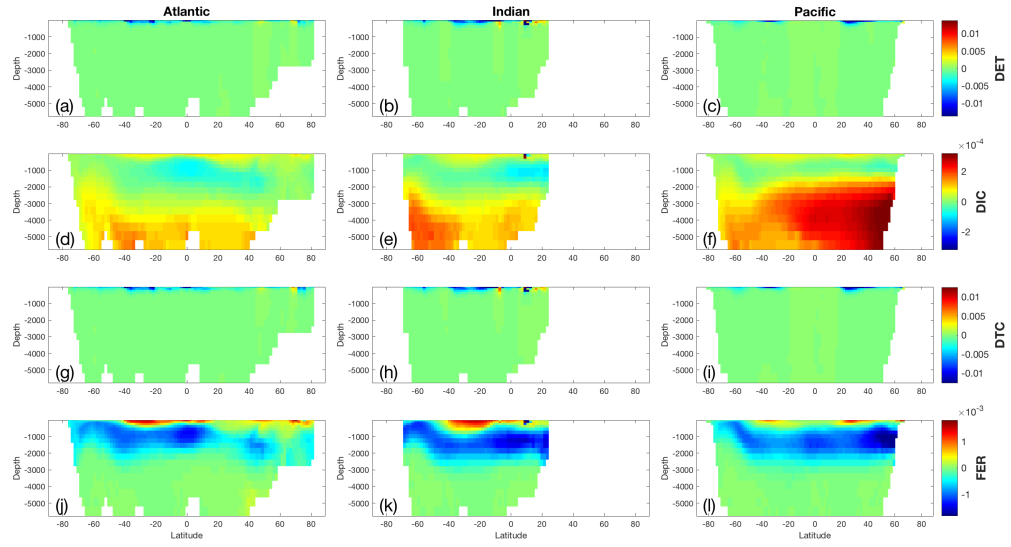


Figure 52: Change in volume-weighted zonally averaged (a-c) DET, (d-f) DIC, (g-i) DTC, and (j-l) FER after a +10% perturbation in x_{fastsi} , the biogenic silicon dissolution length scale, for the (left) Atlantic, (middle) Indian, and (right) Pacific Oceans.

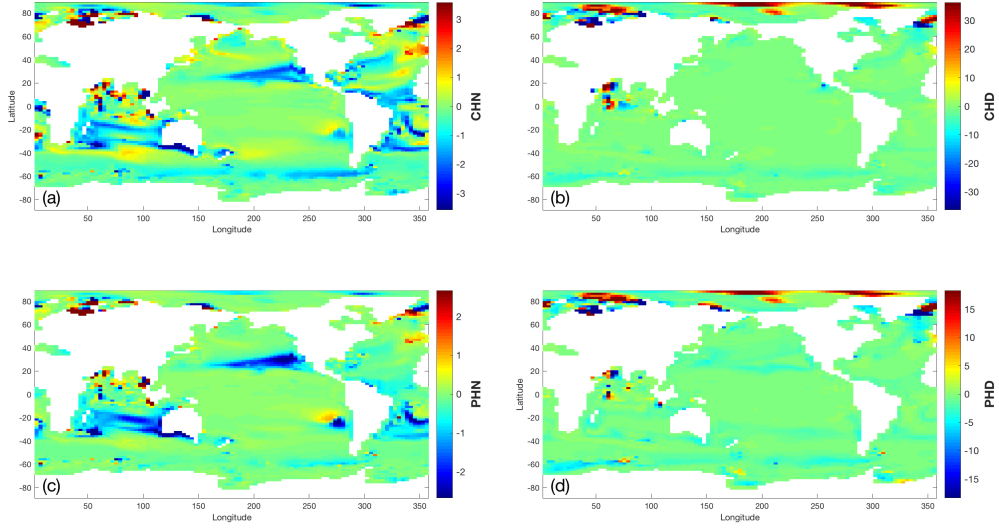


Figure 53: Change in column inventory of (a) CHN, (b) CHD, (c) PHN, and (d) PHD. after a +10% perturbation in xfastsi, the biogenic silicon dissolution length scale.

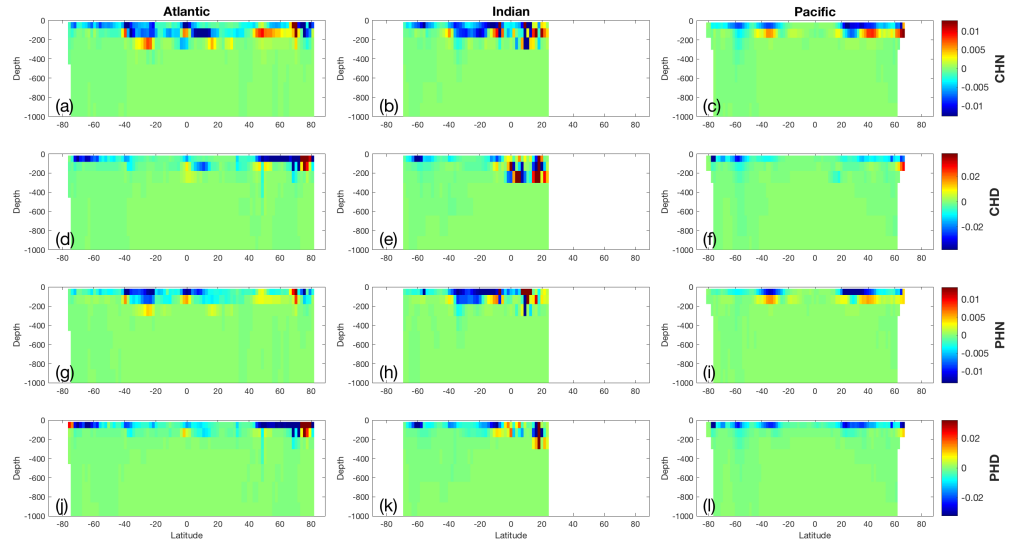


Figure 54: Change in volume-weighted zonally averaged (a-c) CHN, (d-f) CHD, (g-i) PHN, and (j-l) PHD after a +10% perturbation in xfastsi, the biogenic silicon dissolution length scale, for the (left) Atlantic, (middle) Indian, and (right) Pacific Oceans.

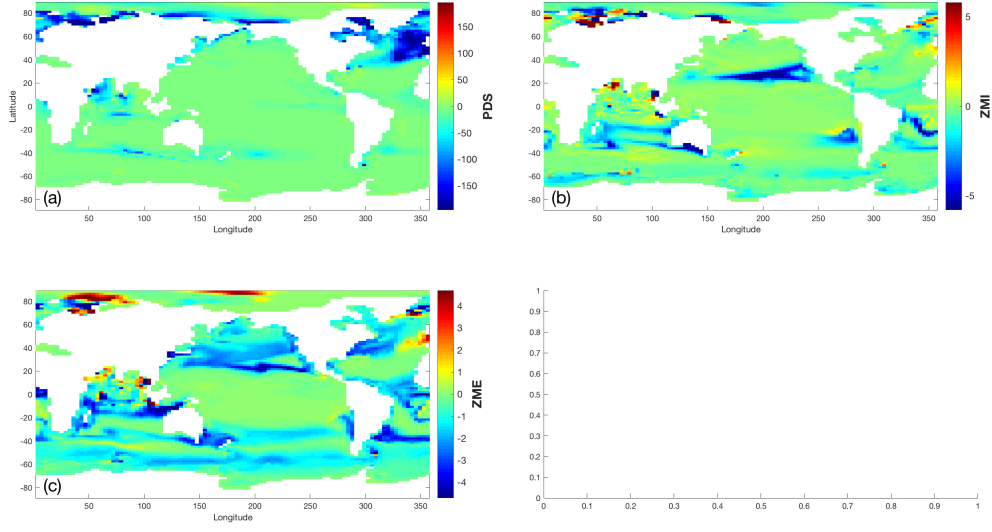


Figure 55: Change in column inventory of (a) PDS, (b) ZMI, and (c) ZME, after a +10% perturbation in xfastsi, the biogenic silicon dissolution length scale.

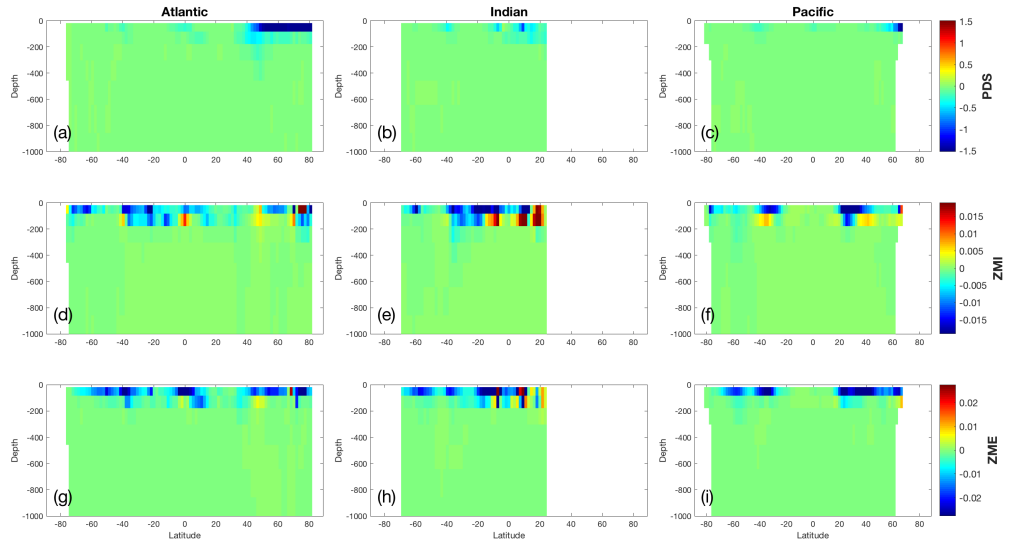


Figure 56: Change in volume-weighted zonally averaged (a-c) PDS, (d-f) ZMI, and (g-i) ZME after a +10% perturbation in xfastsi, the biogenic silicon dissolution length scale, for the (left) Atlantic, (middle) Indian, and (right) Pacific Oceans.

- 9 Parameter `xfrac1`: the fast-sinking fraction of diatom natural mortality losses.

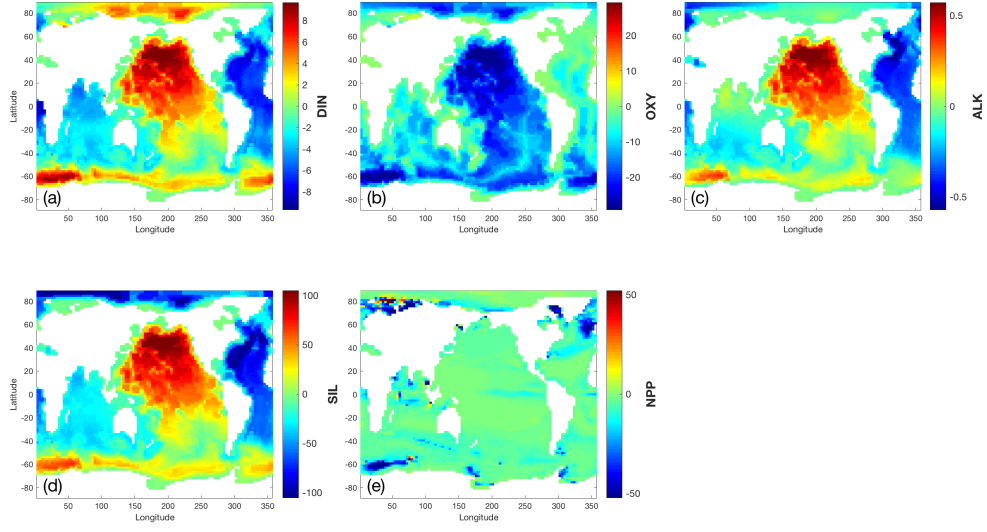


Figure 57: Change in column inventory of (a) DIN, (b) OXY, (c) ALK, (d) SIL, and (e) NPP after a +10% perturbation in xfdfrac1 , the fast-sinking fraction of diatom natural mortality losses.

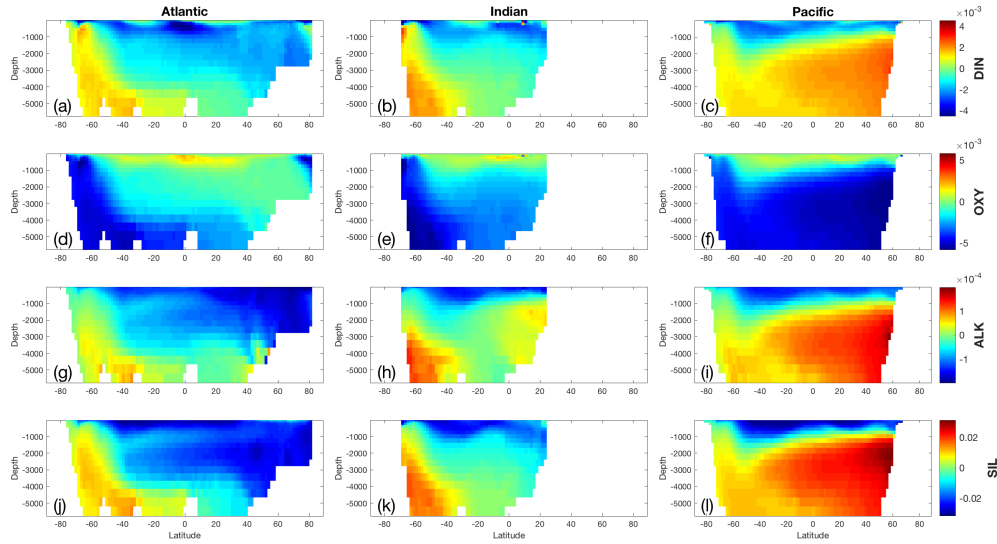


Figure 58: Change in volume-weighted zonally averaged (a-c) DIN, (d-f) OXY, (g-i) ALK, and (j-l) SIL after a +10% perturbation in xfdfrac1 , the fast-sinking fraction of diatom natural mortality losses, for the (left) Atlantic, (middle) Indian, and (right) Pacific Oceans.

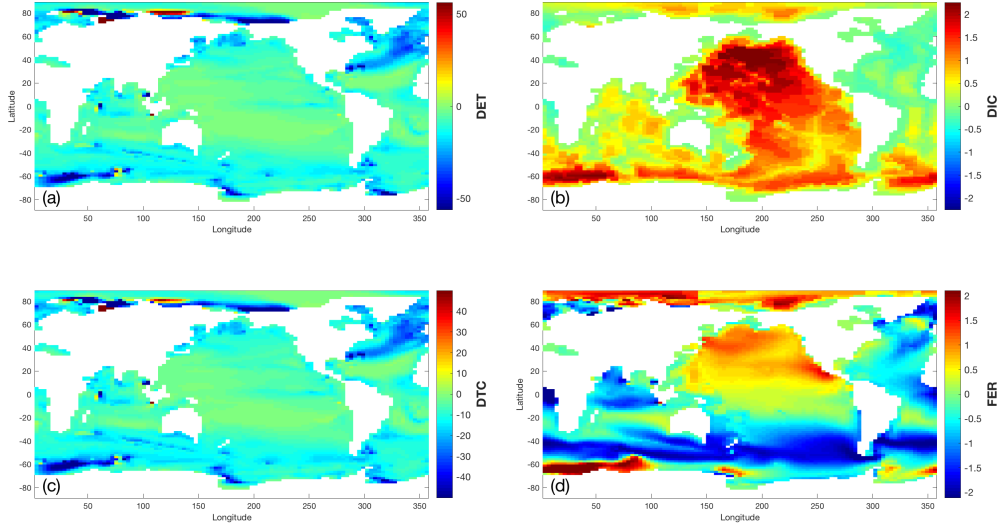


Figure 59: Change in column inventory of (a) DET, (b) DIC, (c) DTC, and (d) FER after a +10% perturbation in $x_{fdfrac1}$, the fast-sinking fraction of diatom natural mortality losses.

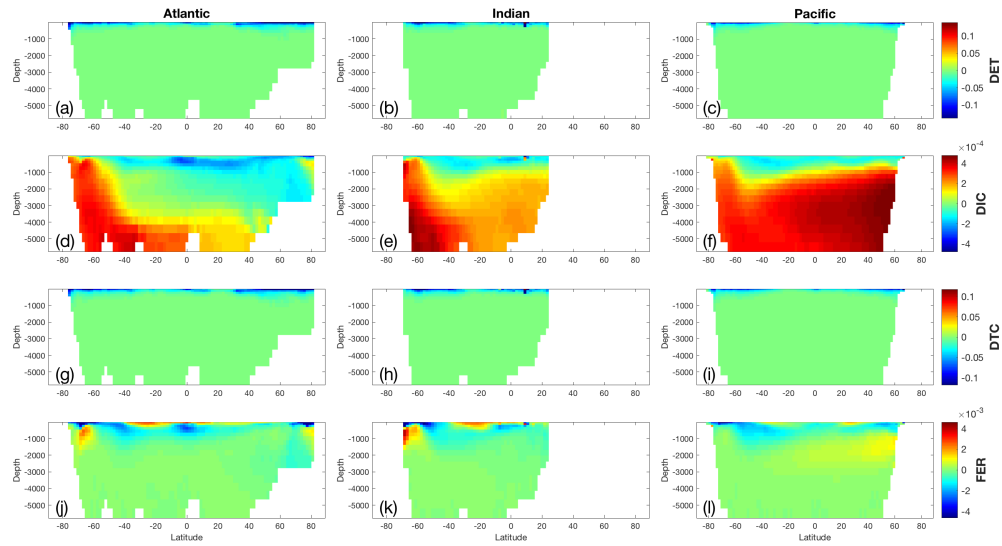


Figure 60: Change in volume-weighted zonally averaged (a-c) DET, (d-f) DIC, (g-i) DTC, and (j-l) FER after a +10% perturbation in $x_{fdfrac1}$, the fast-sinking fraction of diatom natural mortality losses, for the (left) Atlantic, (middle) Indian, and (right) Pacific Oceans.

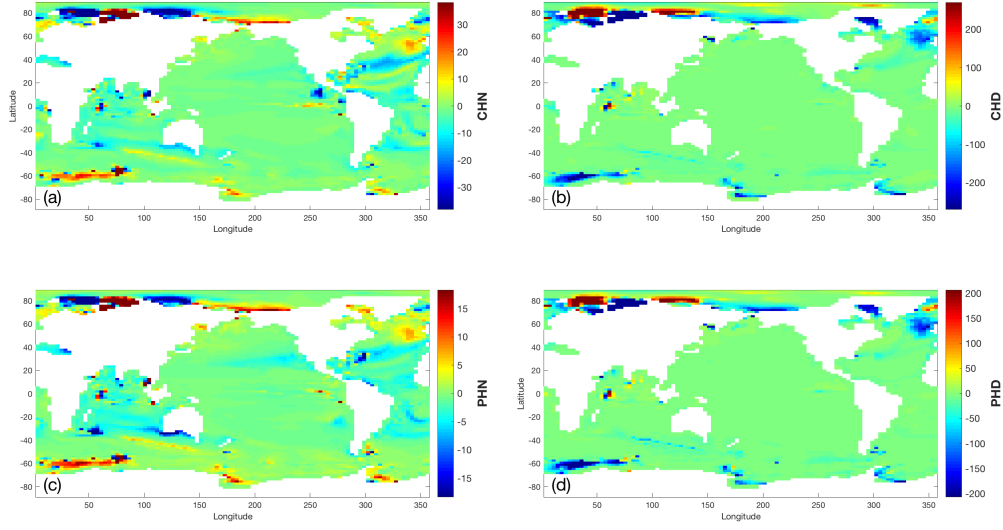


Figure 61: Change in column inventory of (a) CHN, (b) CHD, (c) PHN, and (d) PHD after a +10% perturbation in $xfdfraction1$, the fast-sinking fraction of diatom natural mortality losses.

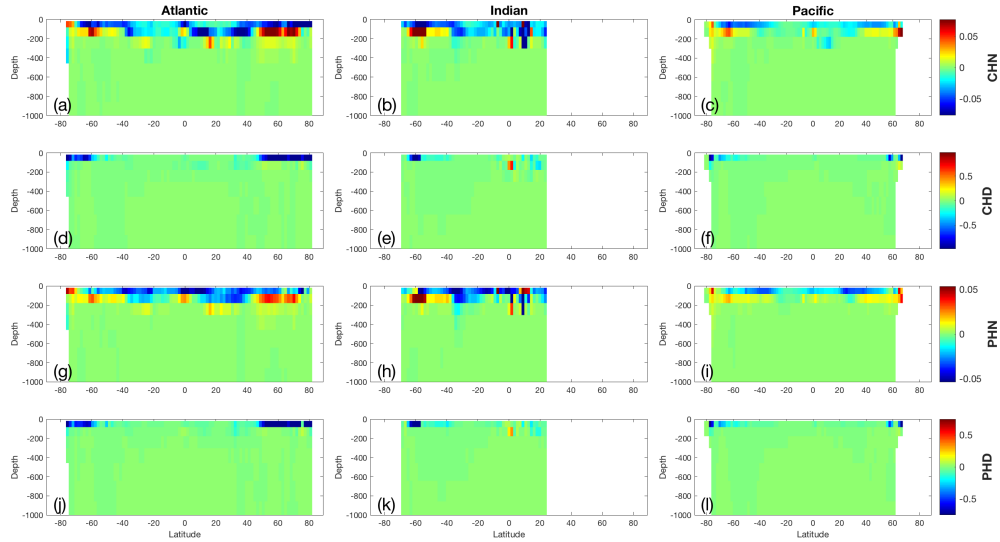


Figure 62: Change in volume-weighted zonally averaged (a-c) CHN, (d-f) CHD, (g-i) PHN, and (j-l) PHD after a +10% perturbation in $xfdfraction1$, the fast-sinking fraction of diatom natural mortality losses, for the (left) Atlantic, (middle) Indian, and (right) Pacific Oceans.

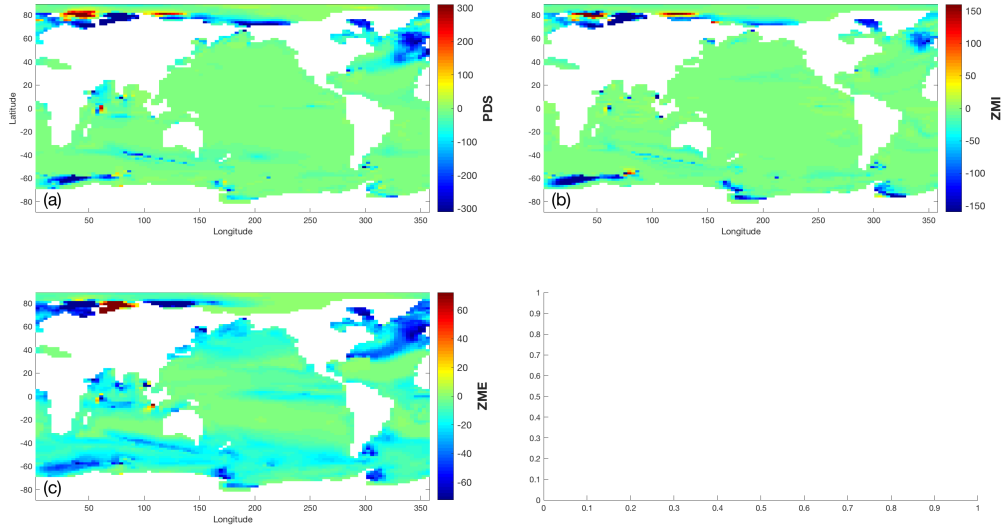


Figure 63: Change in column inventory of (a) PDS, (b) ZMI, and (c) ZME, after a +10% perturbation in $x_{fdfrac1}$, the fast-sinking fraction of diatom natural mortality losses.

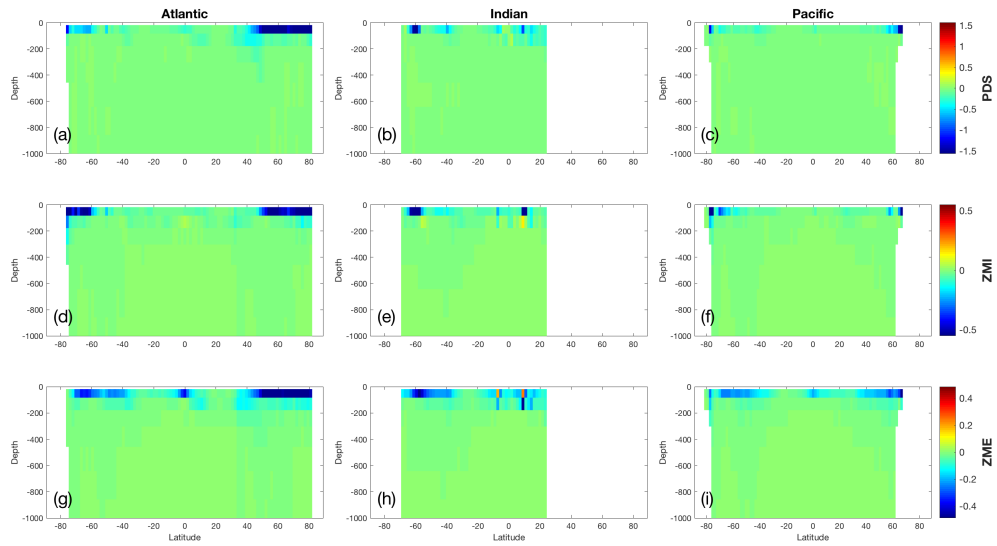


Figure 64: Change in volume-weighted zonally averaged (a-c) PDS, (d-f) ZMI, and (g-i) ZME after a +10% perturbation in $x_{fdfrac1}$, the fast-sinking fraction of diatom natural mortality losses, for the (left) Atlantic, (middle) Indian, and (right) Pacific Oceans.

- 10 Parameter `xfdfrac2`: the fast-sinking fraction of meso-zooplankton mortality losses.

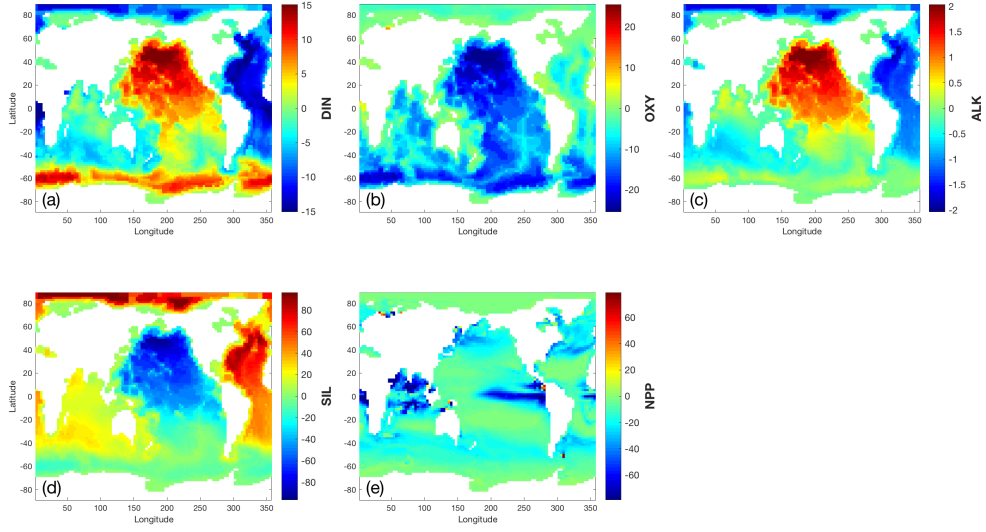


Figure 65: Change in column inventory of (a) DIN, (b) OXY, (c) ALK, (d) SIL, and (e) NPP after a +10% perturbation in xfdfrac2, the fast-sinking fraction of meso-zooplankton mortality losses.

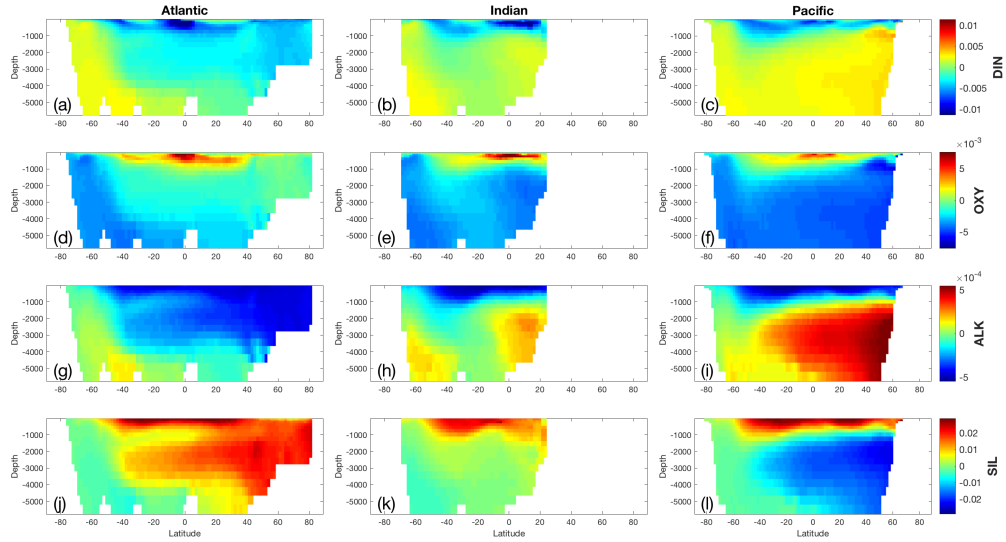


Figure 66: Change in volume-weighted zonally averaged (a-c) DIN, (d-f) OXY, (g-i) ALK, and (j-l) SIL after a +10% perturbation in xfdfrac2, the fast-sinking fraction of meso-zooplankton mortality losses, for the (left) Atlantic, (middle) Indian, and (right) Pacific Oceans.

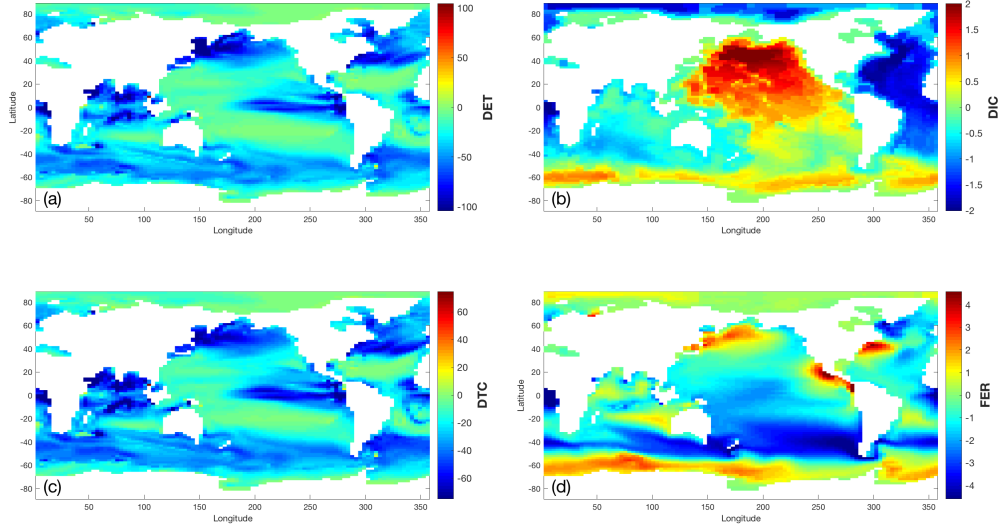


Figure 67: Change in column inventory of (a) DET, (b) DIC, (c) DTC, and (d) FER after a +10% perturbation in $x_{fdfrac2}$, the fast-sinking fraction of meso-zooplankton mortality losses.

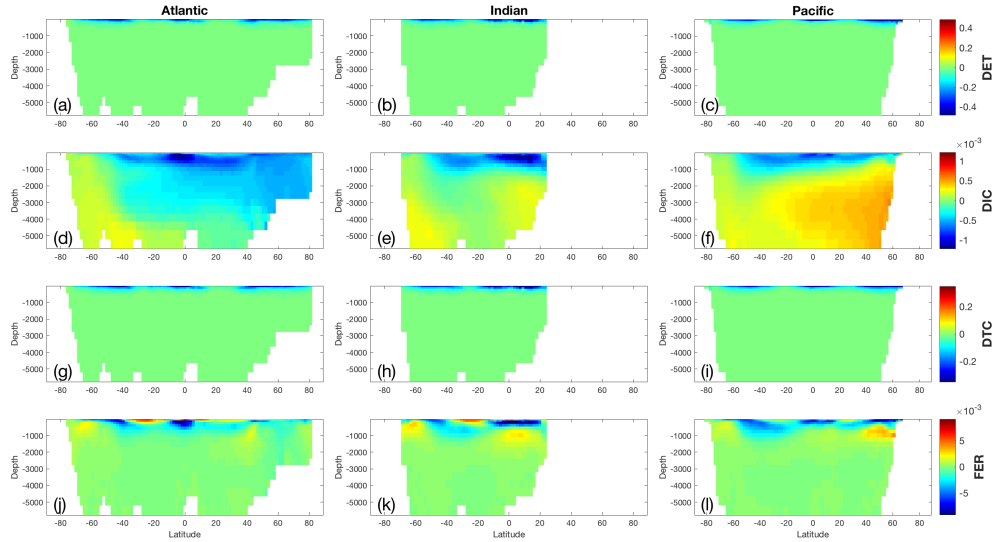


Figure 68: Change in volume-weighted zonally averaged (a-c) DET, (d-f) DIC, (g-i) DTC, and (j-l) FER after a +10% perturbation in $x_{fdfrac2}$, the fast-sinking fraction of meso-zooplankton mortality losses, for the (left) Atlantic, (middle) Indian, and (right) Pacific Oceans.

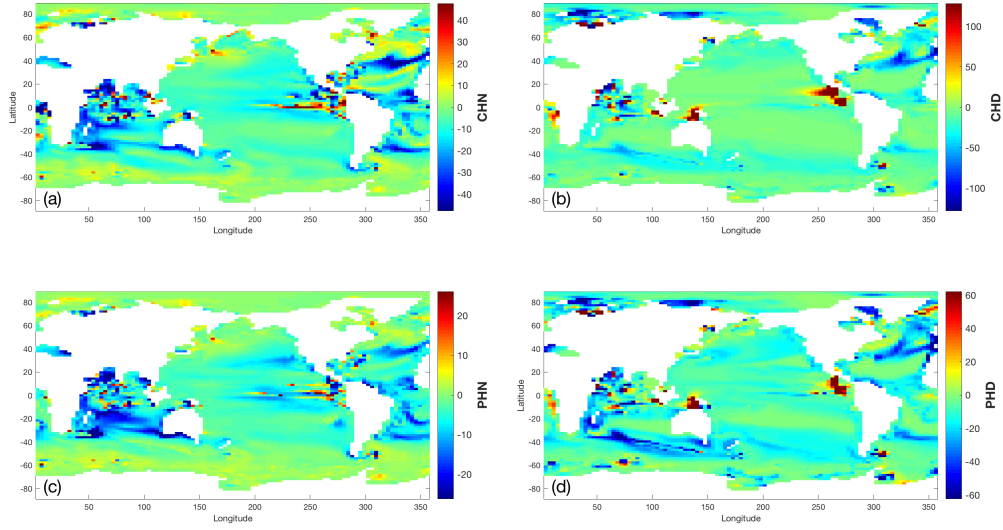


Figure 69: Change in column inventory of (a) CHN, (b) CHD, (c) PHN, and (d) PHD. after a +10% perturbation in $x_{fdfrac2}$, the fast-sinking fraction of meso-zooplankton mortality losses.

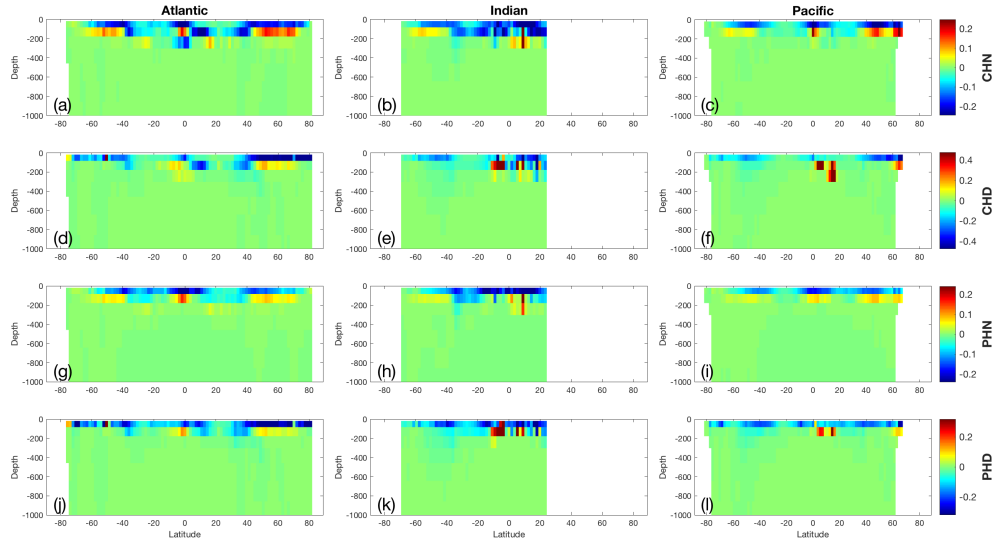


Figure 70: Change in volume-weighted zonally averaged (a-c) CHN, (d-f) CHD, (g-i) PHN, and (j-l) PHD after a +10% perturbation in $x_{fdfrac2}$, the fast-sinking fraction of meso-zooplankton mortality losses, for the (left) Atlantic, (middle) Indian, and (right) Pacific Oceans.

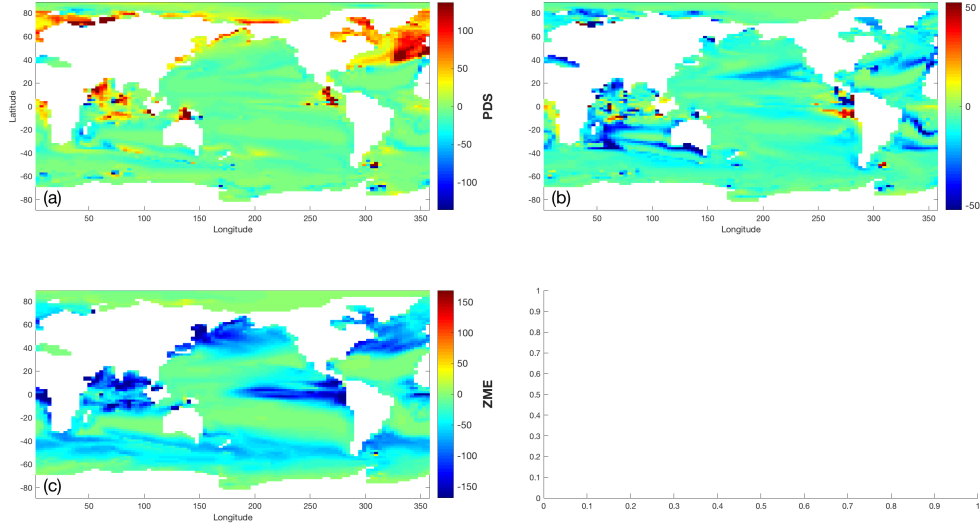


Figure 71: Change in column inventory of (a) PDS, (b) ZMI, and (c) ZME, after a +10% perturbation in x_{df}^{frac2} , the fast-sinking fraction of meso-zooplankton mortality losses.

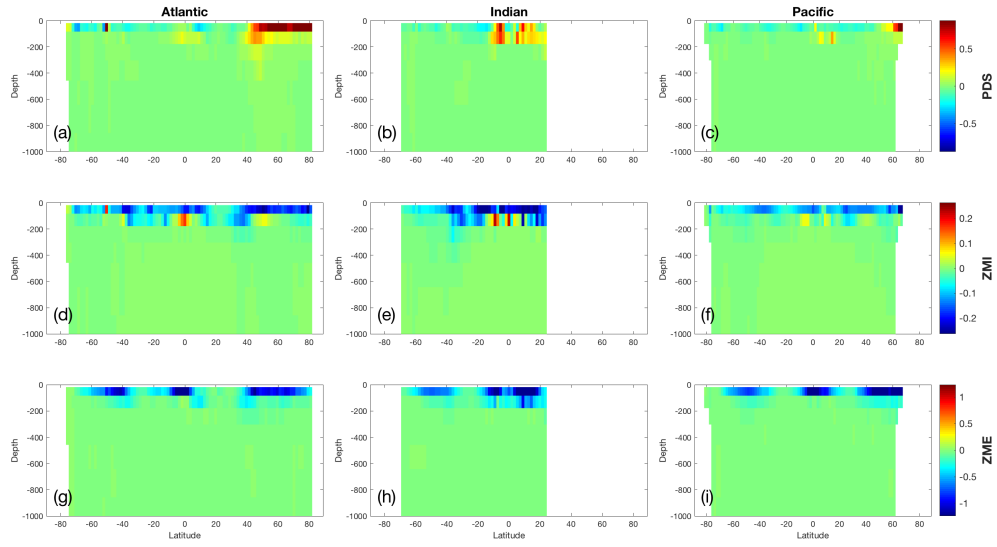


Figure 72: Change in volume-weighted zonally averaged (a-c) PDS, (d-f) ZMI, and (g-i) ZME after a +10% perturbation in x_{df}^{frac2} , the fast-sinking fraction of meso-zooplankton mortality losses, for the (left) Atlantic, (middle) Indian, and (right) Pacific Oceans.

- 11 Parameter `xdffrac3`: the fast-sinking fraction of diatom silicon grazing losses.

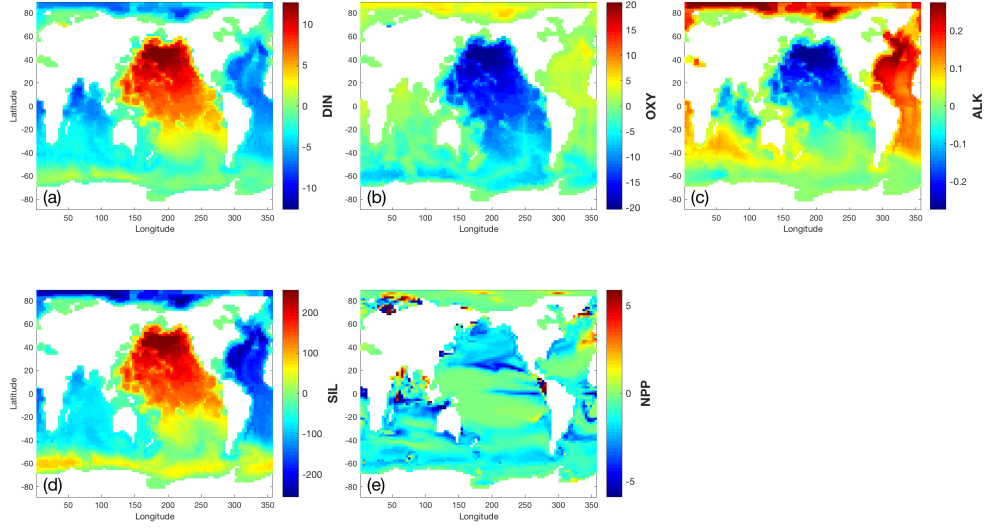


Figure 73: Change in column inventory of (a) DIN, (b) OXY, (c) ALK, (d) SIL, and (e) NPP after a +10% perturbation in xfdfrac3 , the fast-sinking fraction of diatom silicon grazing losses.

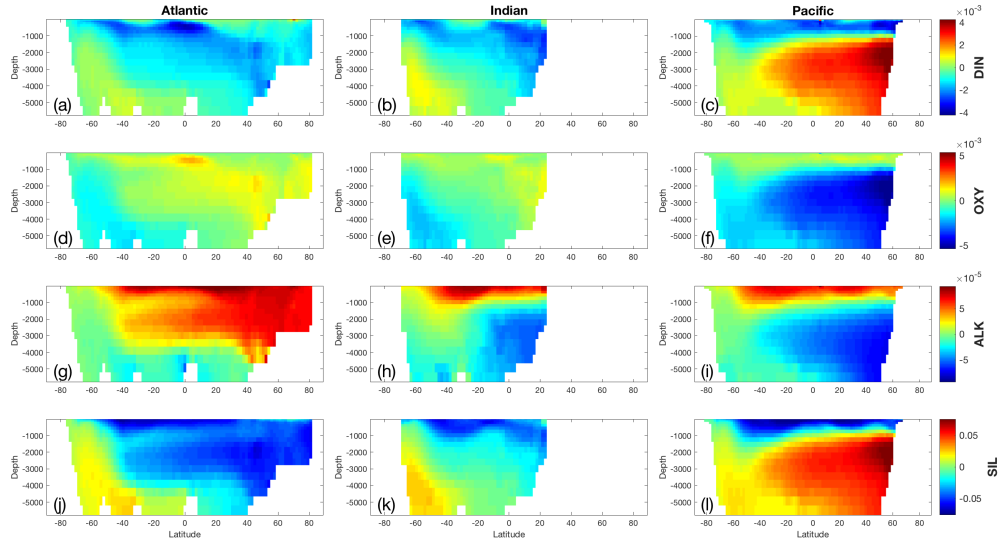


Figure 74: Change in volume-weighted zonally averaged (a-c) DIN, (d-f) OXY, (g-i) ALK, and (j-l) SIL after a +10% perturbation in xfdfrac3 , the fast-sinking fraction of diatom silicon grazing losses, for the (left) Atlantic, (middle) Indian, and (right) Pacific Oceans.

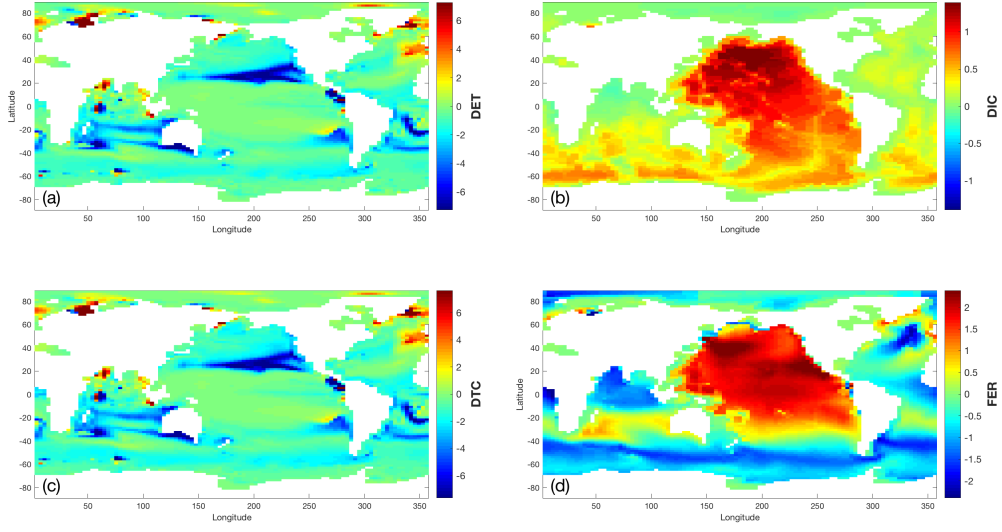


Figure 75: Change in column inventory of (a) DET, (b) DIC, (c) DTC, and (d) FER after a +10% perturbation in xfdfrac3, the fast-sinking fraction of diatom silicon grazing losses.

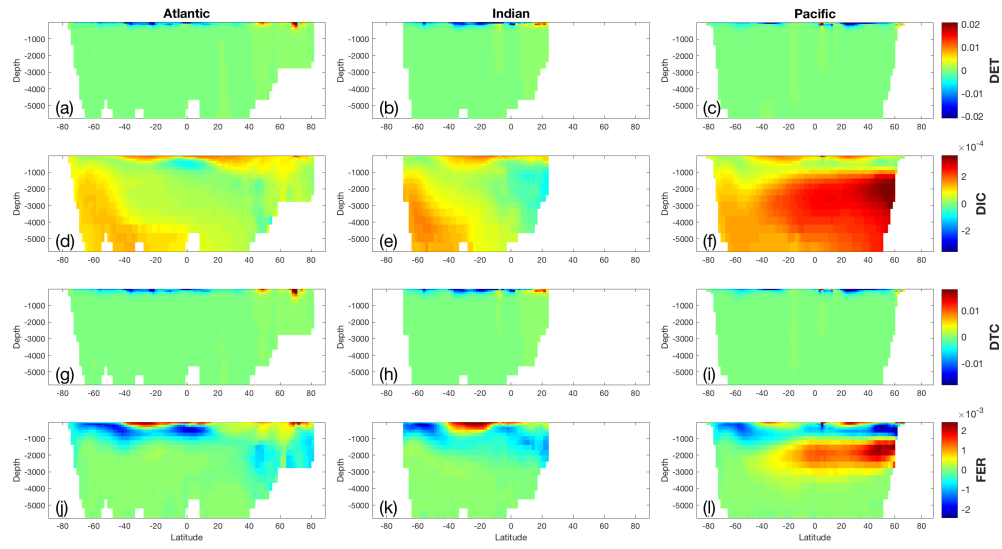


Figure 76: Change in volume-weighted zonally averaged (a-c) DET, (d-f) DIC, (g-i) DTC, and (j-l) FER after a +10% perturbation in xfdfrac3, the fast-sinking fraction of diatom silicon grazing losses, for the (left) Atlantic, (middle) Indian, and (right) Pacific Oceans.

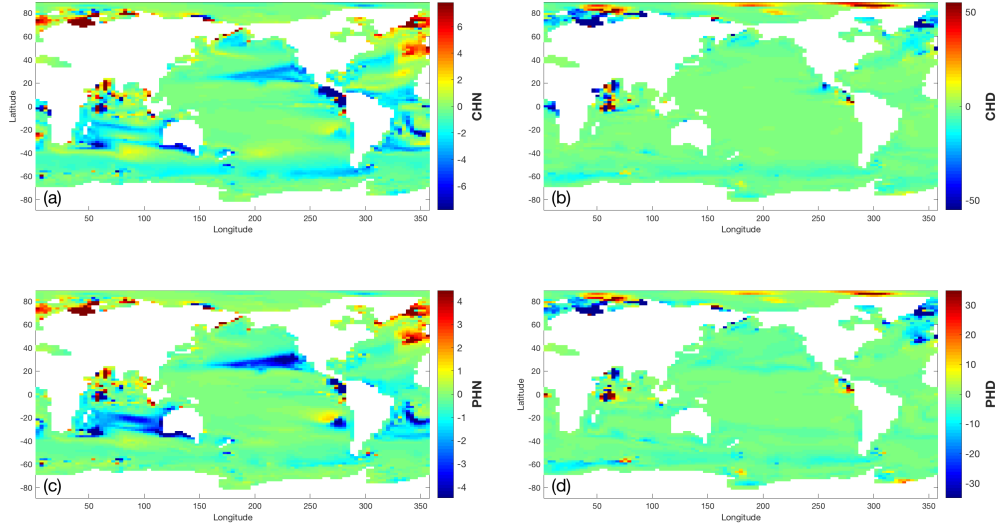


Figure 77: Change in column inventory of (a) CHN, (b) CHD, (c) PHN, and (d) PHD. after a +10% perturbation in $x_{fdfrac3}$, the fast-sinking fraction of diatom silicon grazing losses.

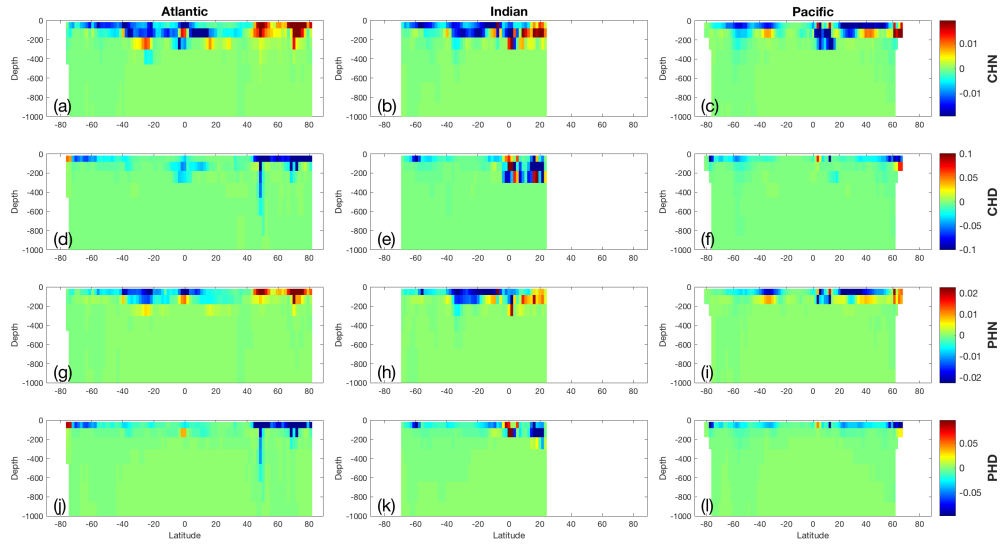


Figure 78: Change in volume-weighted zonally averaged (a-c) CHN, (d-f) CHD, (g-i) PHN, and (j-l) PHD after a +10% perturbation in $x_{fdfrac3}$, the fast-sinking fraction of diatom silicon grazing losses, for the (left) Atlantic, (middle) Indian, and (right) Pacific Oceans.

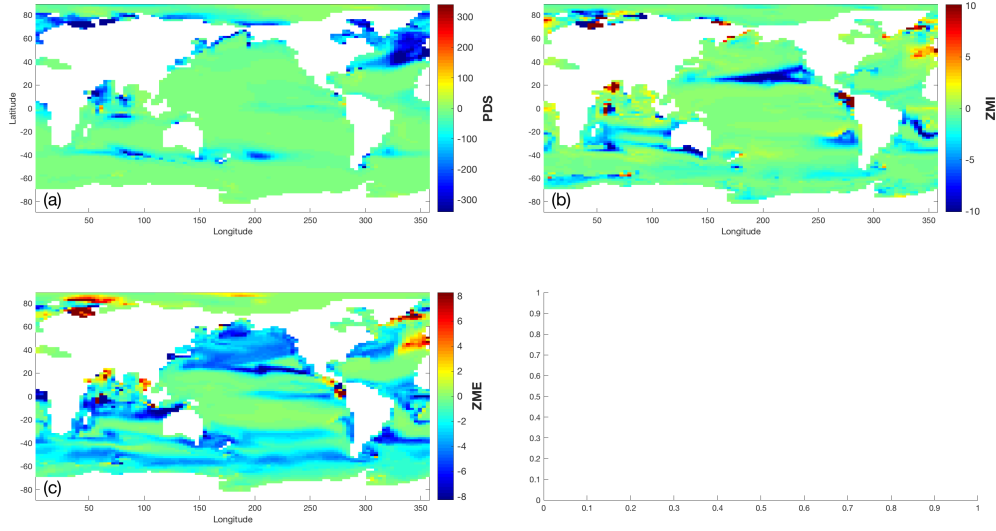


Figure 79: Change in column inventory of (a) PDS, (b) ZMI, and (c) ZME, after a +10% perturbation in xfdfraction , the fast-sinking fraction of diatom silicon grazing losses.

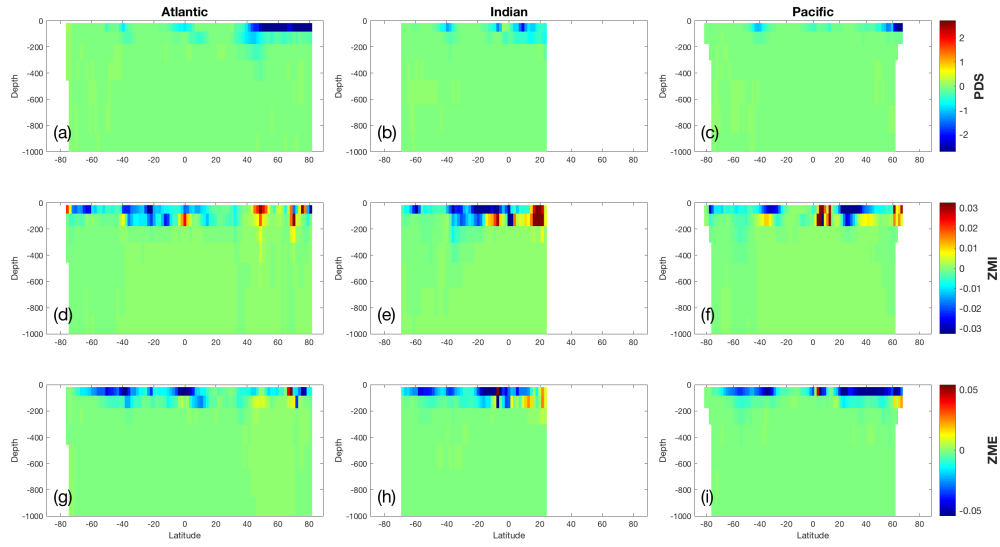


Figure 80: Change in volume-weighted zonally averaged (a-c) PDS, (d-f) ZMI, and (g-i) ZME after a +10% perturbation in xfdfraction , the fast-sinking fraction of diatom silicon grazing losses, for the (left) Atlantic, (middle) Indian, and (right) Pacific Oceans.

12 Parameter `xfld`: the diatom iron nutrient uptake half-saturation constant.

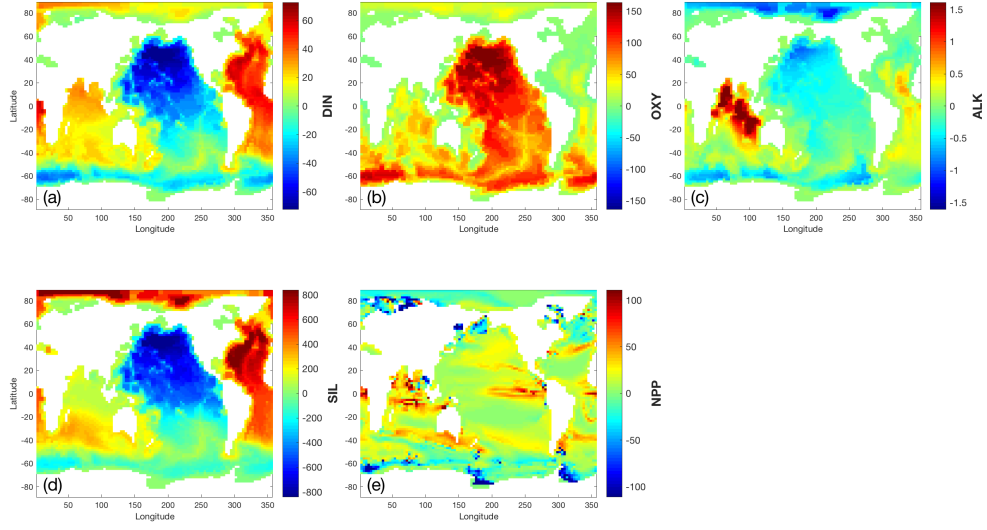


Figure 81: Change in column inventory of (a) DIN, (b) OXY, (c) ALK, (d) SIL, and (e) NPP after a +10% perturbation in x_{fld} , the diatom iron nutrient uptake half-saturation constant.

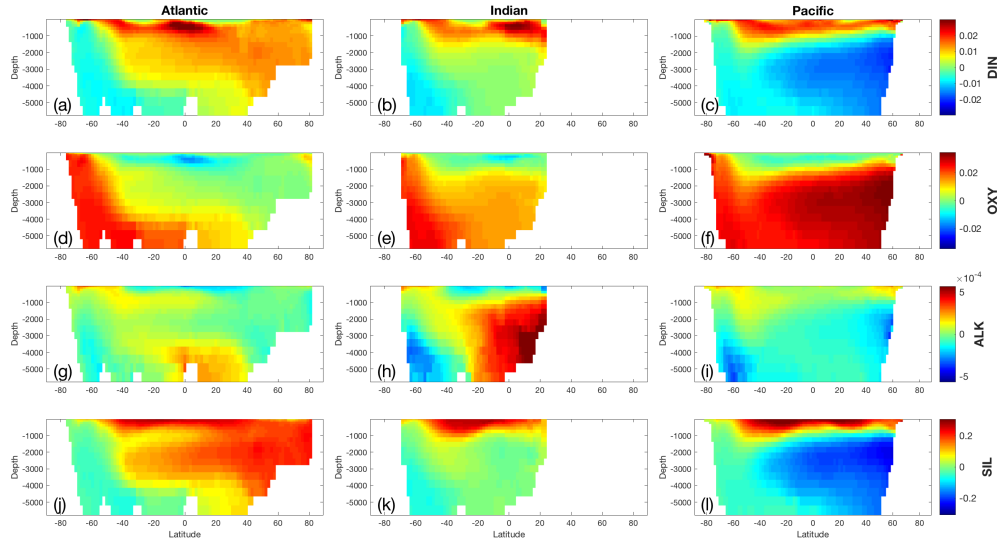


Figure 82: Change in volume-weighted zonally averaged (a-c) DIN, (d-f) OXY, (g-i) ALK, and (j-l) SIL after a +10% perturbation in x_{fld} , the diatom iron nutrient uptake half-saturation constant, for the (left) Atlantic, (middle) Indian, and (right) Pacific Oceans.

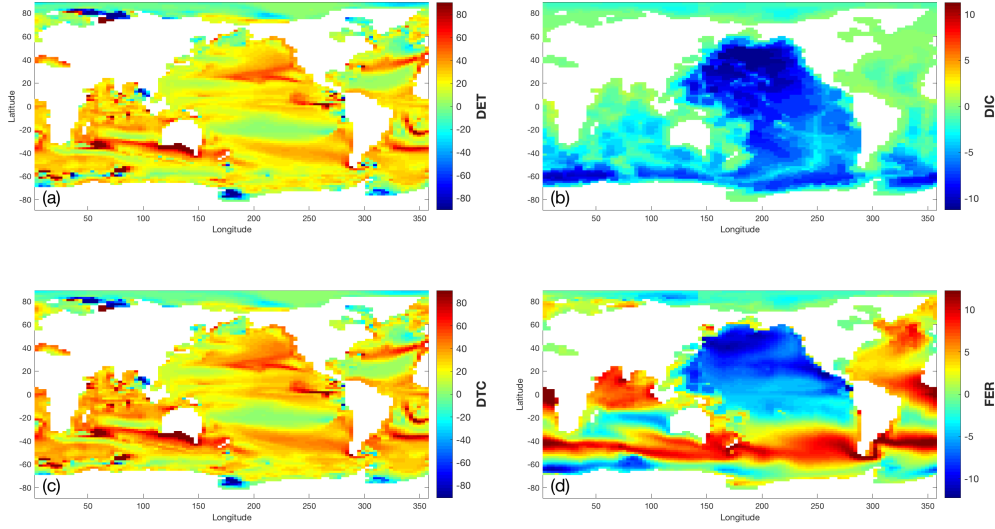


Figure 83: Change in column inventory of (a) DET, (b) DIC, (c) DTC, and (d) FER after a +10% perturbation in x_{fld} , the diatom iron nutrient uptake half-saturation constant.

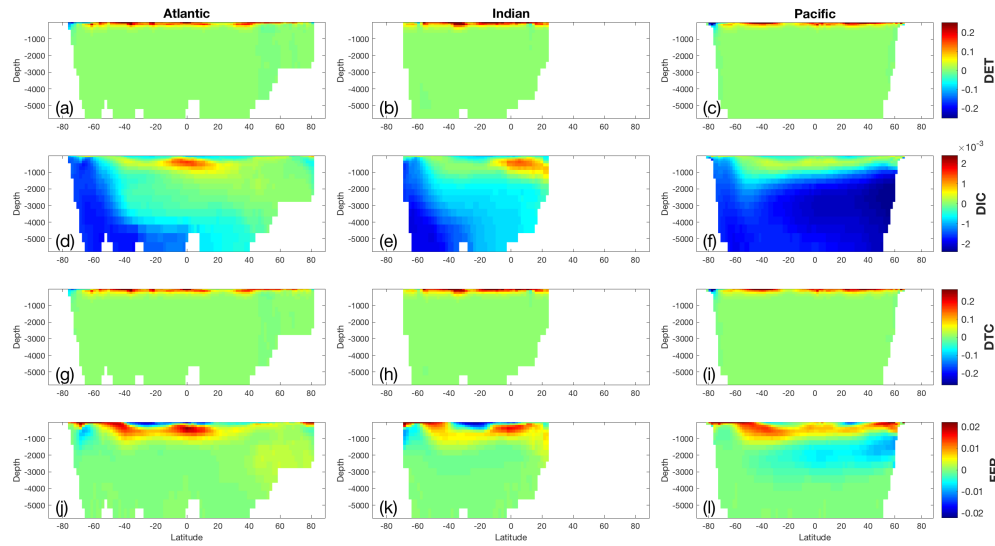


Figure 84: Change in volume-weighted zonally averaged (a-c) DET, (d-f) DIC, (g-i) DTC, and (j-l) FER after a +10% perturbation in x_{fld} , the diatom iron nutrient uptake half-saturation constant, for the (left) Atlantic, (middle) Indian, and (right) Pacific Oceans.

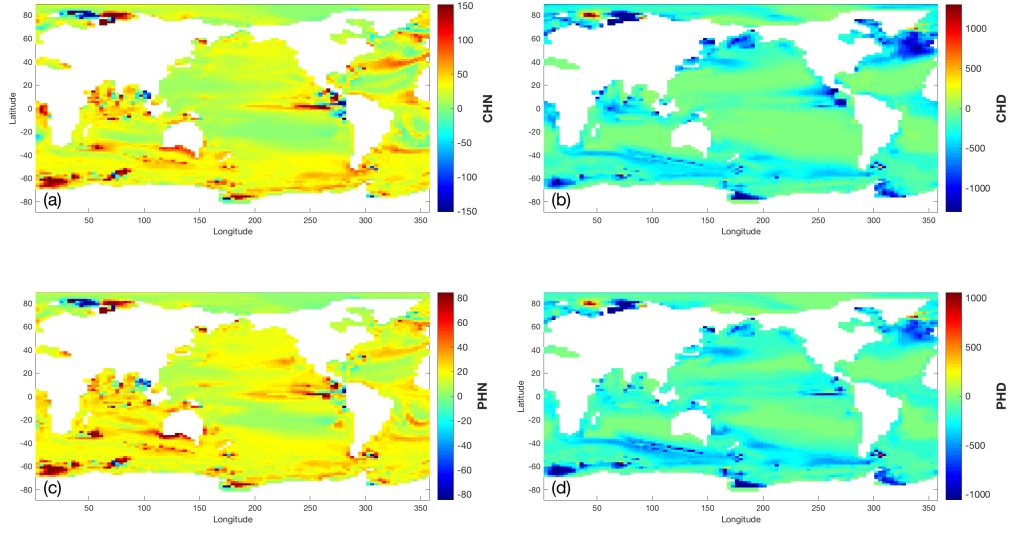


Figure 85: Change in column inventory of (a) CHN, (b) CHD, (c) PHN, and (d) PHD. after a +10% perturbation in x_{fld} , the diatom iron nutrient uptake half-saturation constant.

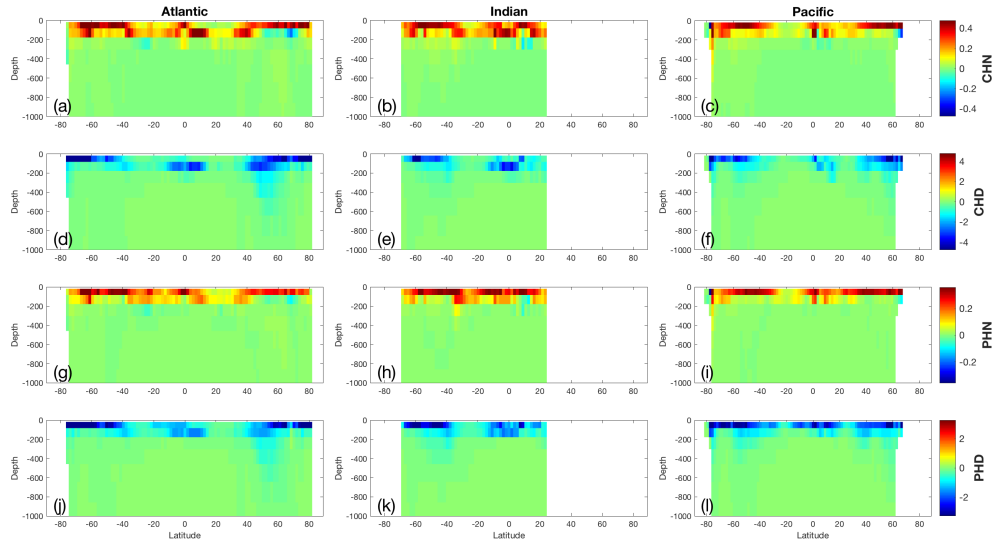


Figure 86: Change in volume-weighted zonally averaged (a-c) CHN, (d-f) CHD, (g-i) PHN, and (j-l) PHD after a +10% perturbation in x_{fld} , the diatom iron nutrient uptake half-saturation constant, for the (left) Atlantic, (middle) Indian, and (right) Pacific Oceans.

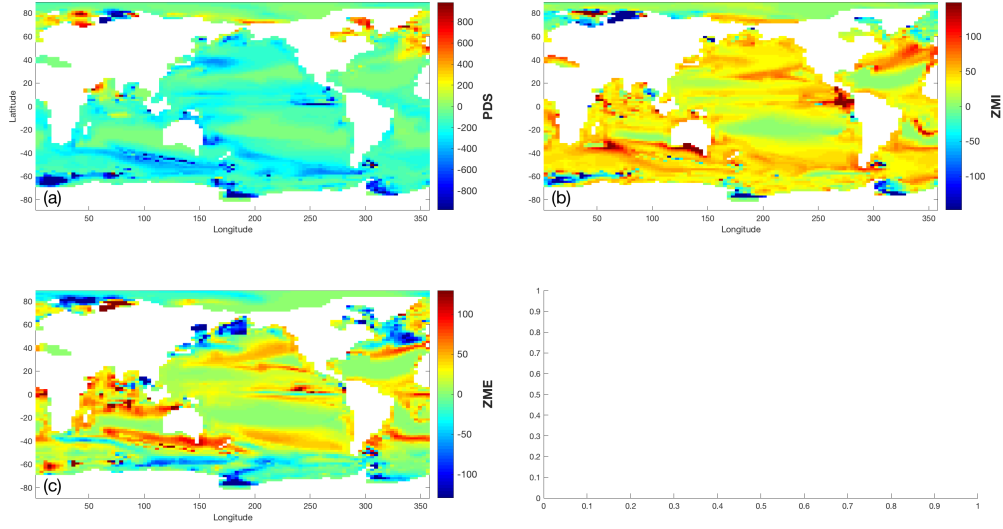


Figure 87: Change in column inventory of (a) PDS, (b) ZMI, and (c) ZME, after a +10% perturbation in x_{fd} , the diatom iron nutrient uptake half-saturation constant.

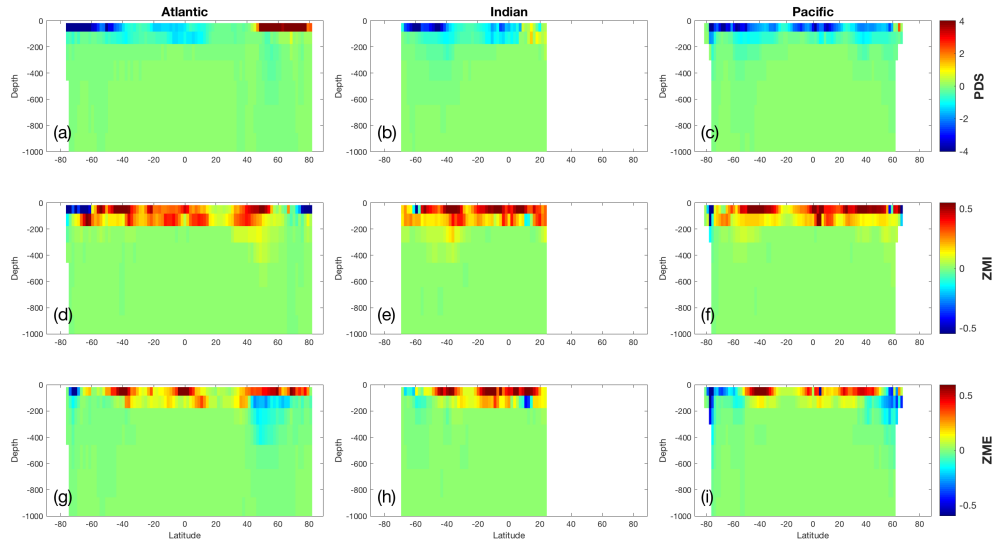


Figure 88: Change in volume-weighted zonally averaged (a-c) PDS, (d-f) ZMI, and (g-i) ZME after a +10% perturbation in x_{fd} , the diatom iron nutrient uptake half-saturation constant, for the (left) Atlantic, (middle) Indian, and (right) Pacific Oceans.

- 13 Parameter `xfln`: the non-diatom iron nutrient uptake half-saturation constant.

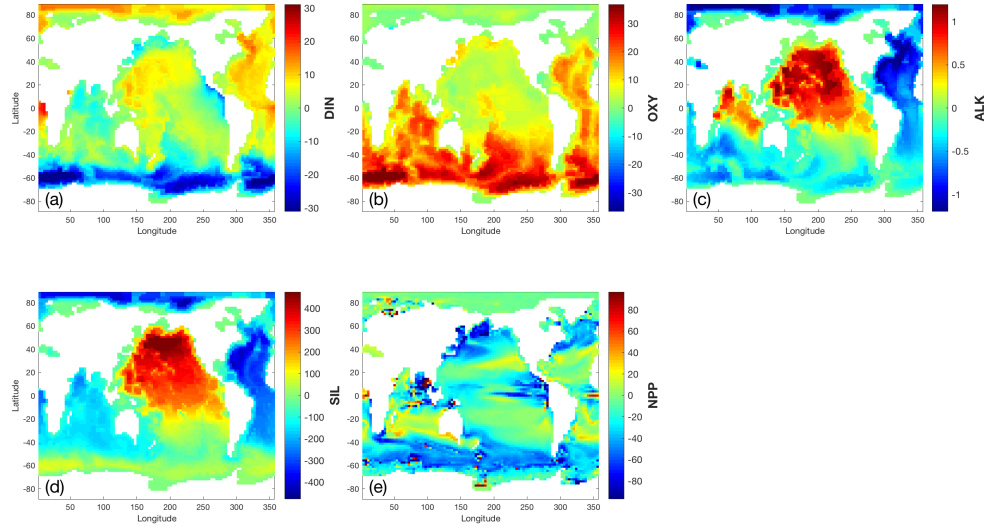


Figure 89: Change in column inventory of (a) DIN, (b) OXY, (c) ALK, (d) SIL, and (e) NPP after a +10% perturbation in x_{fn} , the non-diatom iron nutrient uptake half-saturation constant.

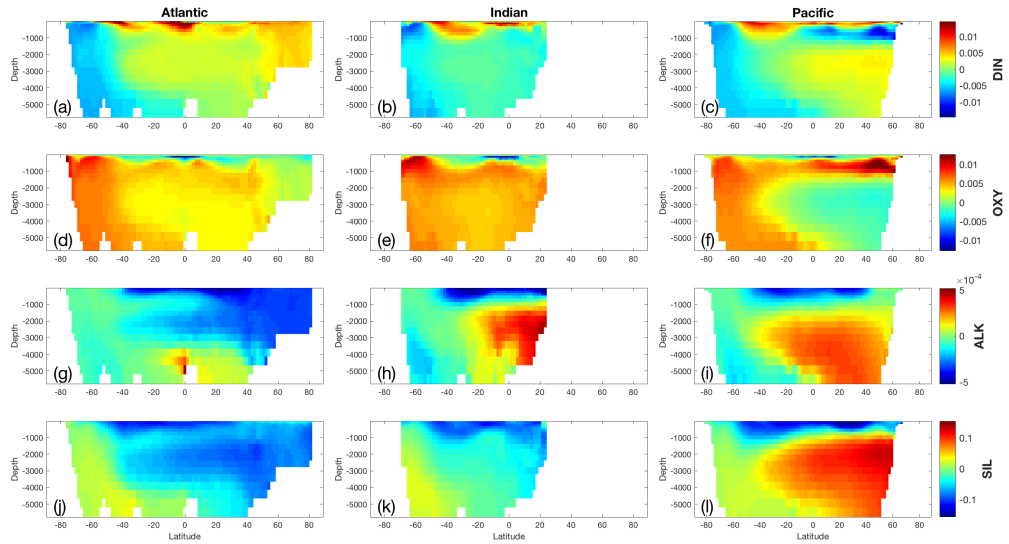


Figure 90: Change in volume-weighted zonally averaged (a-c) DIN, (d-f) OXY, (g-i) ALK, and (j-l) SIL after a +10% perturbation in x_{fn} , the non-diatom iron nutrient uptake half-saturation constant, for the (left) Atlantic, (middle) Indian, and (right) Pacific Oceans.

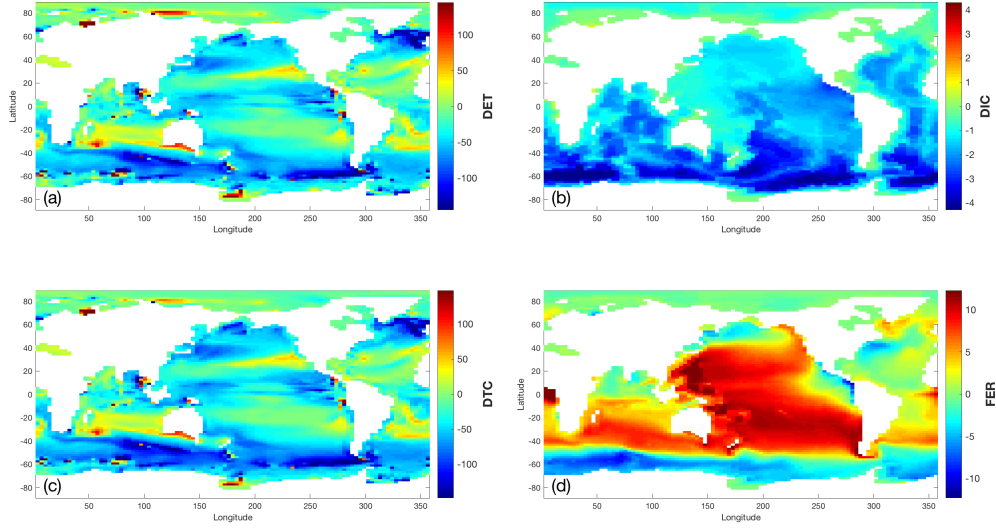


Figure 91: Change in column inventory of (a) DET, (b) DIC, (c) DTC, and (d) FER after a +10% perturbation in x_{fn} , the non-diatom iron nutrient uptake half-saturation constant.

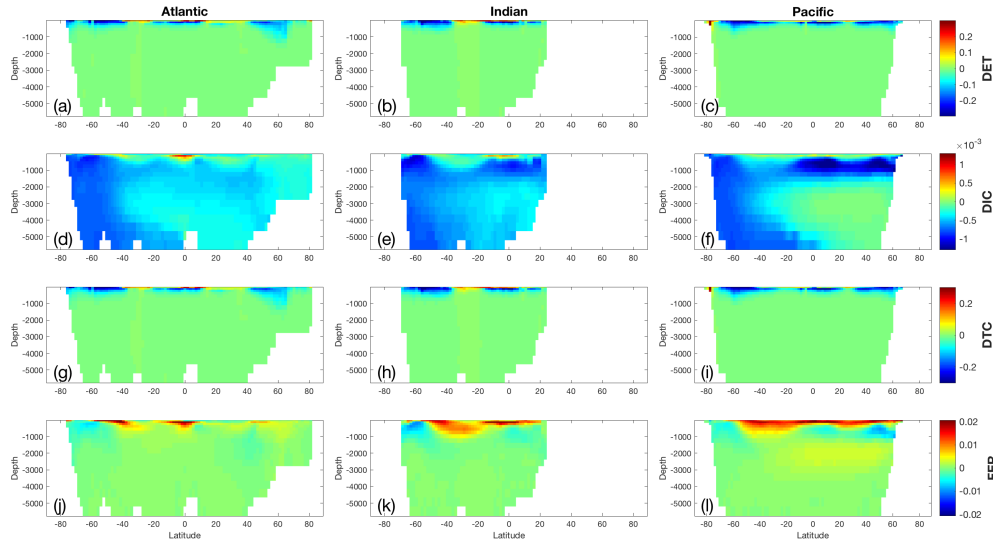


Figure 92: Change in volume-weighted zonally averaged (a-c) DET, (d-f) DIC, (g-i) DTC, and (j-l) FER after a +10% perturbation in x_{fn} , the non-diatom iron nutrient uptake half-saturation constant, for the (left) Atlantic, (middle) Indian, and (right) Pacific Oceans.

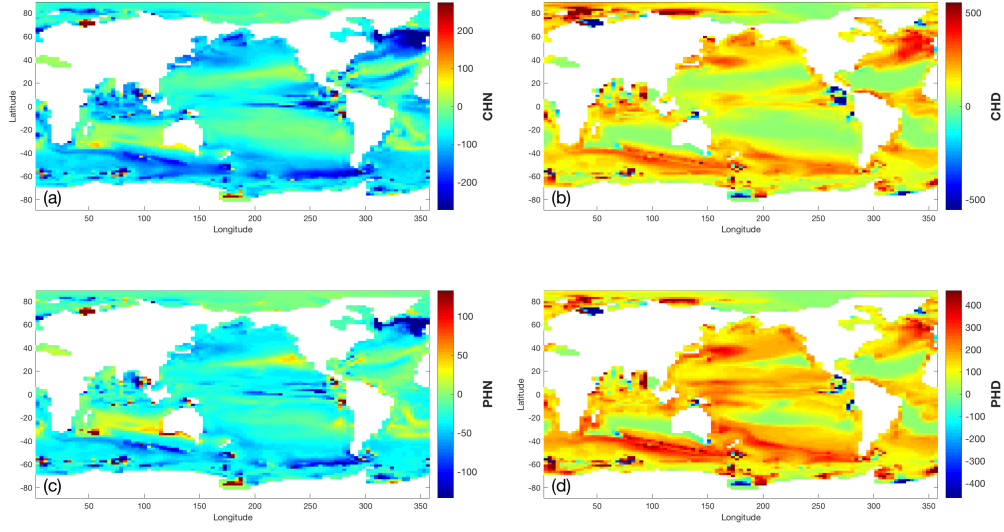


Figure 93: Change in column inventory of (a) CHN, (b) CHD, (c) PHN, and (d) PHD. after a +10% perturbation in x_{fn} , the non-diatom iron nutrient uptake half-saturation constant.

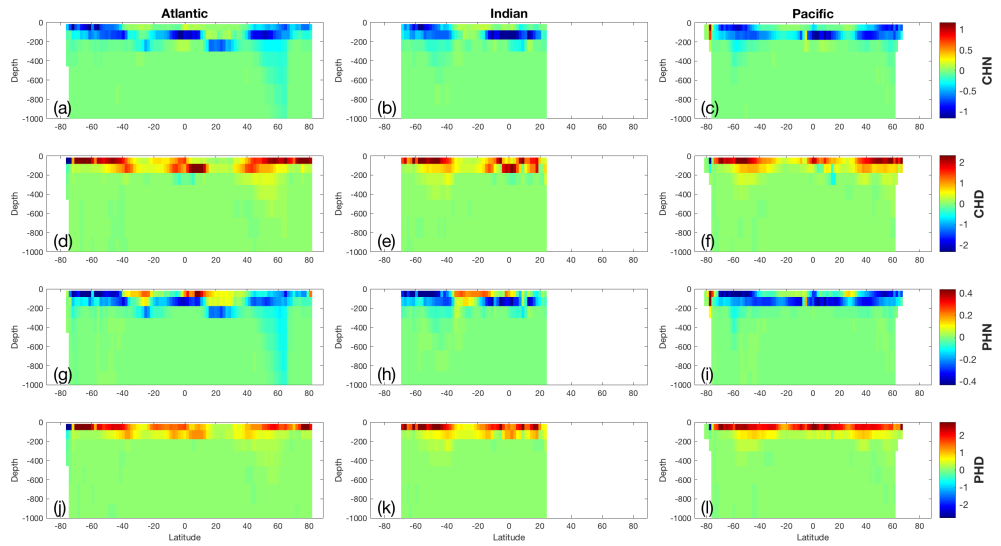


Figure 94: Change in volume-weighted zonally averaged (a-c) CHN, (d-f) CHD, (g-i) PHN, and (j-l) PHD after a +10% perturbation in x_{fn} , the non-diatom iron nutrient uptake half-saturation constant, for the (left) Atlantic, (middle) Indian, and (right) Pacific Oceans.

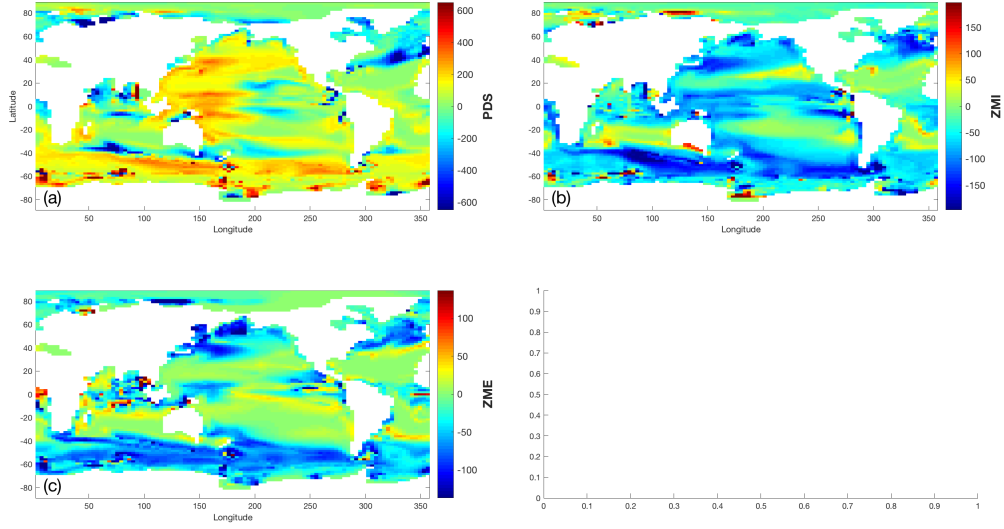


Figure 95: Change in column inventory of (a) PDS, (b) ZMI, and (c) ZME, after a +10% perturbation in x_{fn} , the non-diatom iron nutrient uptake half-saturation constant.

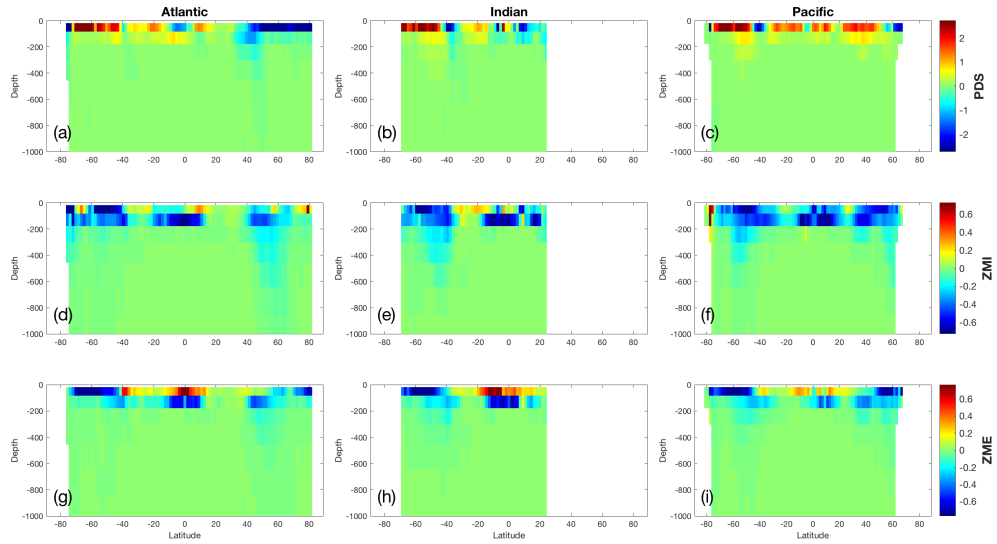


Figure 96: Change in volume-weighted zonally averaged (a-c) PDS, (d-f) ZMI, and (g-i) ZME after a +10% perturbation in x_{fn} , the non-diatom iron nutrient uptake half-saturation constant, for the (left) Atlantic, (middle) Indian, and (right) Pacific Oceans.

- 14 Parameter `xgme`: the maximum meso-zooplankton grazing rate.

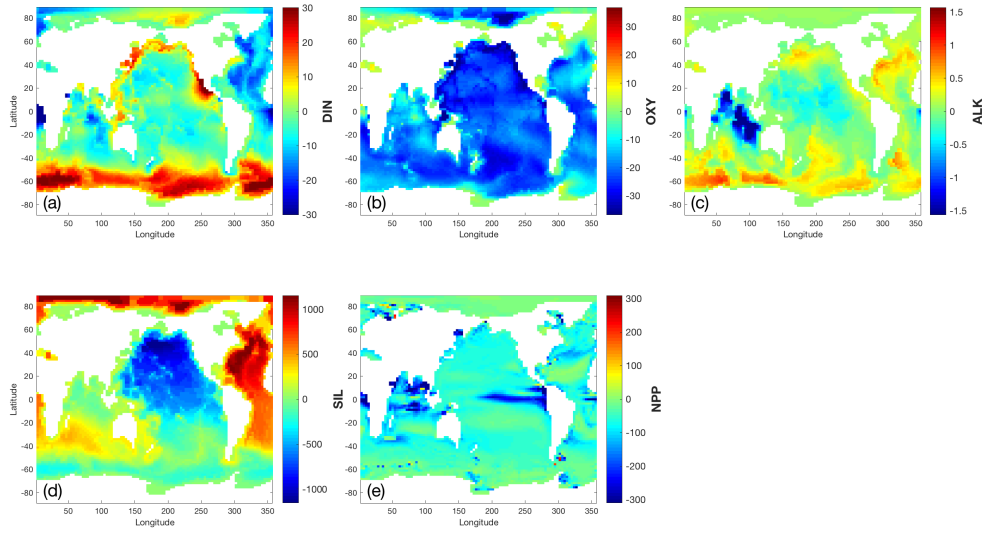


Figure 97: Change in column inventory of (a) DIN, (b) OXY, (c) ALK, (d) SIL, and (e) NPP after a +10% perturbation in x_{gme} , the maximum meso-zooplankton grazing rate.

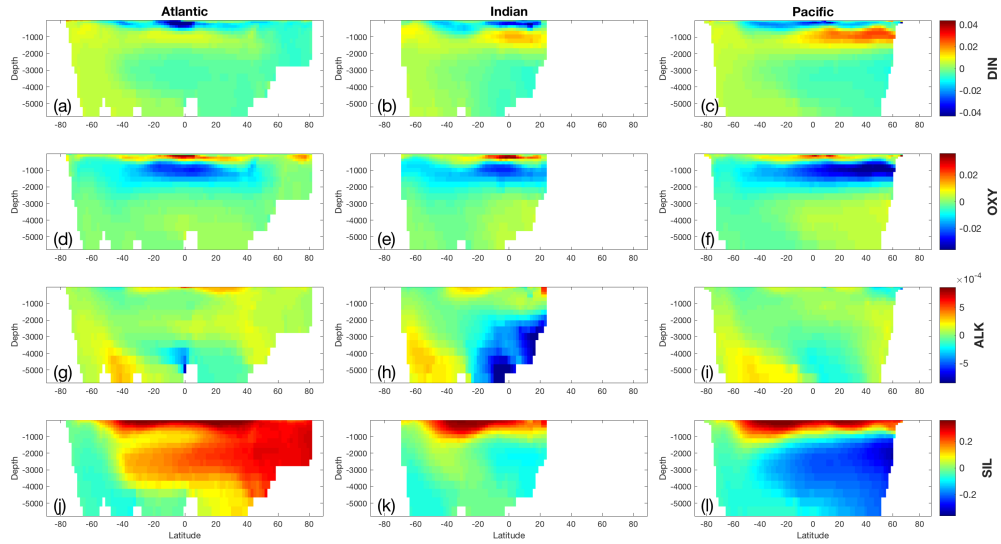


Figure 98: Change in volume-weighted zonally averaged (a-c) DIN, (d-f) OXY, (g-i) ALK, and (j-l) SIL after a +10% perturbation in x_{gme} , the maximum meso-zooplankton grazing rate, for the (left) Atlantic, (middle) Indian, and (right) Pacific Oceans.

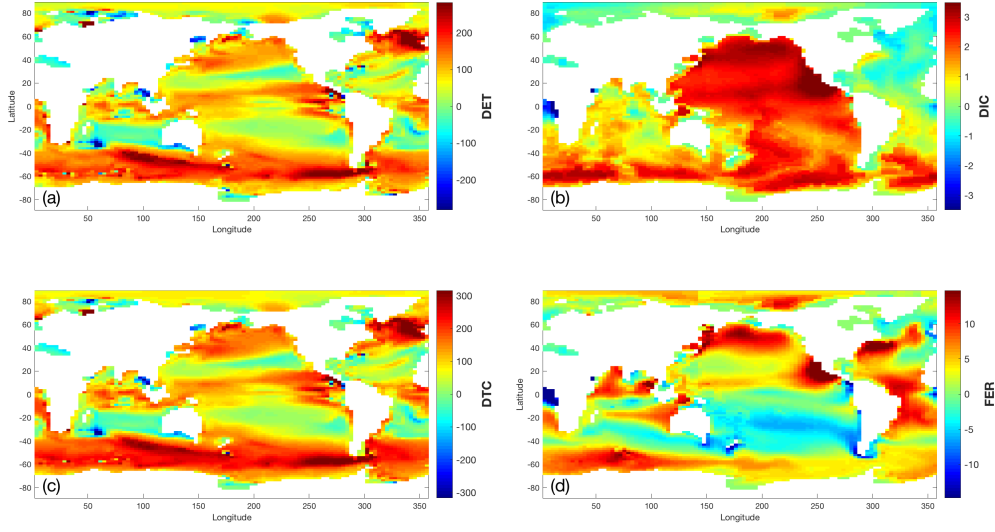


Figure 99: Change in column inventory of (a) DET, (b) DIC, (c) DTC, and (d) FER after a +10% perturbation in x_{gme} , the maximum meso-zooplankton grazing rate.

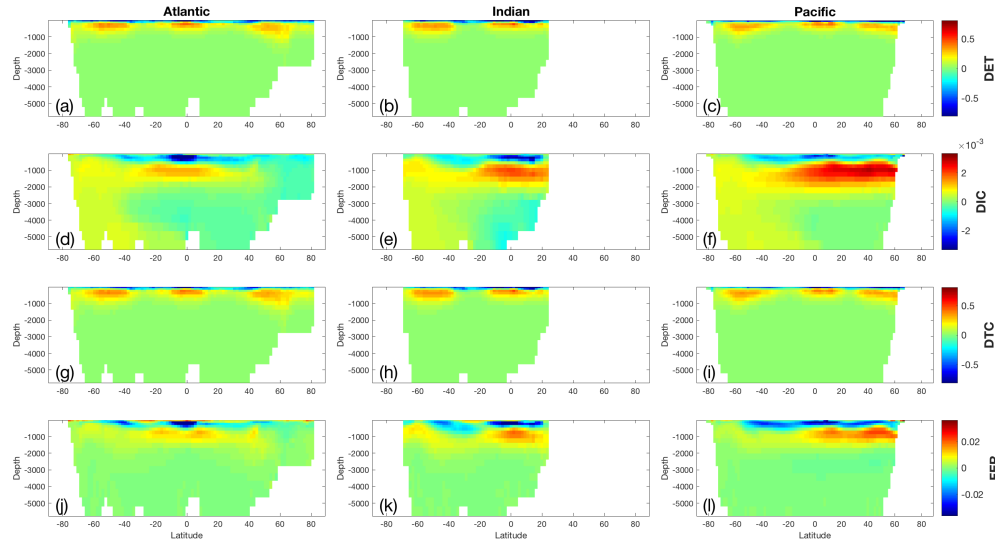


Figure 100: Change in volume-weighted zonally averaged (a-c) DET, (d-f) DIC, (g-i) DTC, and (j-l) FER after a +10% perturbation in x_{gme} , the maximum meso-zooplankton grazing rate, for the (left) Atlantic, (middle) Indian, and (right) Pacific Oceans.

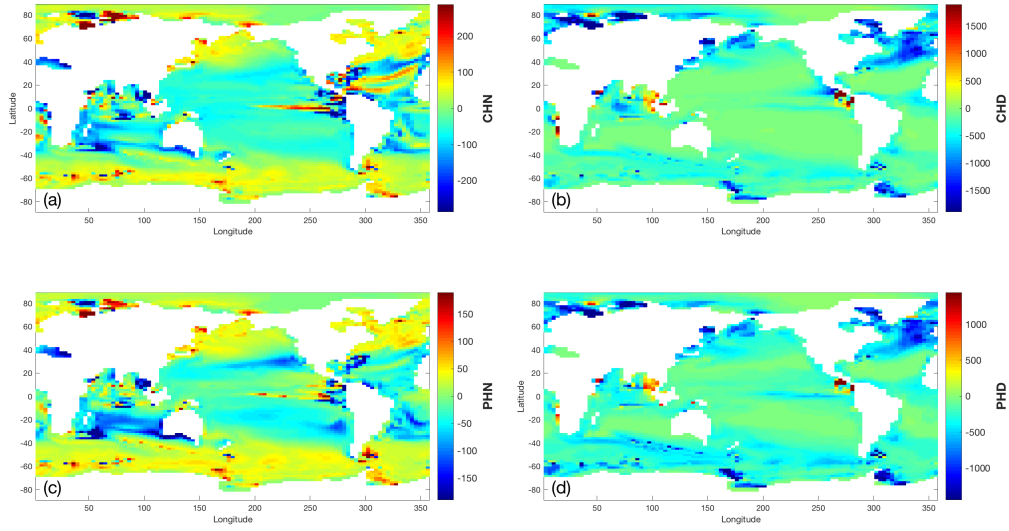


Figure 101: Change in column inventory of (a) CHN, (b) CHD, (c) PHN, and (d) PHD. after a +10% perturbation in x_{gme} , the maximum meso-zooplankton grazing rate.

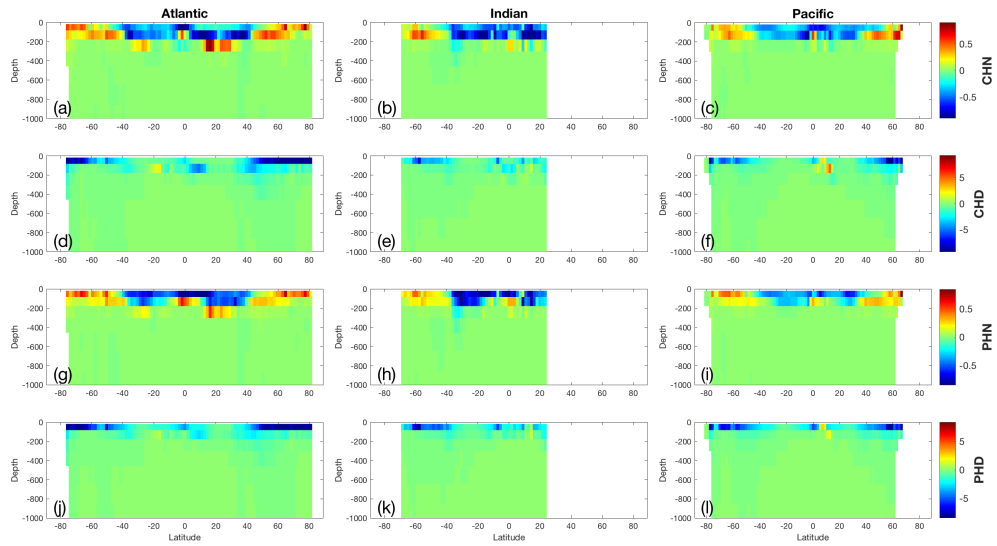


Figure 102: Change in volume-weighted zonally averaged (a-c) CHN, (d-f) CHD, (g-i) PHN, and (j-l) PHD after a +10% perturbation in x_{gme} , the maximum meso-zooplankton grazing rate, for the (left) Atlantic, (middle) Indian, and (right) Pacific Oceans.

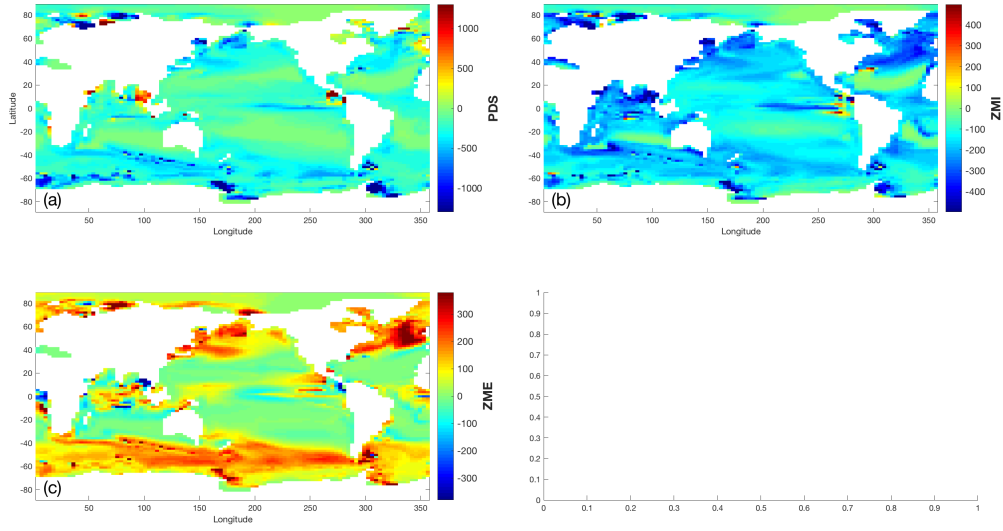


Figure 103: Change in column inventory of (a) PDS, (b) ZMI, and (c) ZME, after a +10% perturbation in x_{gme} , the maximum meso-zooplankton grazing rate.

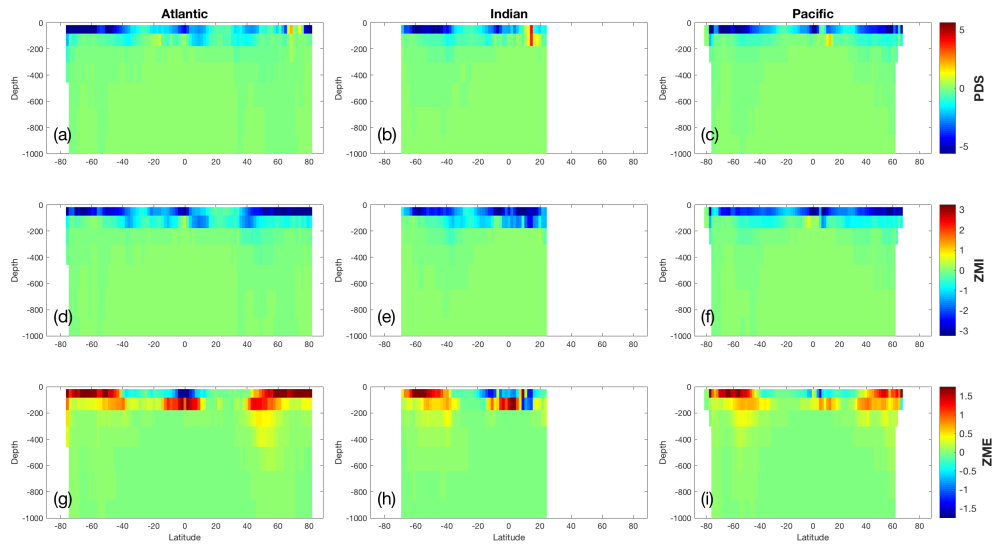


Figure 104: Change in volume-weighted zonally averaged (a-c) PDS, (d-f) ZMI, and (g-i) ZME after a +10% perturbation in x_{gme} , the maximum meso-zooplankton grazing rate, for the (left) Atlantic, (middle) Indian, and (right) Pacific Oceans.

- 15 Parameter `xgmi`: the maximum micro-zooplankton grazing rate.

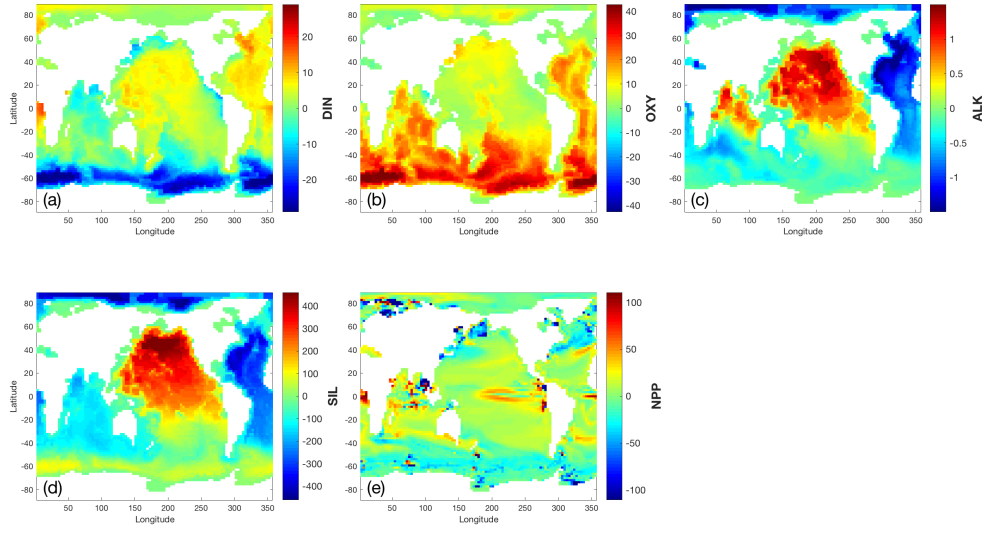


Figure 105: Change in column inventory of (a) DIN, (b) OXY, (c) ALK, (d) SIL, and (e) NPP after a +10% perturbation in x_{gmi} , the maximum micro-zooplankton grazing rate.

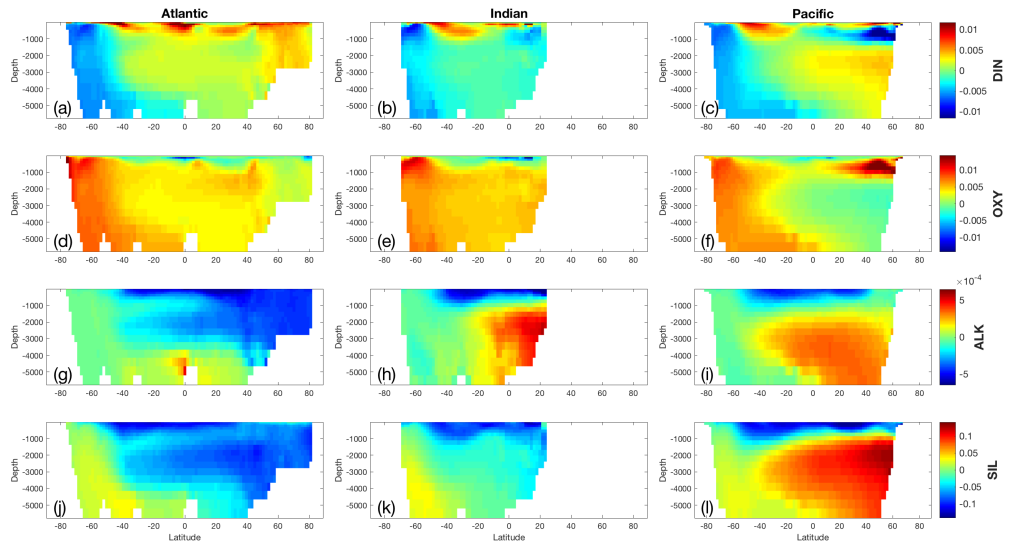


Figure 106: Change in volume-weighted zonally averaged (a-c) DIN, (d-f) OXY, (g-i) ALK, and (j-l) SIL after a +10% perturbation in x_{gmi} , the maximum micro-zooplankton grazing rate, for the (left) Atlantic, (middle) Indian, and (right) Pacific Oceans.

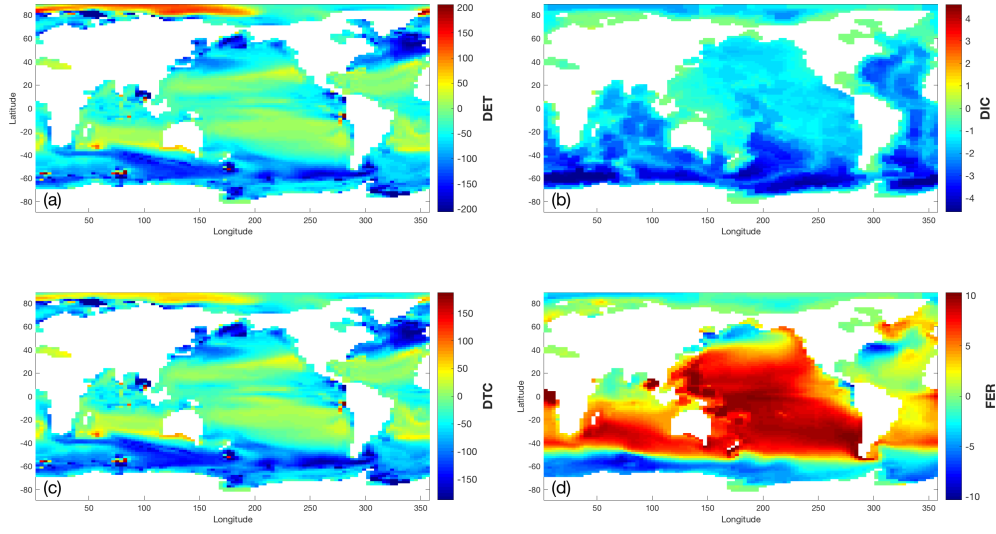


Figure 107: Change in column inventory of (a) DET, (b) DIC, (c) DTC, and (d) FER after a +10% perturbation in x_{gmi} , the maximum micro-zooplankton grazing rate.

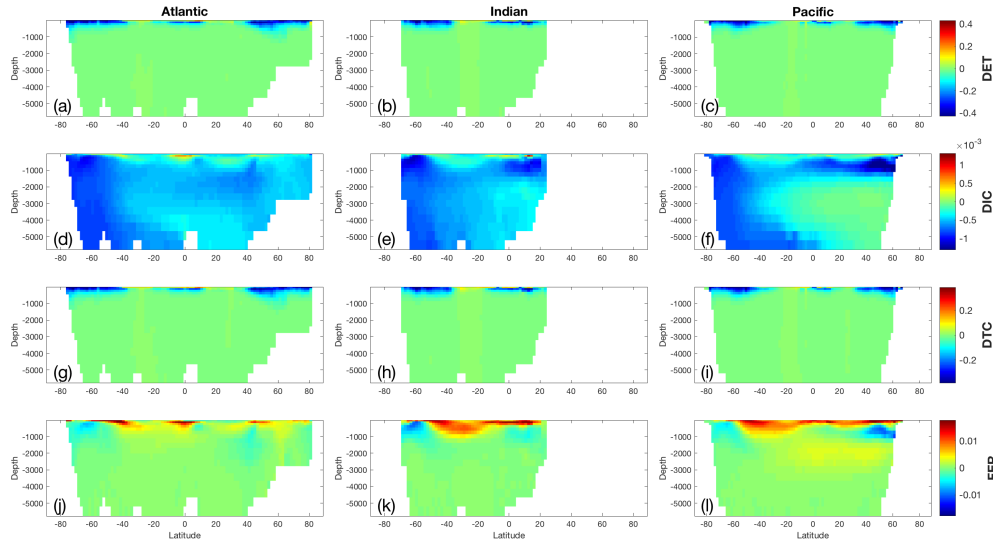


Figure 108: Change in volume-weighted zonally averaged (a-c) DET, (d-f) DIC, (g-i) DTC, and (j-l) FER after a +10% perturbation in x_{gmi} , the maximum micro-zooplankton grazing rate, for the (left) Atlantic, (middle) Indian, and (right) Pacific Oceans.

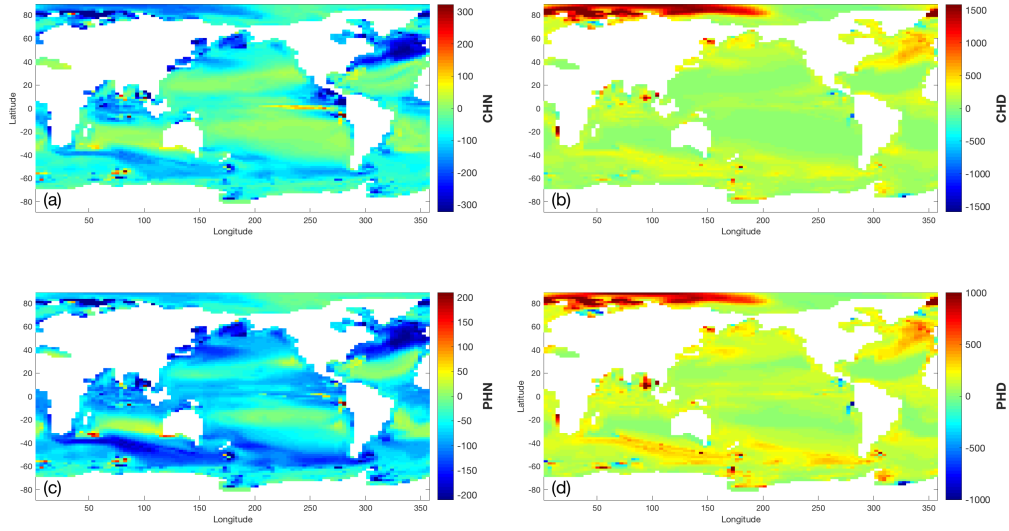


Figure 109: Change in column inventory of (a) CHN, (b) CHD, (c) PHN, and (d) PHD. after a +10% perturbation in x_{gmi} , the maximum micro-zooplankton grazing rate.

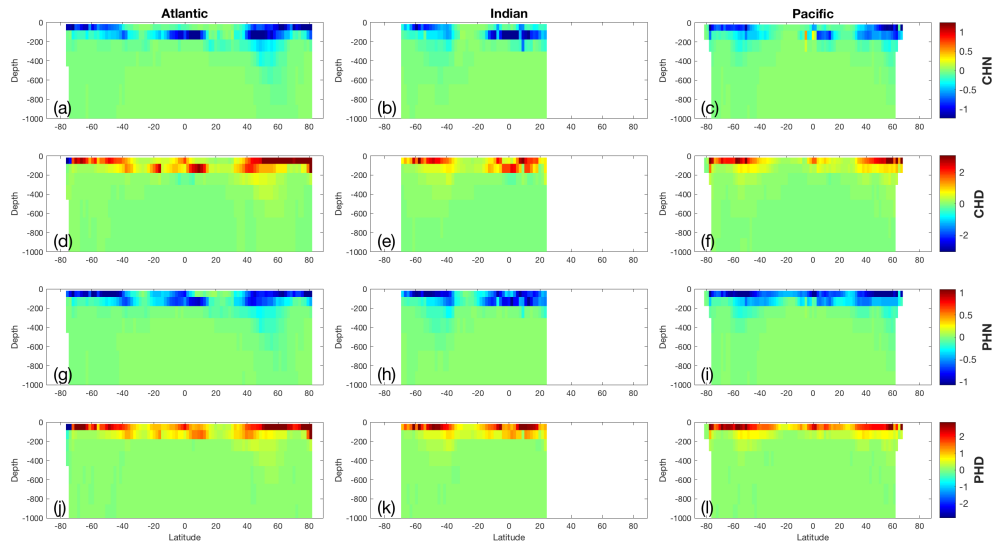


Figure 110: Change in volume-weighted zonally averaged (a-c) CHN, (d-f) CHD, (g-i) PHN, and (j-l) PHD after a +10% perturbation in x_{gmi} , the maximum micro-zooplankton grazing rate, for the (left) Atlantic, (middle) Indian, and (right) Pacific Oceans.

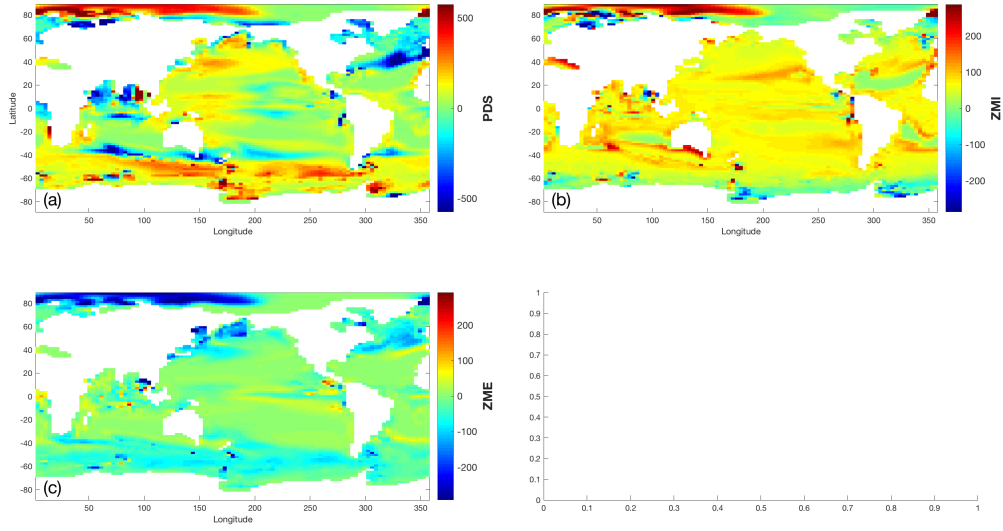


Figure 111: Change in column inventory of (a) PDS, (b) ZMI, and (c) ZME, after a +10% perturbation in x_{gmi} , the maximum micro-zooplankton grazing rate.

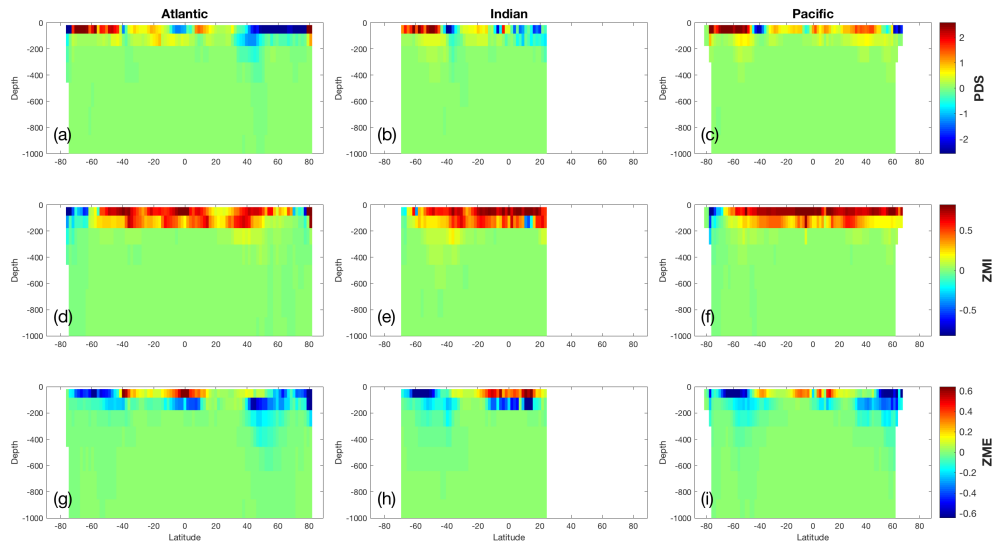


Figure 112: Change in volume-weighted zonally averaged (a-c) PDS, (d-f) ZMI, and (g-i) ZME after a +10% perturbation in x_{gmi} , the maximum micro-zooplankton grazing rate, for the (left) Atlantic, (middle) Indian, and (right) Pacific Oceans.

16 Parameter xmd: the detrital nitrogen remineralisation rate.

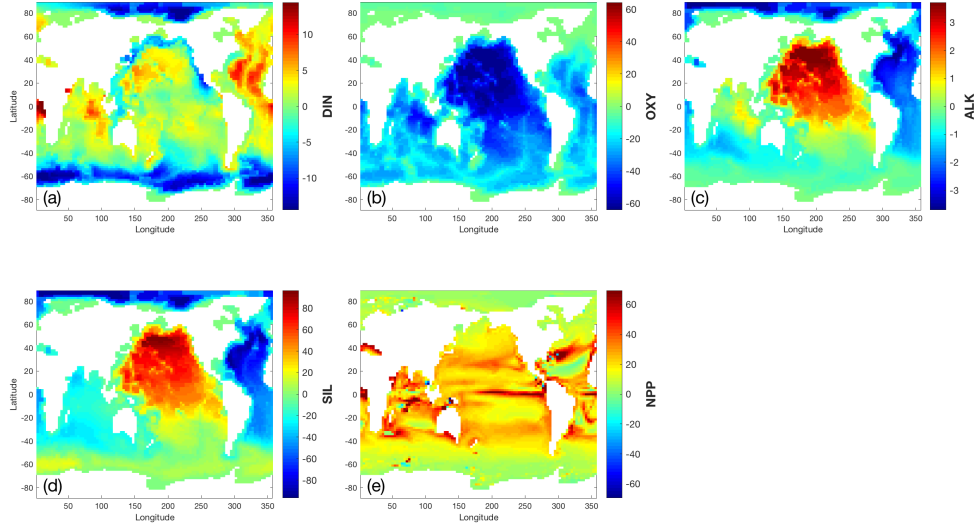


Figure 113: Change in column inventory of (a) DIN, (b) OXY, (c) ALK, (d) SIL, and (e) NPP after a +10% perturbation in x_{md} , the detrital nitrogen remineralisation rate.

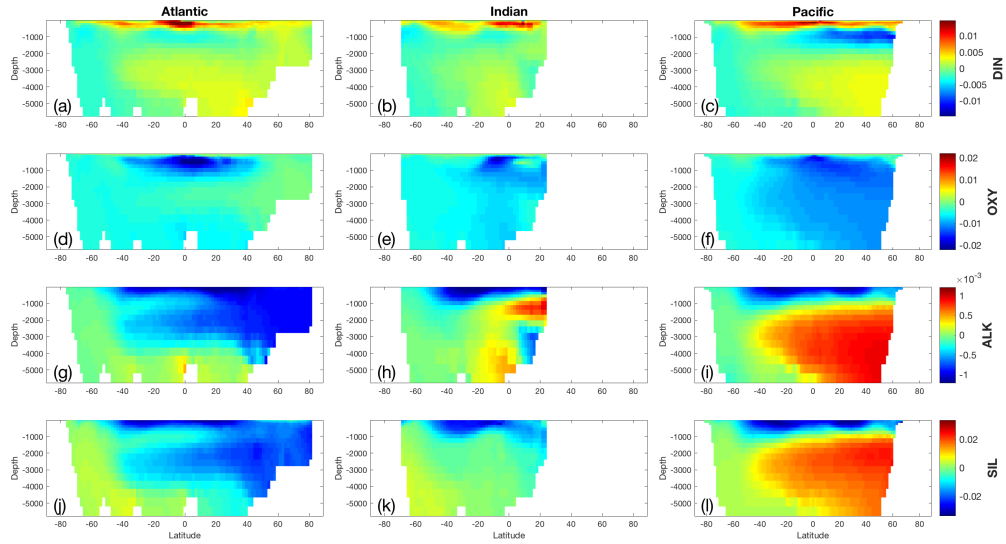


Figure 114: Change in volume-weighted zonally averaged (a-c) DIN, (d-f) OXY, (g-i) ALK, and (j-l) SIL after a +10% perturbation in x_{md} , the detrital nitrogen remineralisation rate, for the (left) Atlantic, (middle) Indian, and (right) Pacific Oceans.

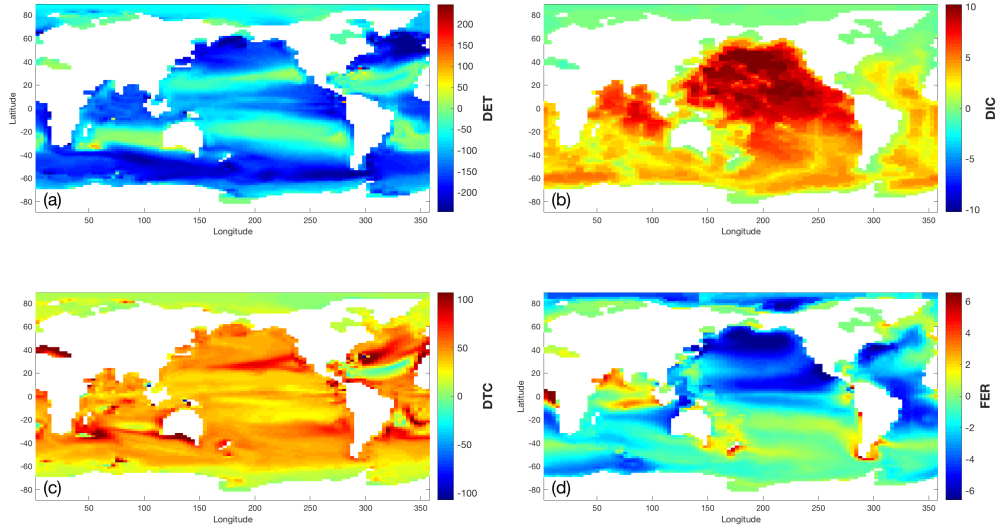


Figure 115: Change in column inventory of (a) DET, (b) DIC, (c) DTC, and (d) FER after a +10% perturbation in xmd, the detrital nitrogen remineralisation rate.

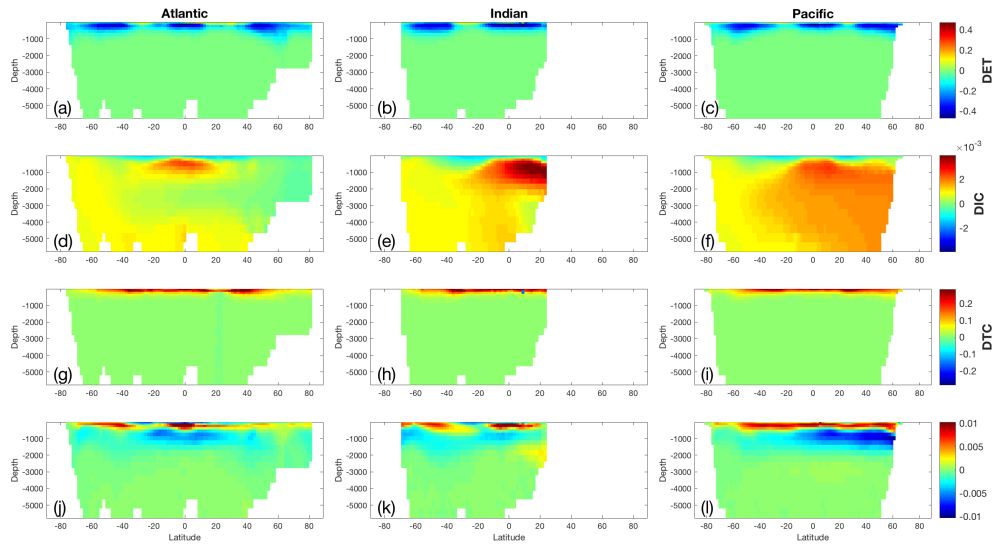


Figure 116: Change in volume-weighted zonally averaged (a-c) DET, (d-f) DIC, (g-i) DTC, and (j-l) FER after a +10% perturbation in xmd, the detrital nitrogen remineralisation rate, for the (left) Atlantic, (middle) Indian, and (right) Pacific Oceans.

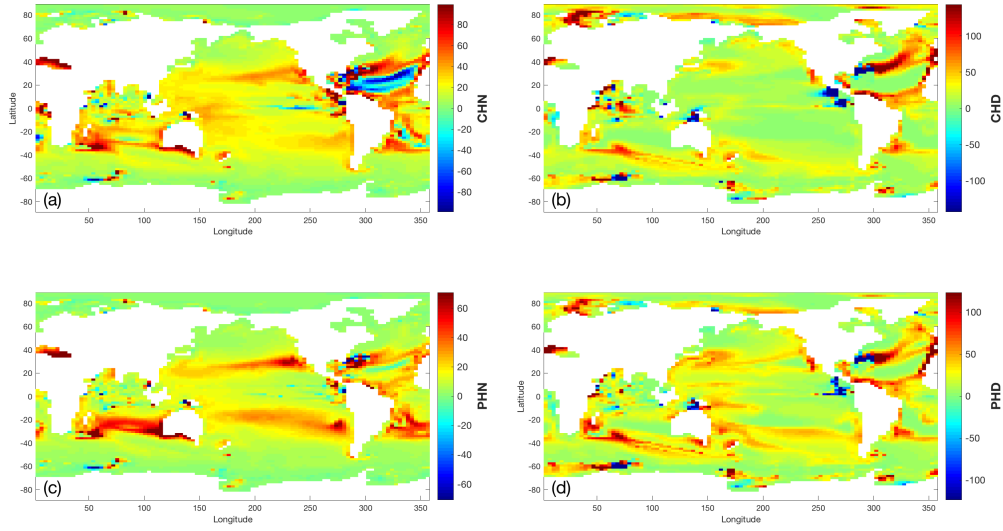


Figure 117: Change in column inventory of (a) CHN, (b) CHD, (c) PHN, and (d) PHD. after a +10% perturbation in xmd, the detrital nitrogen remineralisation rate.

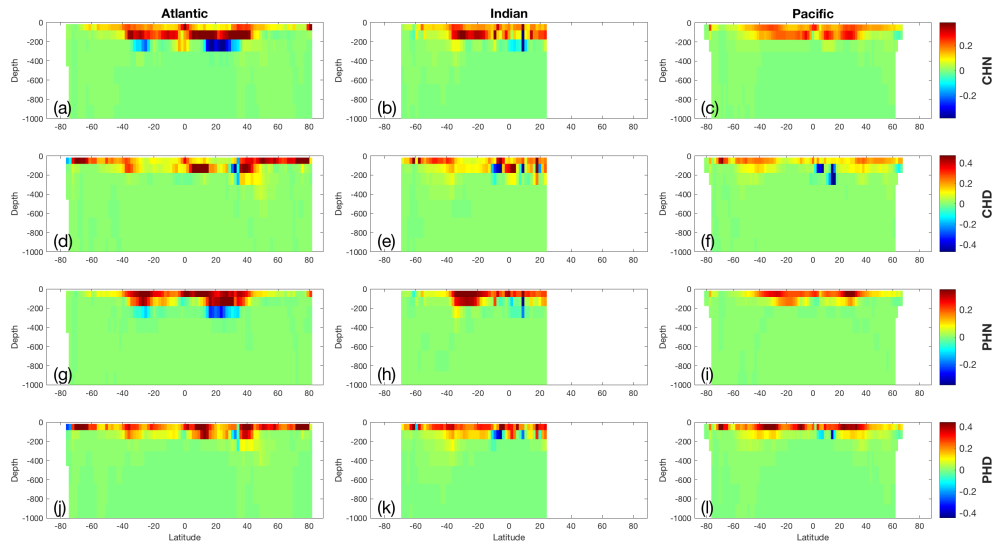


Figure 118: Change in volume-weighted zonally averaged (a-c) CHN, (d-f) CHD, (g-i) PHN, and (j-l) PHD after a +10% perturbation in xmd, the detrital nitrogen remineralisation rate, for the (left) Atlantic, (middle) Indian, and (right) Pacific Oceans.

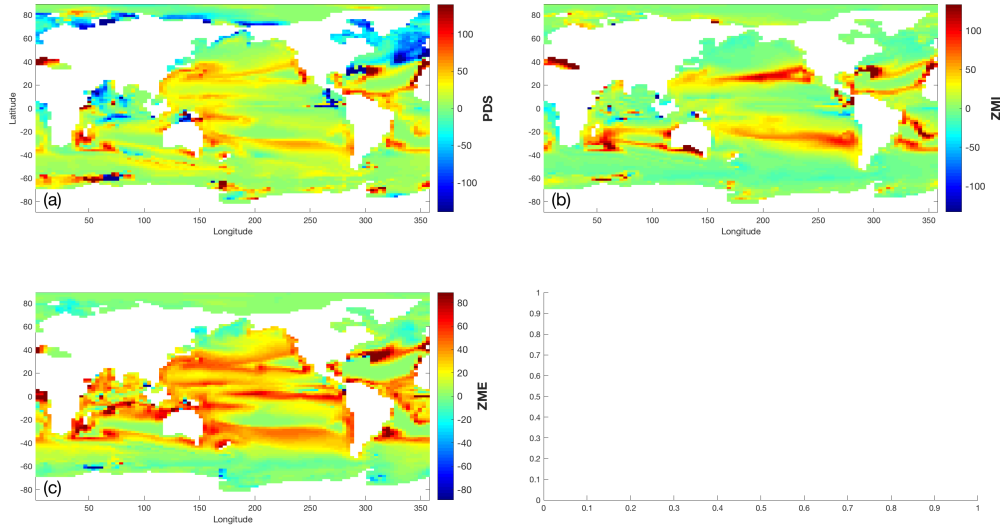


Figure 119: Change in column inventory of (a) PDS, (b) ZMI, and (c) ZME, after a +10% perturbation in xmd, the detrital nitrogen remineralisation rate.

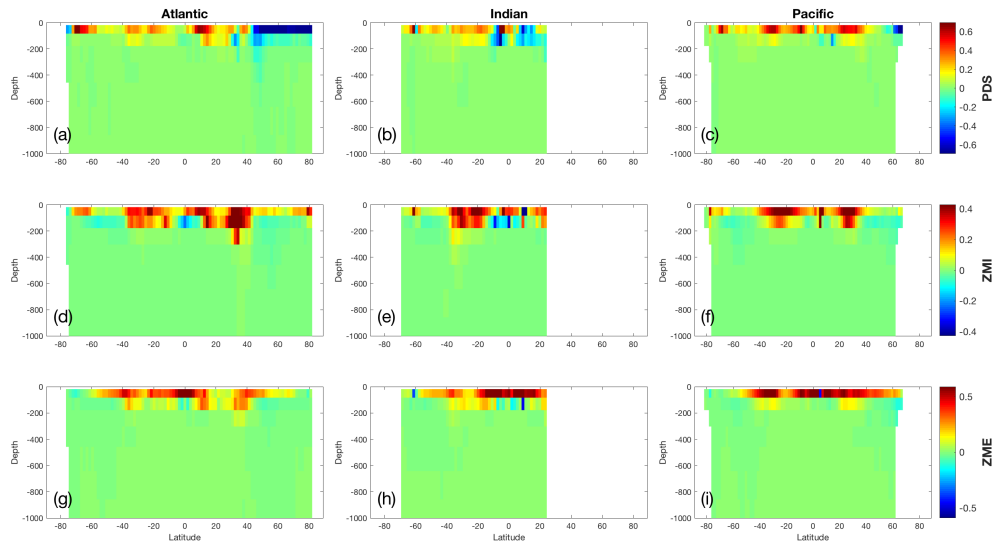


Figure 120: Change in volume-weighted zonally averaged (a-c) PDS, (d-f) ZMI, and (g-i) ZME after a +10% perturbation in xmd, the detrital nitrogen remineralisation rate, for the (left) Atlantic, (middle) Indian, and (right) Pacific Oceans.

- 17 Parameter xmdc: the detrital carbon remineralisation rate.

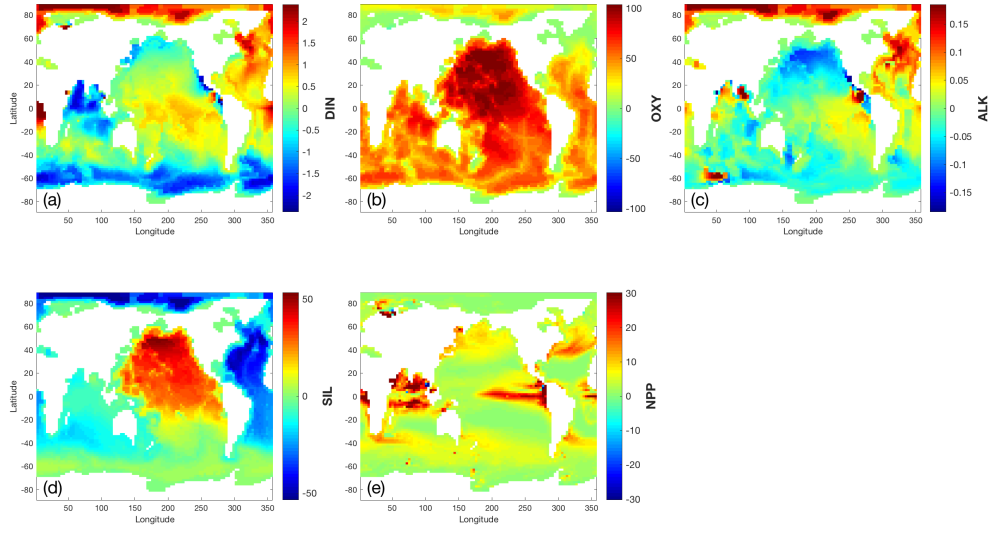


Figure 121: Change in column inventory of (a) DIN, (b) OXY, (c) ALK, (d) SIL, and (e) NPP after a +10% perturbation in xmdc, the detrital carbon remineralisation rate.

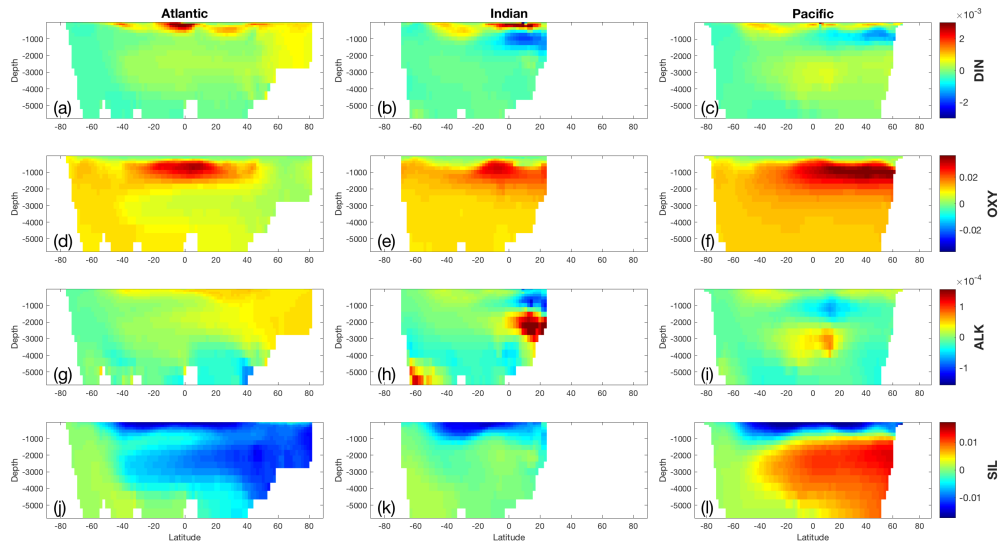


Figure 122: Change in volume-weighted zonally averaged (a-c) DIN, (d-f) OXY, (g-i) ALK, and (j-l) SIL after a +10% perturbation in xmdc, the detrital carbon remineralisation rate, for the (left) Atlantic, (middle) Indian, and (right) Pacific Oceans.

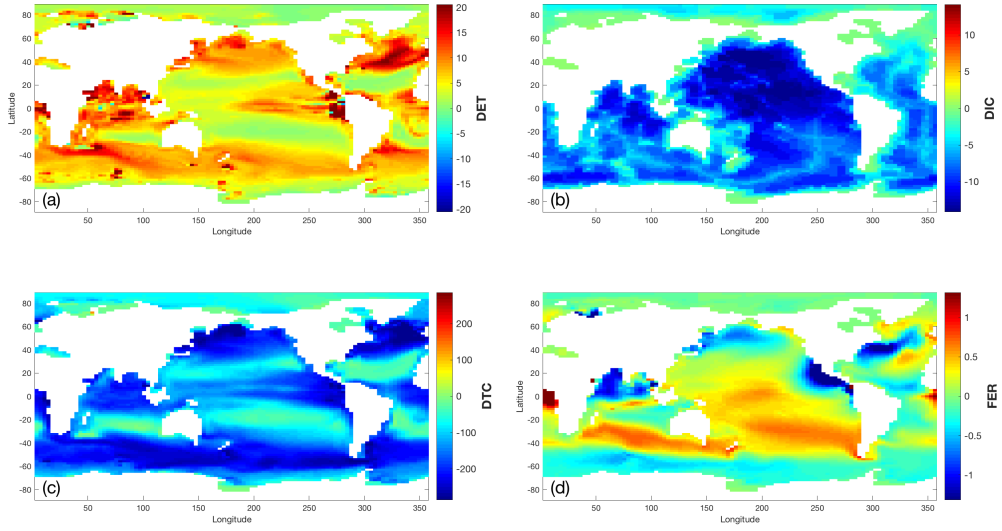


Figure 123: Change in column inventory of (a) DET, (b) DIC, (c) DTC, and (d) FER after a +10% perturbation in xmdc, the detrital carbon remineralisation rate.

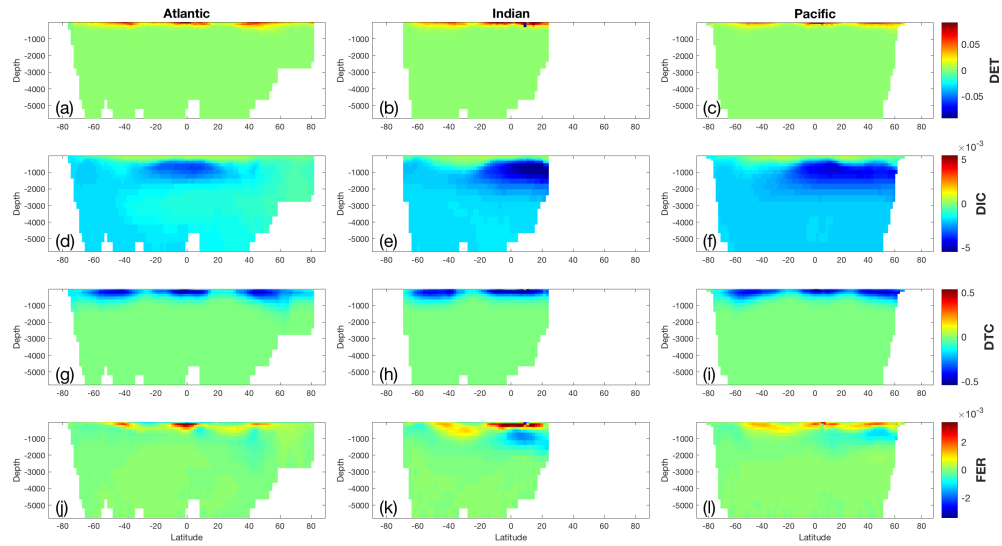


Figure 124: Change in volume-weighted zonally averaged (a-c) DET, (d-f) DIC, (g-i) DTC, and (j-l) FER after a +10% perturbation in xmdc, the detrital carbon remineralisation rate, for the (left) Atlantic, (middle) Indian, and (right) Pacific Oceans.

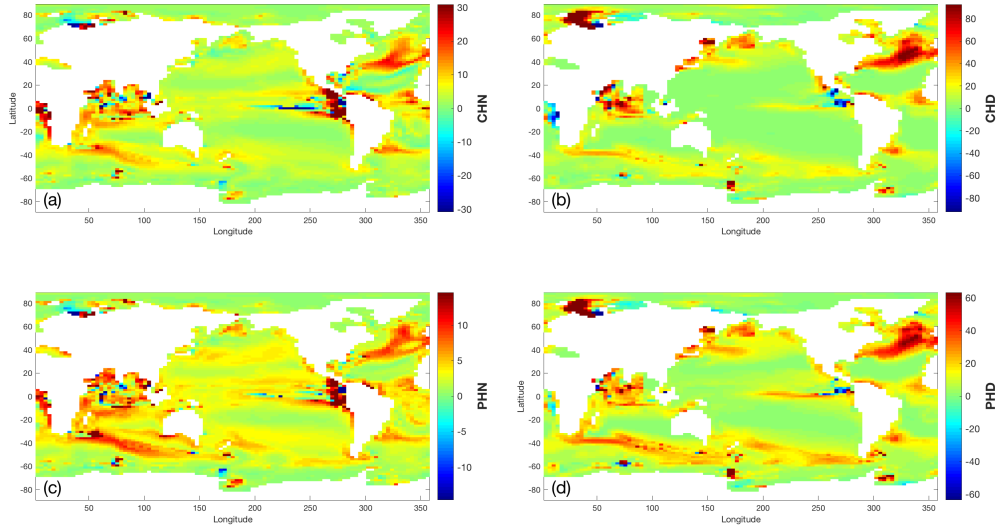


Figure 125: Change in column inventory of (a) CHN, (b) CHD, (c) PHN, and (d) PHD. after a +10% perturbation in xmdc, the detrital carbon remineralisation rate.

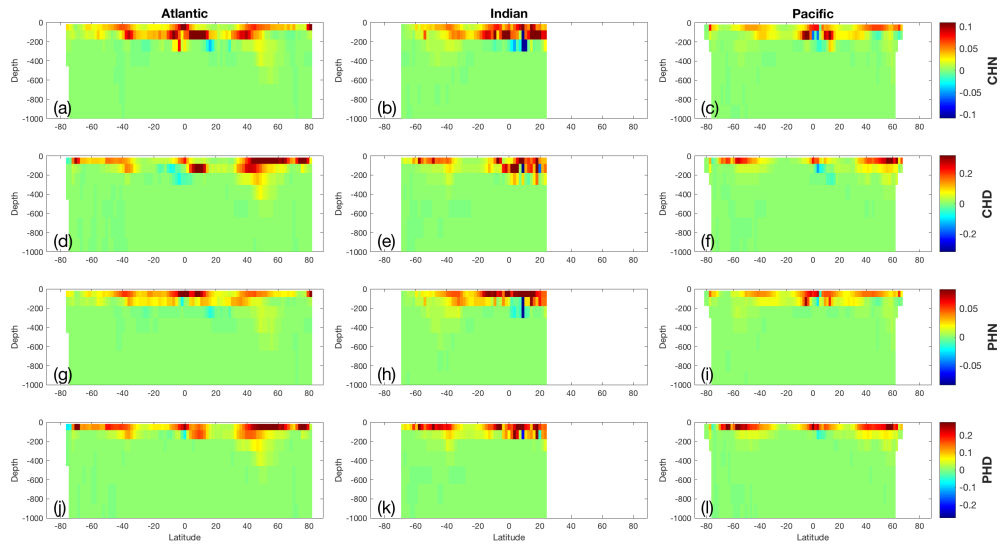


Figure 126: Change in volume-weighted zonally averaged (a-c) CHN, (d-f) CHD, (g-i) PHN, and (j-l) PHD after a +10% perturbation in xmdc, the detrital carbon remineralisation rate, for the (left) Atlantic, (middle) Indian, and (right) Pacific Oceans.

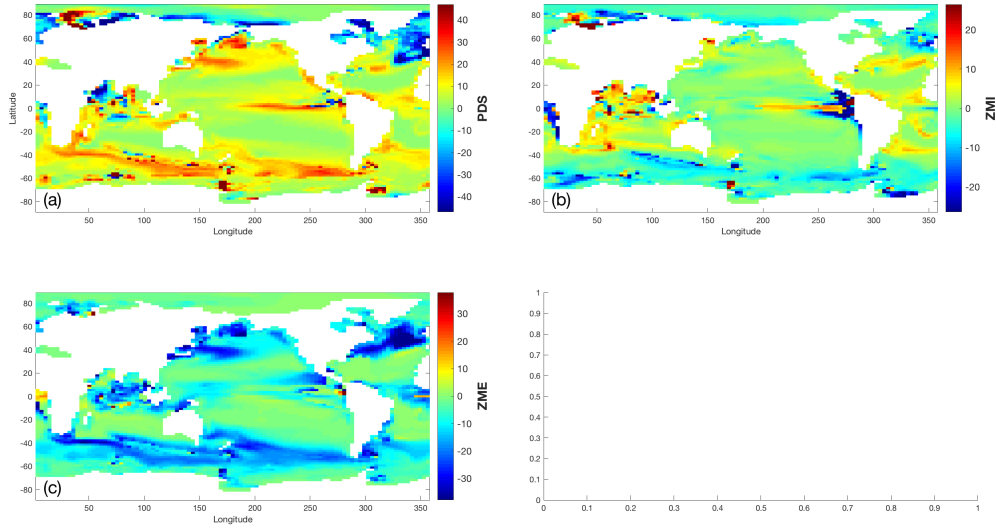


Figure 127: Change in column inventory of (a) PDS, (b) ZMI, and (c) ZME, after a +10% perturbation in xmdc, the detrital carbon remineralisation rate.

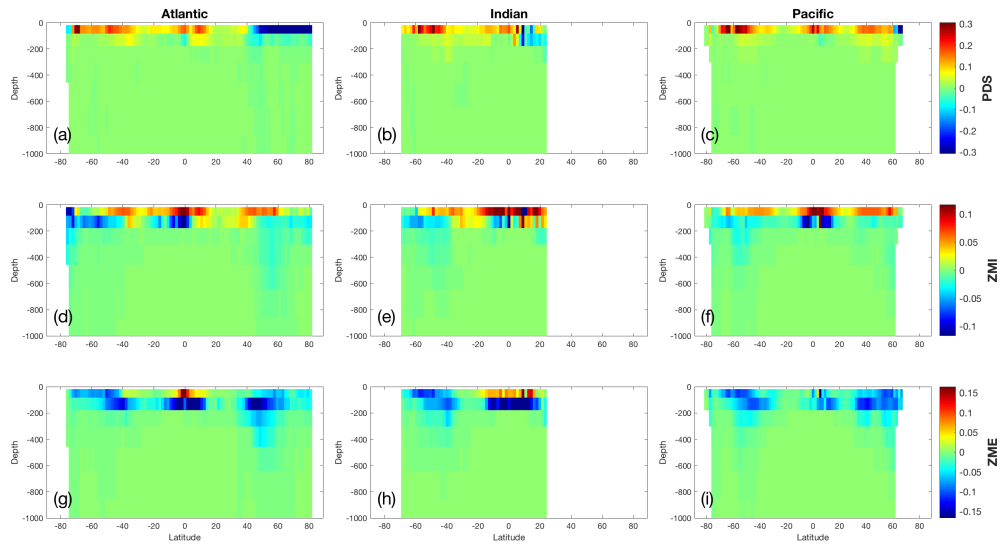


Figure 128: Change in volume-weighted zonally averaged (a-c) PDS, (d-f) ZMI, and (g-i) ZME after a +10% perturbation in xmdc, the detrital carbon remineralisation rate, for the (left) Atlantic, (middle) Indian, and (right) Pacific Oceans.

- 18 Parameter `xmzme`: the meso-zooplankton maximum loss rate.

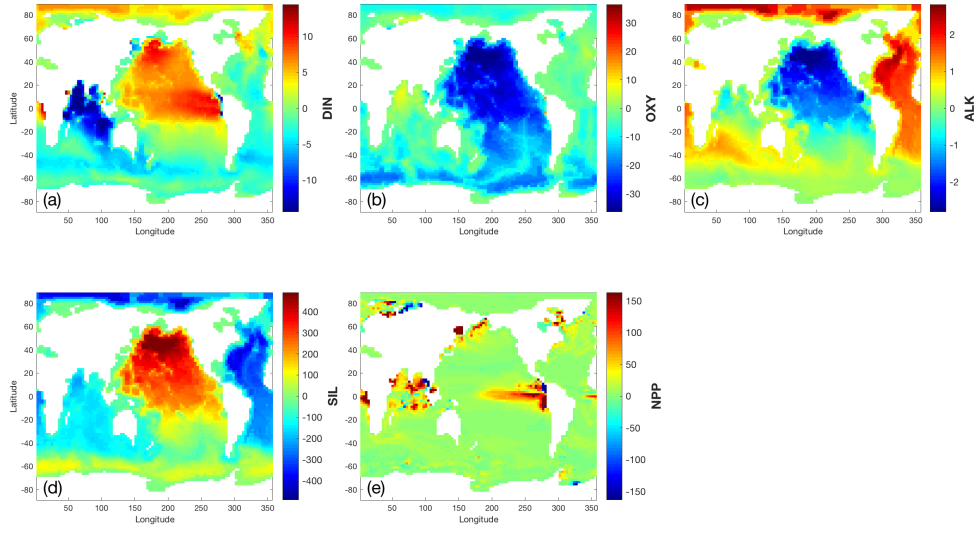


Figure 129: Change in column inventory of (a) DIN, (b) OXY, (c) ALK, (d) SIL, and (e) NPP after a +10% perturbation in x_{mzme} , the meso-zooplankton maximum loss rate.

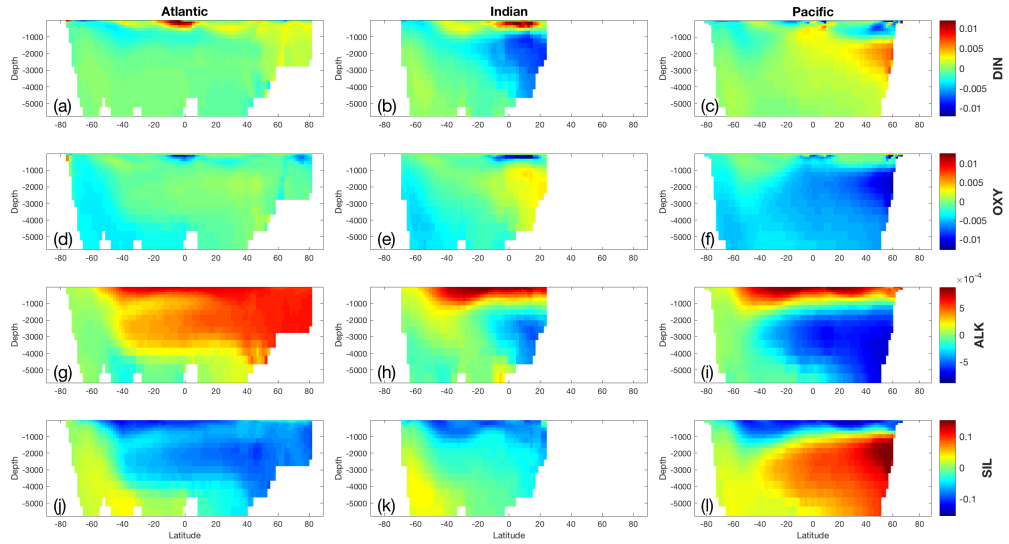


Figure 130: Change in volume-weighted zonally averaged (a-c) DIN, (d-f) OXY, (g-i) ALK, and (j-l) SIL after a +10% perturbation in x_{mzme} , the meso-zooplankton maximum loss rate, for the (left) Atlantic, (middle) Indian, and (right) Pacific Oceans.

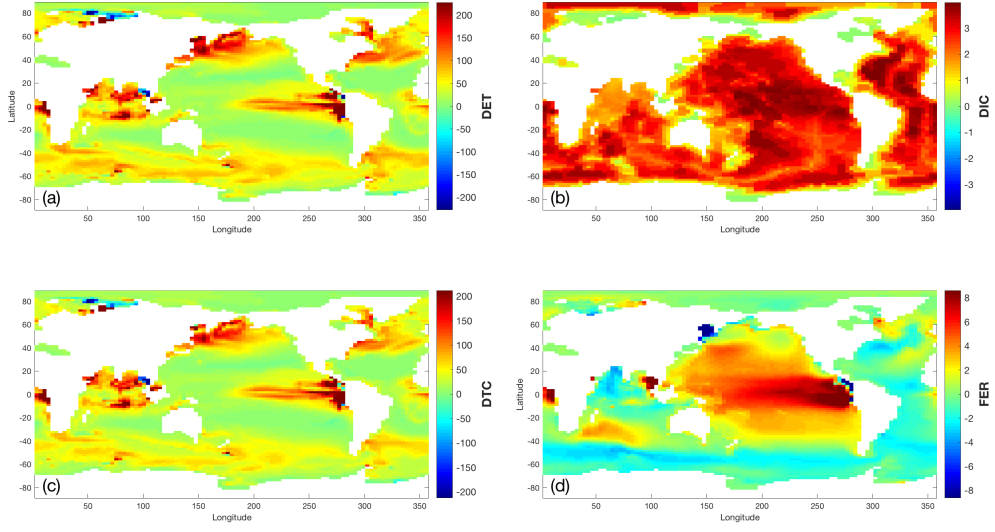


Figure 131: Change in column inventory of (a) DET, (b) DIC, (c) DTC, and (d) FER after a +10% perturbation in xzmze, the meso-zooplankton maximum loss rate.

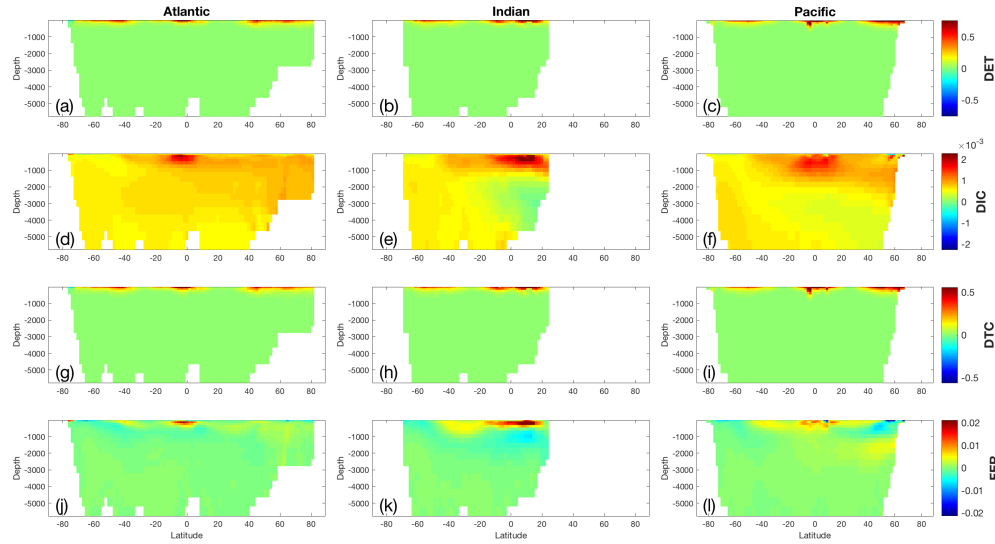


Figure 132: Change in volume-weighted zonally averaged (a-c) DET, (d-f) DIC, (g-i) DTC, and (j-l) FER after a +10% perturbation in xzmze, the meso-zooplankton maximum loss rate, for the (left) Atlantic, (middle) Indian, and (right) Pacific Oceans.

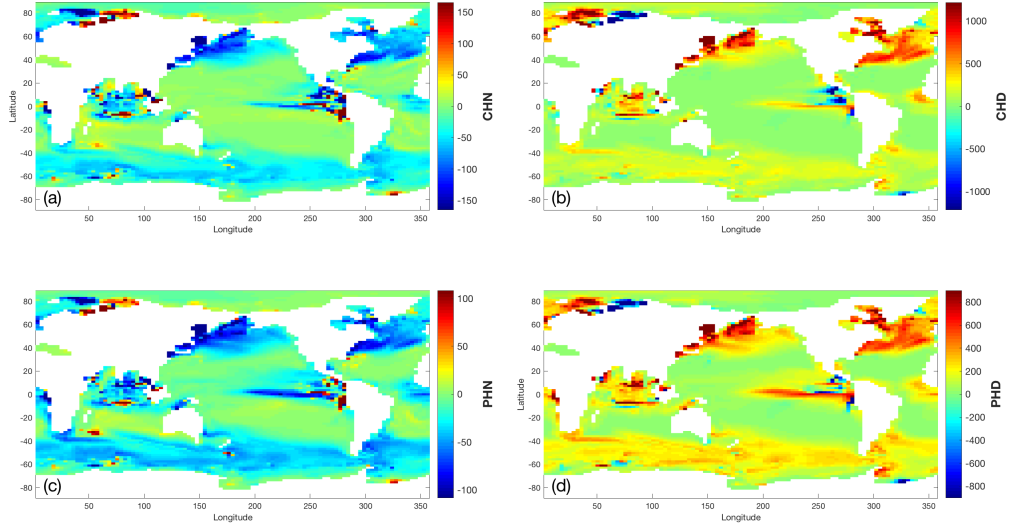


Figure 133: Change in column inventory of (a) CHN, (b) CHD, (c) PHN, and (d) PHD. after a +10% perturbation in xzmze, the meso-zooplankton maximum loss rate.

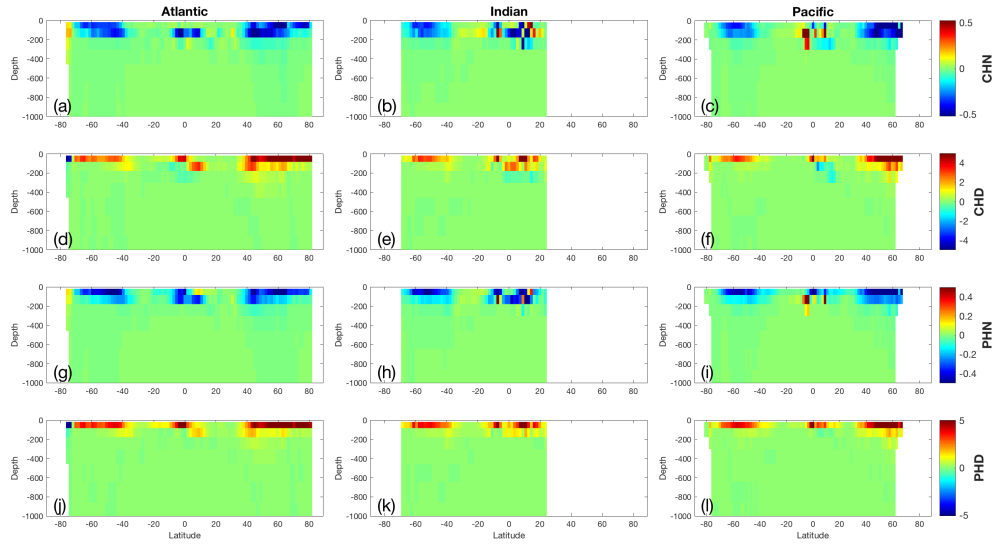


Figure 134: Change in volume-weighted zonally averaged (a-c) CHN, (d-f) CHD, (g-i) PHN, and (j-l) PHD after a +10% perturbation in xzmze, the meso-zooplankton maximum loss rate, for the (left) Atlantic, (middle) Indian, and (right) Pacific Oceans.

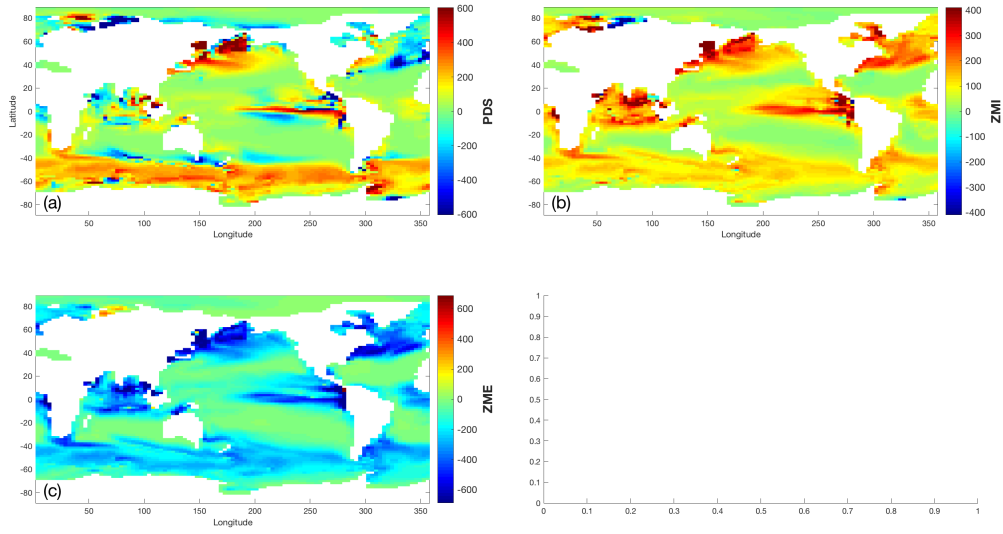


Figure 135: Change in column inventory of (a) PDS, (b) ZMI, and (c) ZME, after a +10% perturbation in x_{mzme} , the meso-zooplankton maximum loss rate.

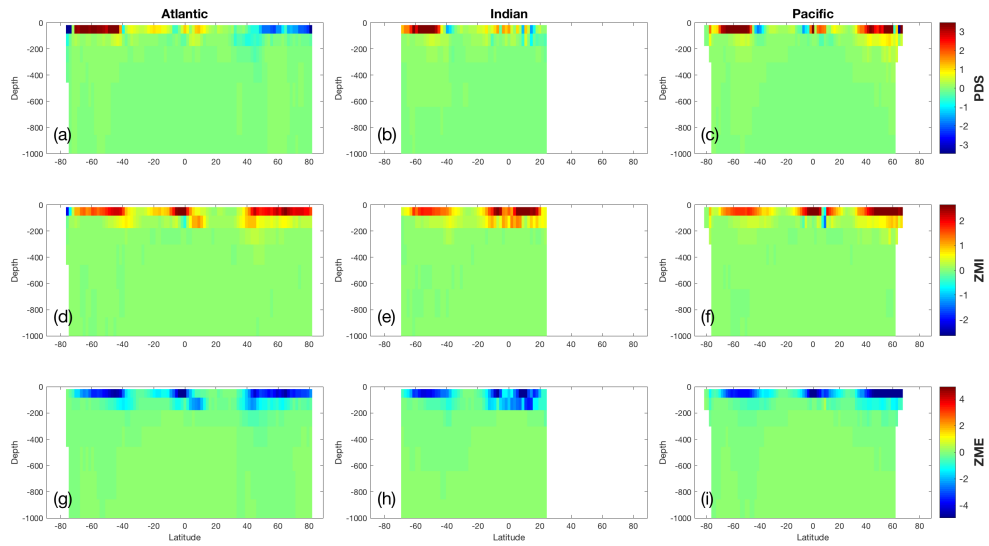


Figure 136: Change in volume-weighted zonally averaged (a-c) PDS, (d-f) ZMI, and (g-i) ZME after a +10% perturbation in x_{mzme} , the meso-zooplankton maximum loss rate, for the (left) Atlantic, (middle) Indian, and (right) Pacific Oceans.

- 19 Parameter `xmzmi`: the micro-zooplankton maximum loss rate.

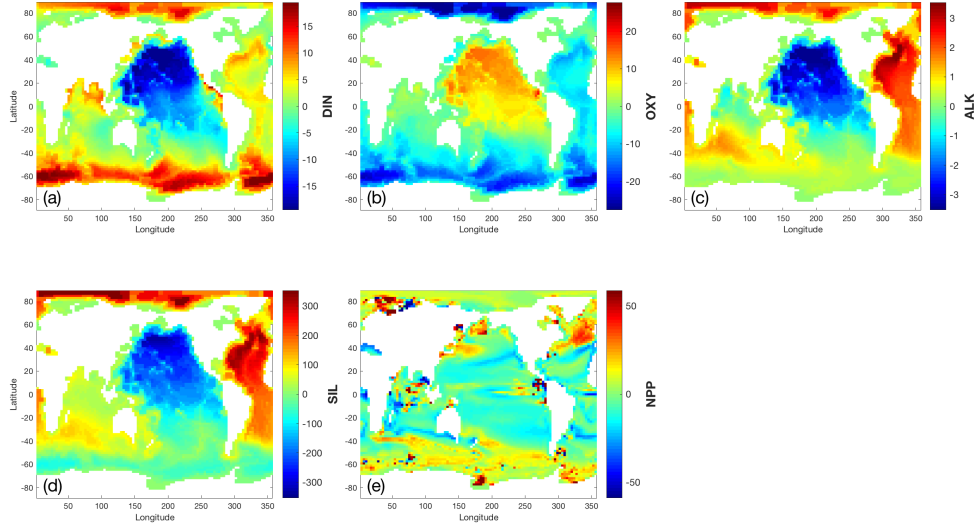


Figure 137: Change in column inventory of (a) DIN, (b) OXY, (c) ALK, (d) SIL, and (e) NPP after a +10% perturbation in x_{mzmi} , the micro-zooplankton maximum loss rate.

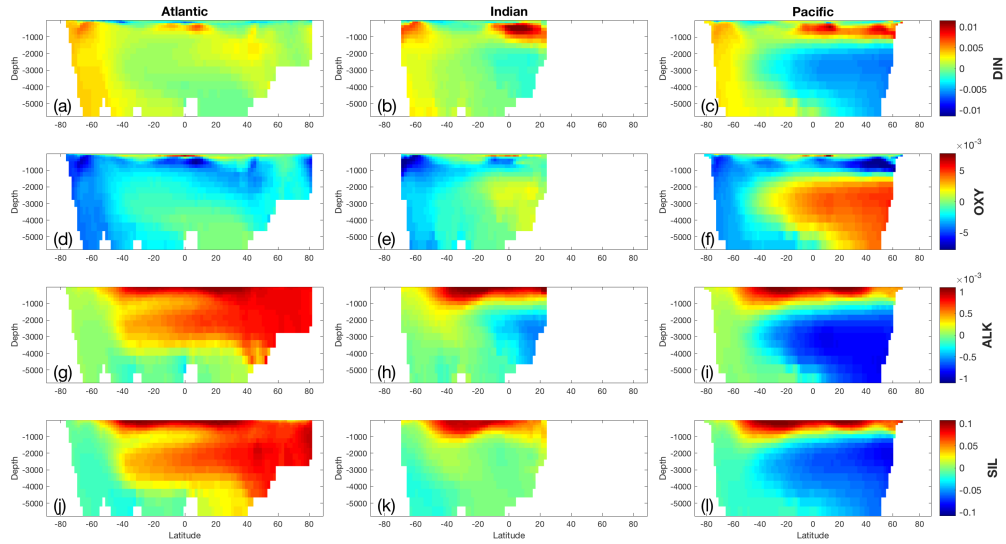


Figure 138: Change in volume-weighted zonally averaged (a-c) DIN, (d-f) OXY, (g-i) ALK, and (j-l) SIL after a +10% perturbation in x_{mzmi} , the micro-zooplankton maximum loss rate, for the (left) Atlantic, (middle) Indian, and (right) Pacific Oceans.

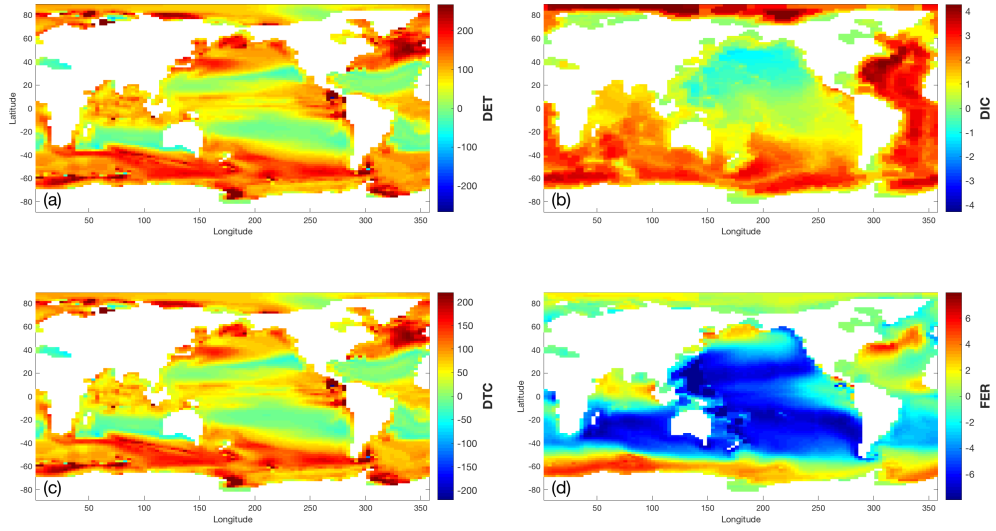


Figure 139: Change in column inventory of (a) DET, (b) DIC, (c) DTC, and (d) FER after a +10% perturbation in xzmzi, the micro-zooplankton maximum loss rate.

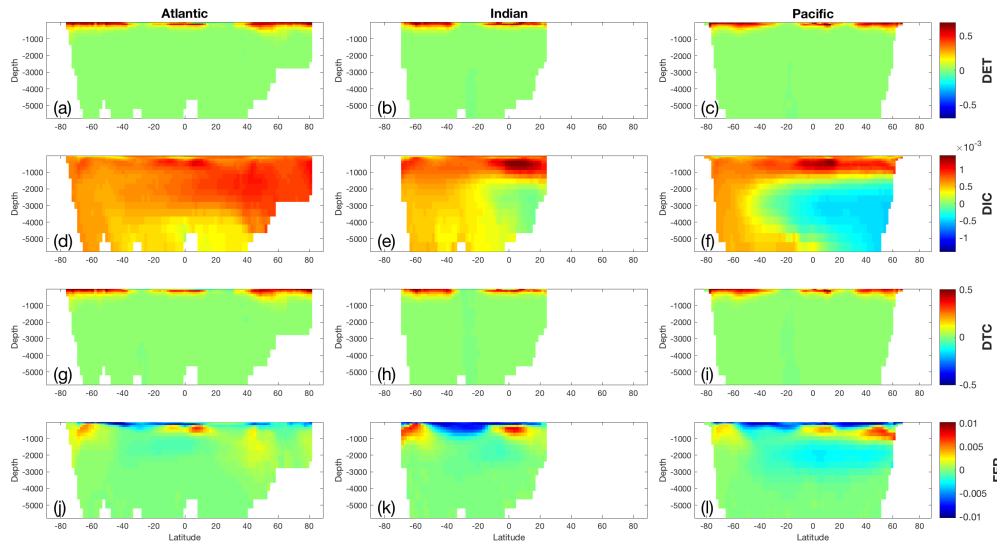


Figure 140: Change in volume-weighted zonally averaged (a-c) DET, (d-f) DIC, (g-i) DTC, and (j-l) FER after a +10% perturbation in xzmzi, the micro-zooplankton maximum loss rate, for the (left) Atlantic, (middle) Indian, and (right) Pacific Oceans.

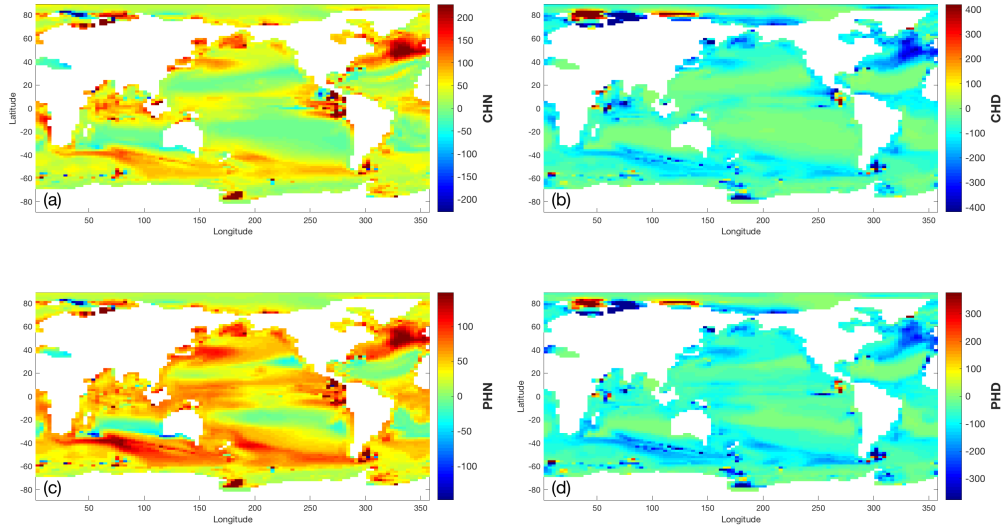


Figure 141: Change in column inventory of (a) CHN, (b) CHD, (c) PHN, and (d) PHD. after a +10% perturbation in xzmzi, the micro-zooplankton maximum loss rate.

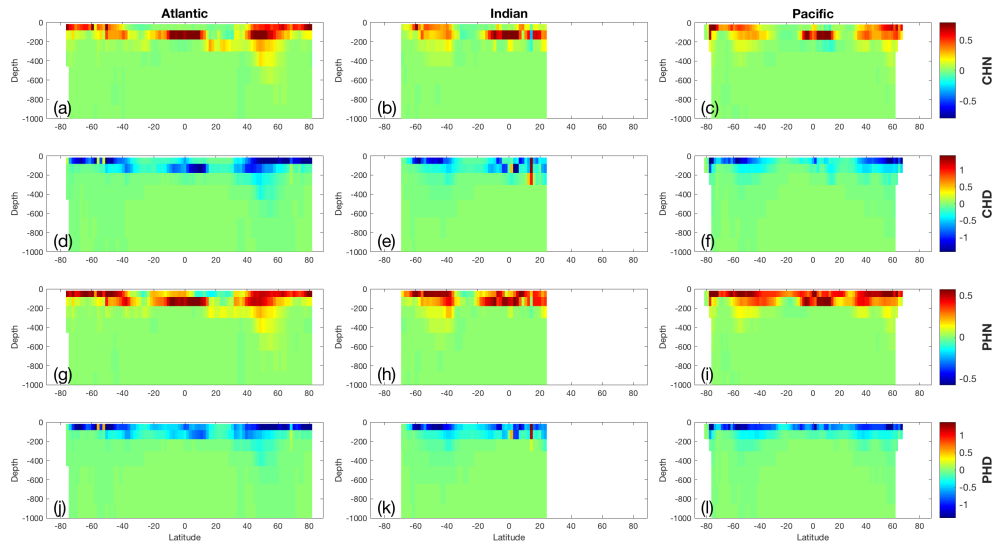


Figure 142: Change in volume-weighted zonally averaged (a-c) CHN, (d-f) CHD, (g-i) PHN, and (j-l) PHD after a +10% perturbation in xzmzi, the micro-zooplankton maximum loss rate, for the (left) Atlantic, (middle) Indian, and (right) Pacific Oceans.

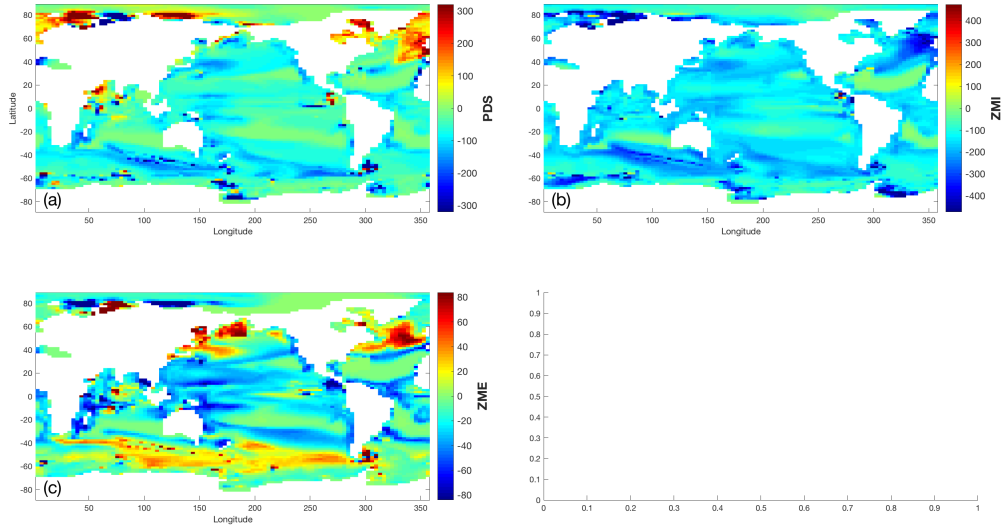


Figure 143: Change in column inventory of (a) PDS, (b) ZMI, and (c) ZME, after a +10% perturbation in x_{mzmi} , the micro-zooplankton maximum loss rate.

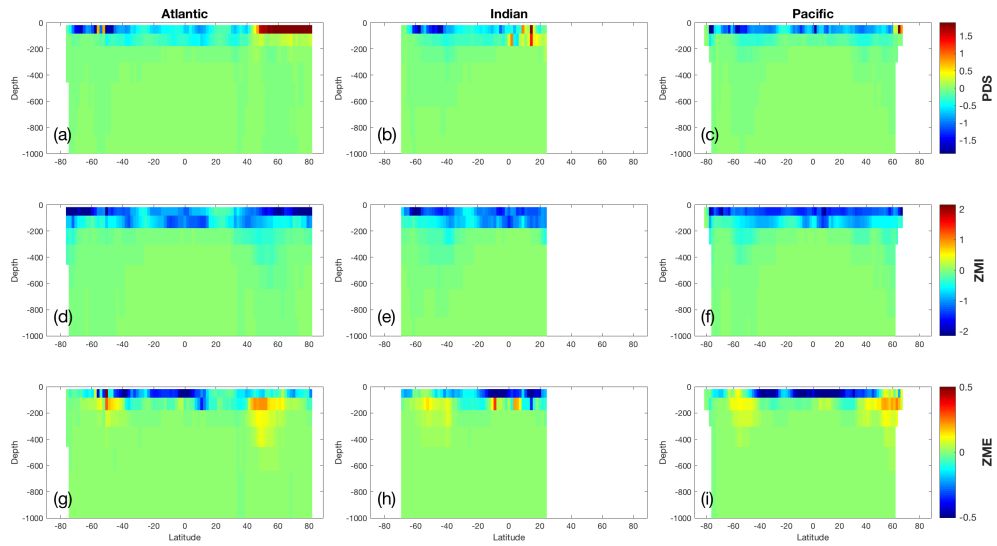


Figure 144: Change in volume-weighted zonally averaged (a-c) PDS, (d-f) ZMI, and (g-i) ZME after a +10% perturbation in x_{mzmi} , the micro-zooplankton maximum loss rate, for the (left) Atlantic, (middle) Indian, and (right) Pacific Oceans.

- 20 Parameter `xnld`: the diatom nitrogen nutrient uptake half-saturation constant.

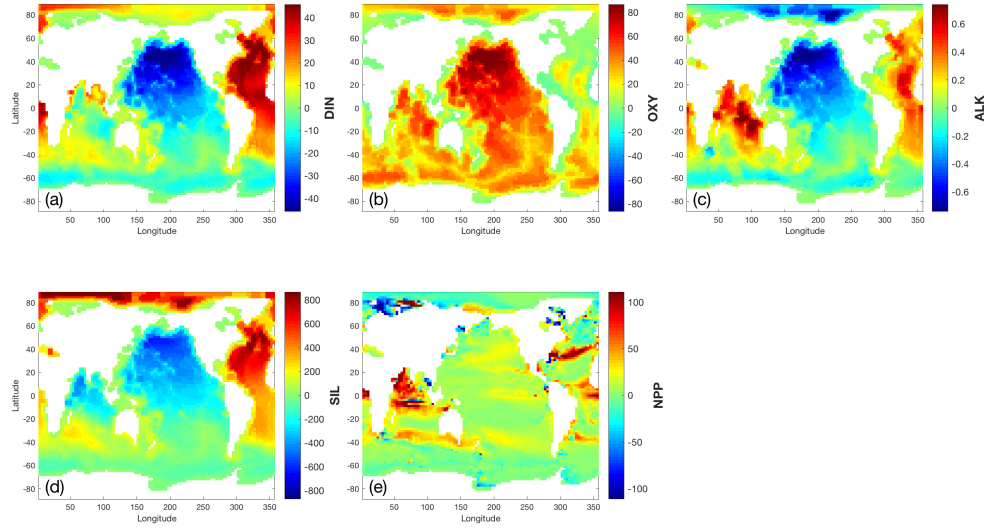


Figure 145: Change in column inventory of (a) DIN, (b) OXY, (c) ALK, (d) SIL, and (e) NPP after a +10% perturbation in $xnld$, the diatom nitrogen nutrient uptake half-saturation constant.

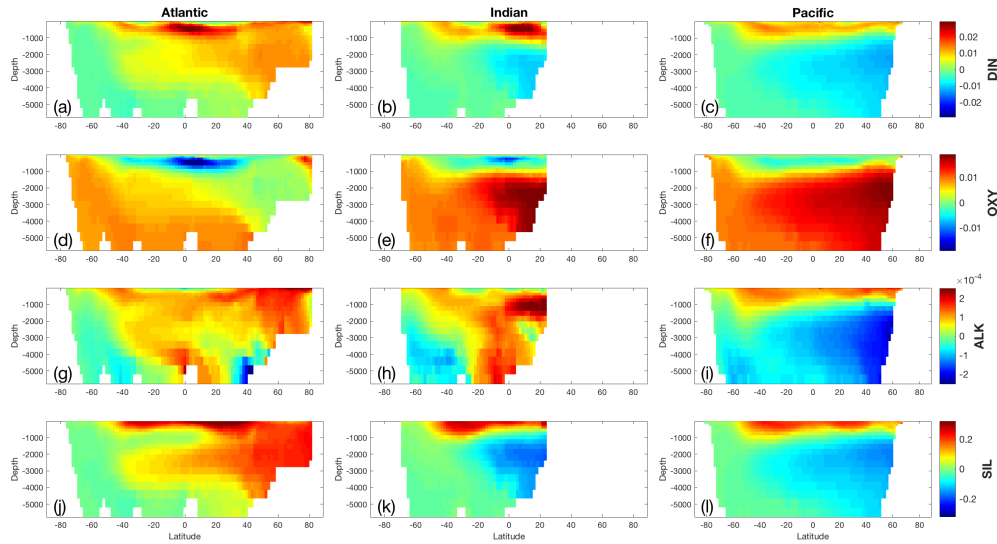


Figure 146: Change in volume-weighted zonally averaged (a-c) DIN, (d-f) OXY, (g-i) ALK, and (j-l) SIL after a +10% perturbation in $xnld$, the diatom nitrogen nutrient uptake half-saturation constant, for the (left) Atlantic, (middle) Indian, and (right) Pacific Oceans.

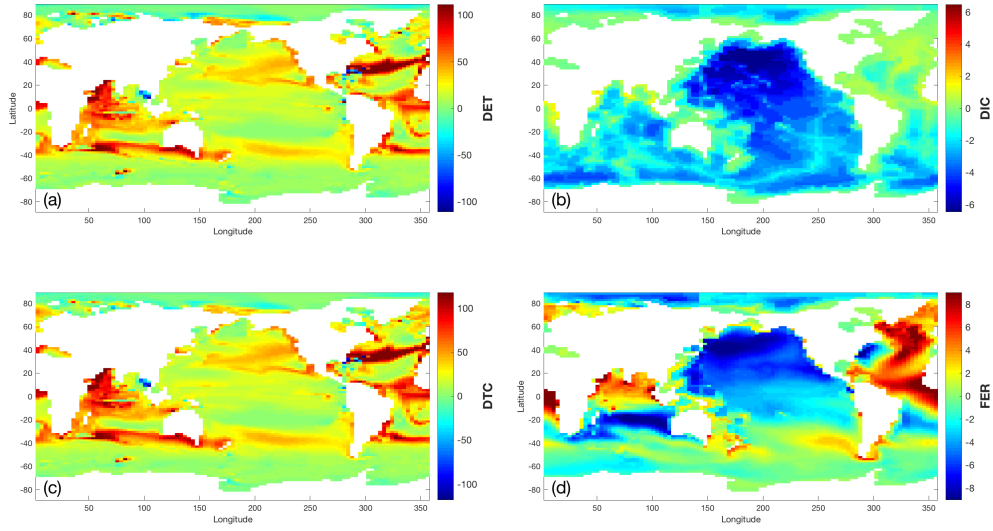


Figure 147: Change in column inventory of (a) DET, (b) DIC, (c) DTC, and (d) FER after a +10% perturbation in $xnld$, the diatom nitrogen nutrient uptake half-saturation constant.

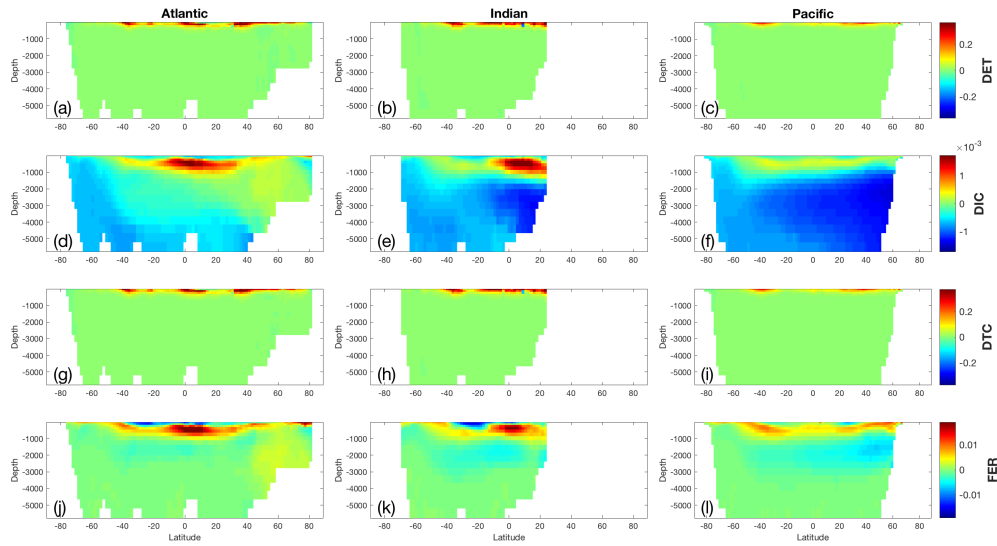


Figure 148: Change in volume-weighted zonally averaged (a-c) DET, (d-f) DIC, (g-i) DTC, and (j-l) FER after a +10% perturbation in $xnld$, the diatom nitrogen nutrient uptake half-saturation constant, for the (left) Atlantic, (middle) Indian, and (right) Pacific Oceans.

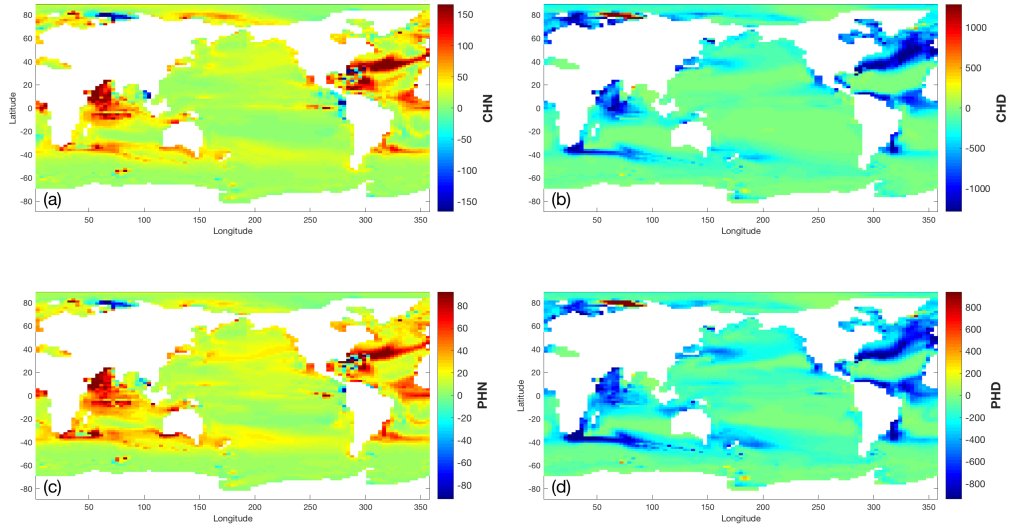


Figure 149: Change in column inventory of (a) CHN, (b) CHD, (c) PHN, and (d) PHD after a +10% perturbation in x_{nld} , the diatom nitrogen nutrient uptake half-saturation constant.

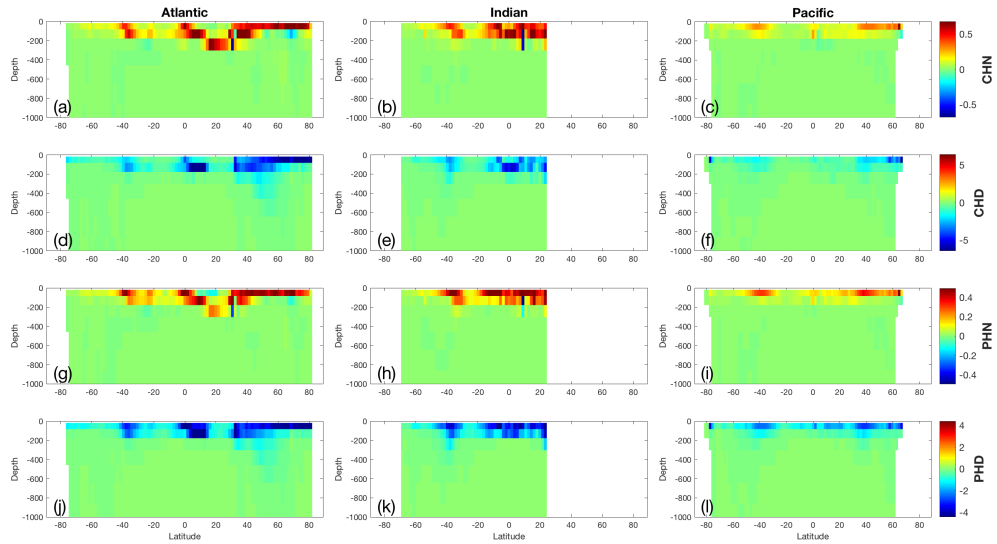


Figure 150: Change in volume-weighted zonally averaged (a-c) CHN, (d-f) CHD, (g-i) PHN, and (j-l) PHD after a +10% perturbation in x_{nld} , the diatom nitrogen nutrient uptake half-saturation constant, for the (left) Atlantic, (middle) Indian, and (right) Pacific Oceans.

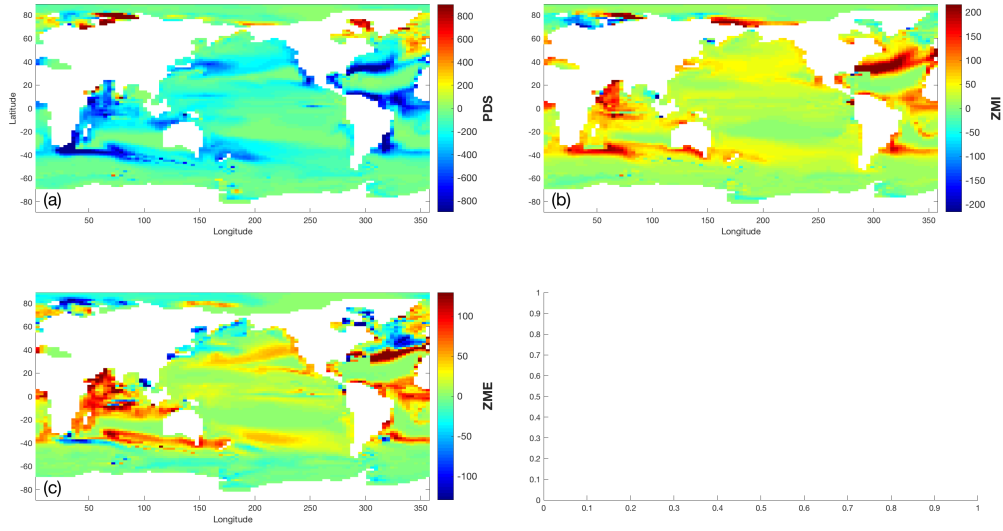


Figure 151: Change in column inventory of (a) PDS, (b) ZMI, and (c) ZME, after a +10% perturbation in $xnld$, the diatom nitrogen nutrient uptake half-saturation constant.

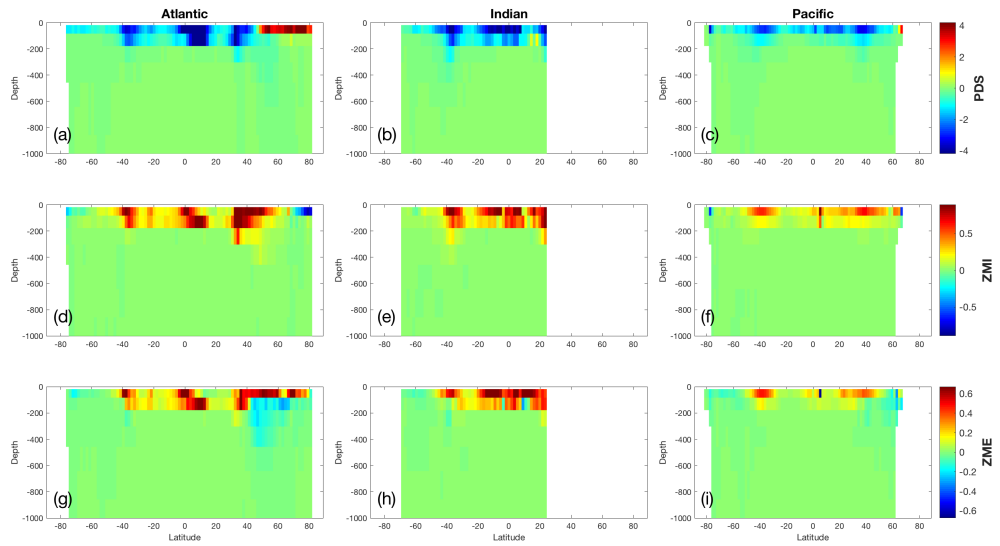


Figure 152: Change in volume-weighted zonally averaged (a-c) PDS, (d-f) ZMI, and (g-i) ZME after a +10% perturbation in $xnld$, the diatom nitrogen nutrient uptake half-saturation constant, for the (left) Atlantic, (middle) Indian, and (right) Pacific Oceans.

- 21 Parameter `xnln`: the non-diatom nitrogen nutrient uptake half-saturation constant.

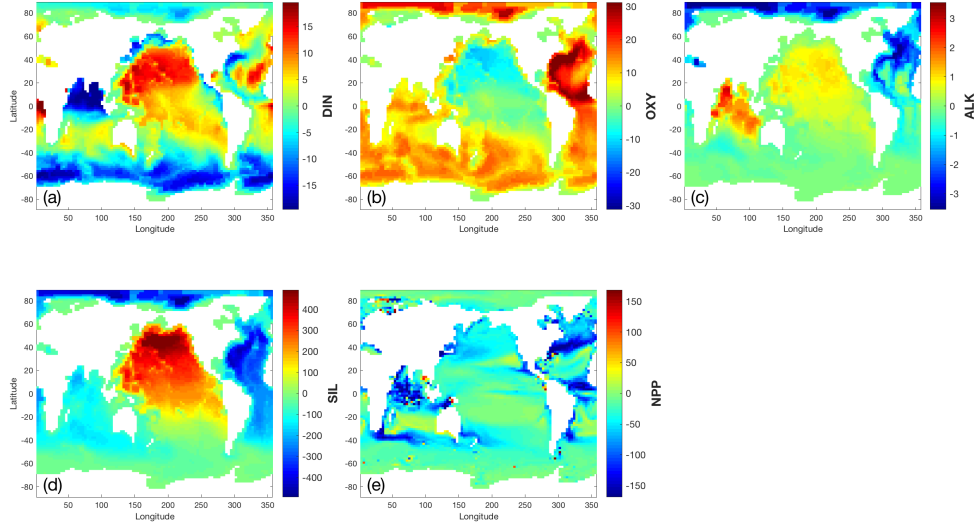


Figure 153: Change in column inventory of (a) DIN, (b) OXY, (c) ALK, (d) SIL, and (e) NPP after a +10% perturbation in $x_{nl,n}$, the non-diatom nitrogen nutrient uptake half-saturation constant.

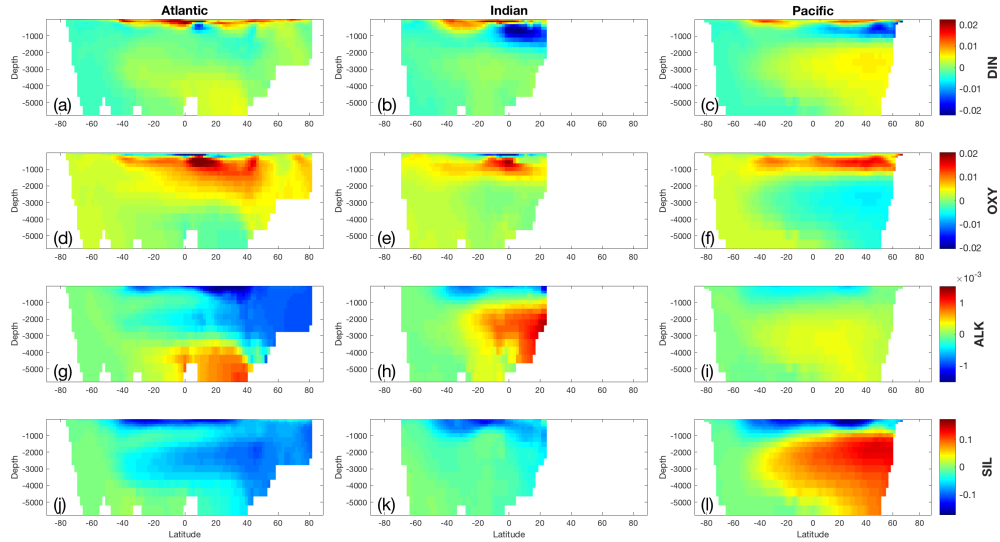


Figure 154: Change in volume-weighted zonally averaged (a-c) DIN, (d-f) OXY, (g-i) ALK, and (j-l) SIL after a +10% perturbation in $x_{nl,n}$, the non-diatom nitrogen nutrient uptake half-saturation constant, for the (left) Atlantic, (middle) Indian, and (right) Pacific Oceans.

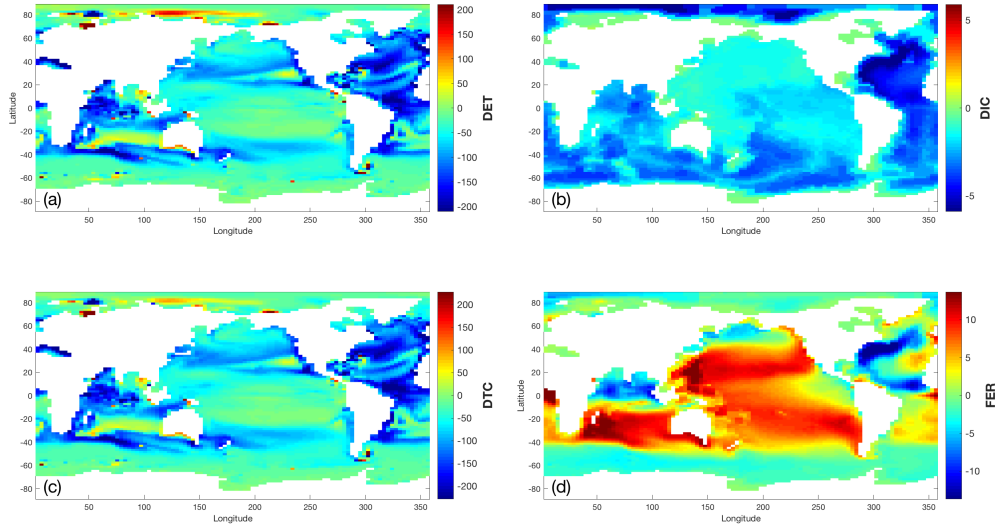


Figure 155: Change in column inventory of (a) DET, (b) DIC, (c) DTC, and (d) FER after a +10% perturbation in x_{nlm} , the non-diatom nitrogen nutrient uptake half-saturation constant.

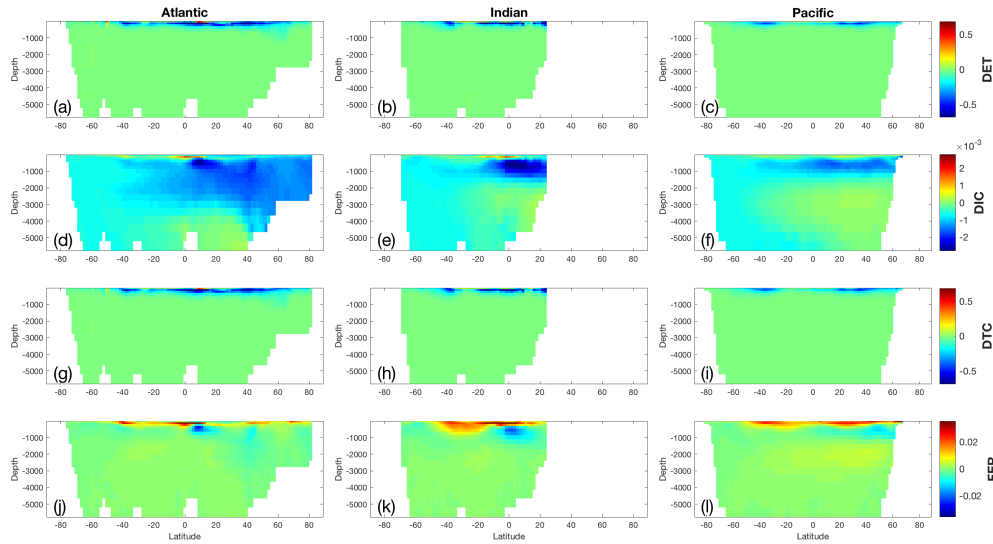


Figure 156: Change in volume-weighted zonally averaged (a-c) DET, (d-f) DIC, (g-i) DTC, and (j-l) FER after a +10% perturbation in x_{nlm} , the non-diatom nitrogen nutrient uptake half-saturation constant, for the (left) Atlantic, (middle) Indian, and (right) Pacific Oceans.

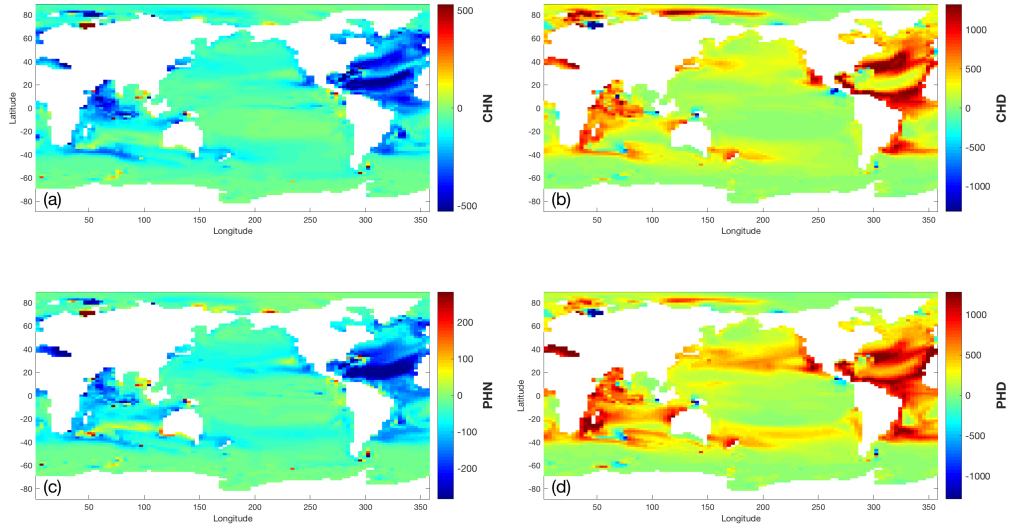


Figure 157: Change in column inventory of (a) CHN, (b) CHD, (c) PHN, and (d) PHD after a +10% perturbation in x_{nlm} , the non-diatom nitrogen nutrient uptake half-saturation constant.

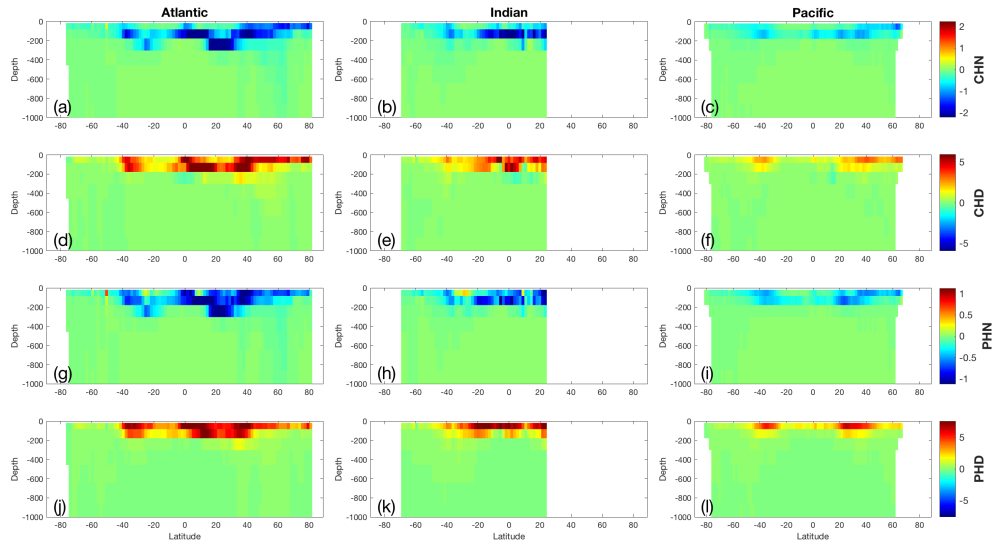


Figure 158: Change in volume-weighted zonally averaged (a-c) CHN, (d-f) CHD, (g-i) PHN, and (j-l) PHD after a +10% perturbation in x_{nlm} , the non-diatom nitrogen nutrient uptake half-saturation constant, for the (left) Atlantic, (middle) Indian, and (right) Pacific Oceans.

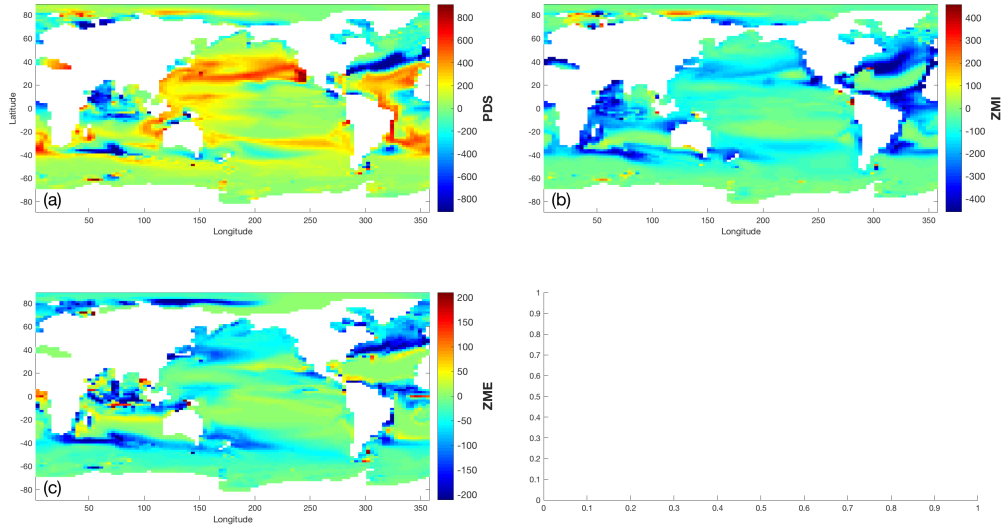


Figure 159: Change in column inventory of (a) PDS, (b) ZMI, and (c) ZME, after a +10% perturbation in x_{nlm} , the non-diatom nitrogen nutrient uptake half-saturation constant.

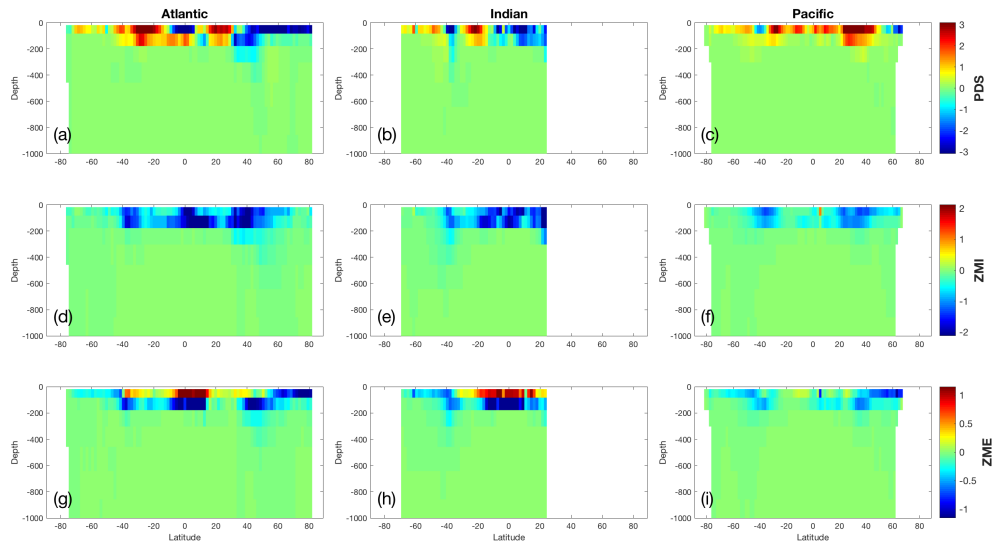


Figure 160: Change in volume-weighted zonally averaged (a-c) PDS, (d-f) ZMI, and (g-i) ZME after a +10% perturbation in x_{nlm} , the non-diatom nitrogen nutrient uptake half-saturation constant, for the (left) Atlantic, (middle) Indian, and (right) Pacific Oceans.

22 Parameter xsld: the diatom silicon nutrient uptake half-saturation constant.

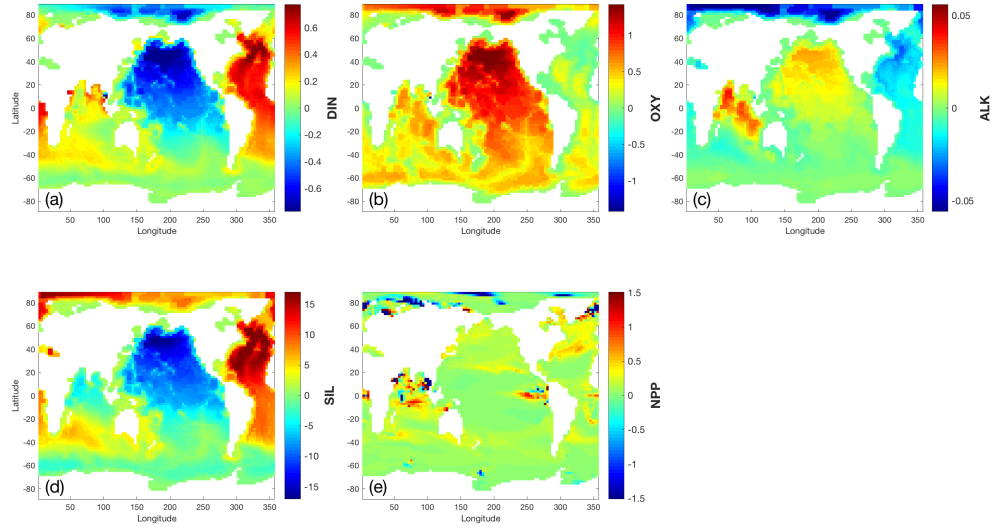


Figure 161: Change in column inventory of (a) DIN, (b) OXY, (c) ALK, (d) SIL, and (e) NPP after a +10% perturbation in $xsld$, the diatom silicon nutrient uptake half-saturation constant.

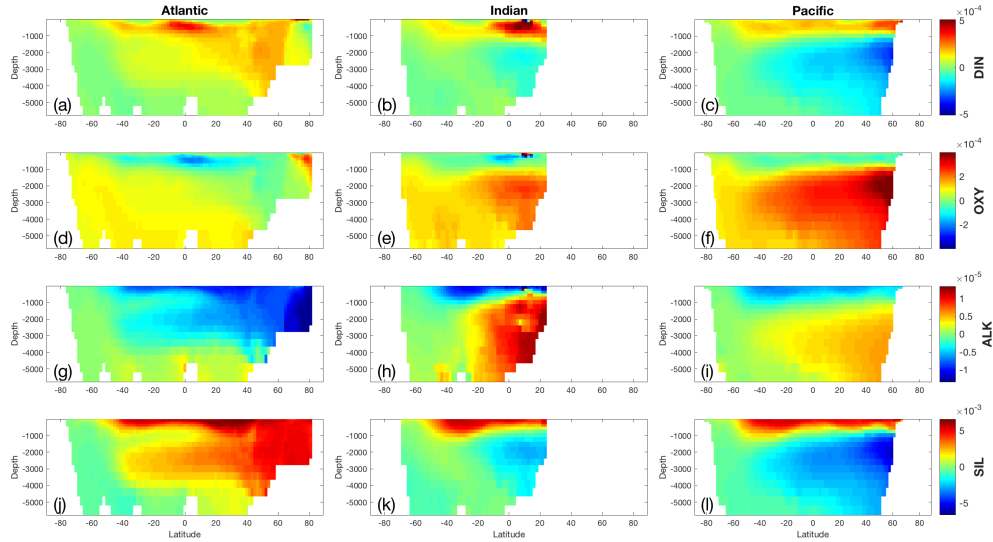


Figure 162: Change in volume-weighted zonally averaged (a-c) DIN, (d-f) OXY, (g-i) ALK, and (j-l) SIL after a +10% perturbation in $xsld$, the diatom silicon nutrient uptake half-saturation constant, for the (left) Atlantic, (middle) Indian, and (right) Pacific Oceans.

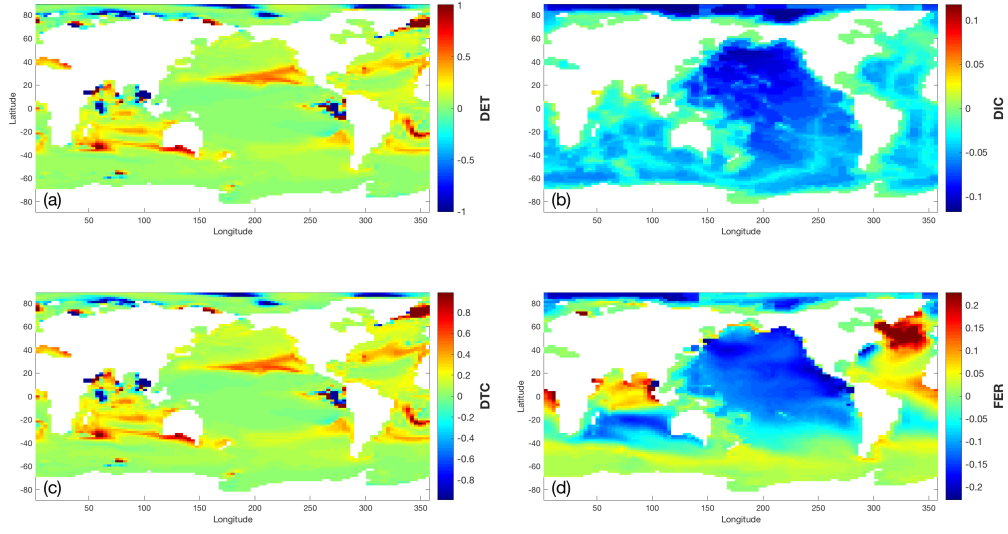


Figure 163: Change in column inventory of (a) DET, (b) DIC, (c) DTC, and (d) FER after a +10% perturbation in xsld, the diatom silicon nutrient uptake half-saturation constant.

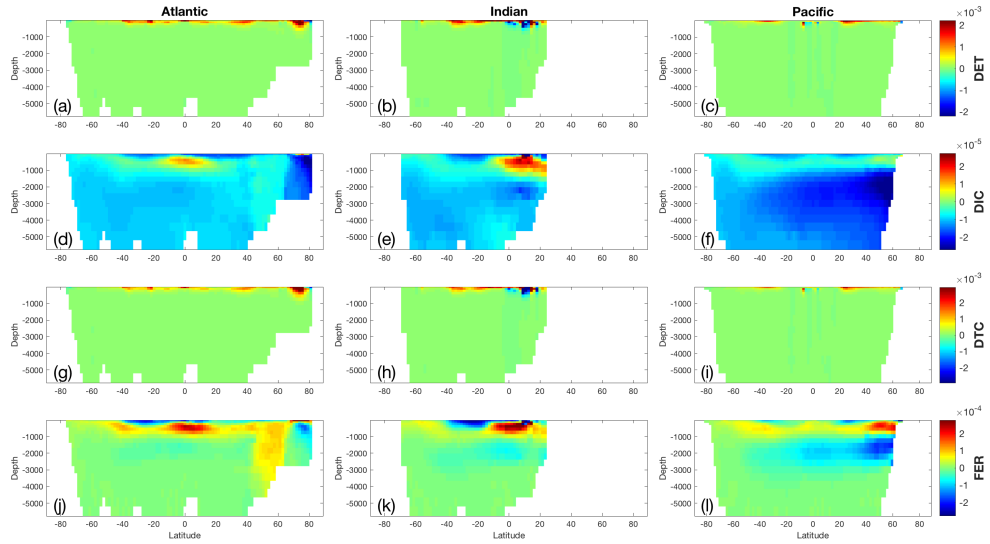


Figure 164: Change in volume-weighted zonally averaged (a-c) DET, (d-f) DIC, (g-i) DTC, and (j-l) FER after a +10% perturbation in xsld, the diatom silicon nutrient uptake half-saturation constant, for the (left) Atlantic, (middle) Indian, and (right) Pacific Oceans.

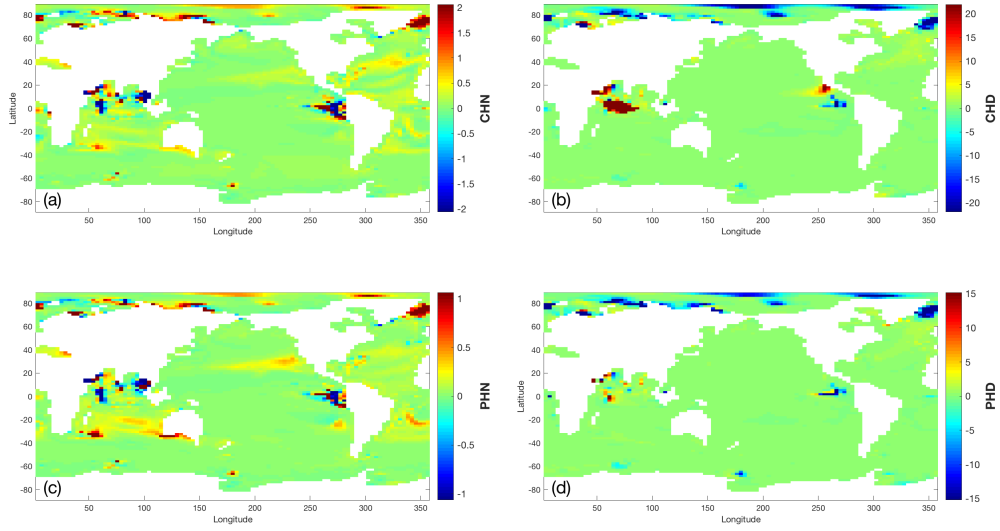


Figure 165: Change in column inventory of (a) CHN, (b) CHD, (c) PHN, and (d) PHD. after a +10% perturbation in $xsld$, the diatom silicon nutrient uptake half-saturation constant.

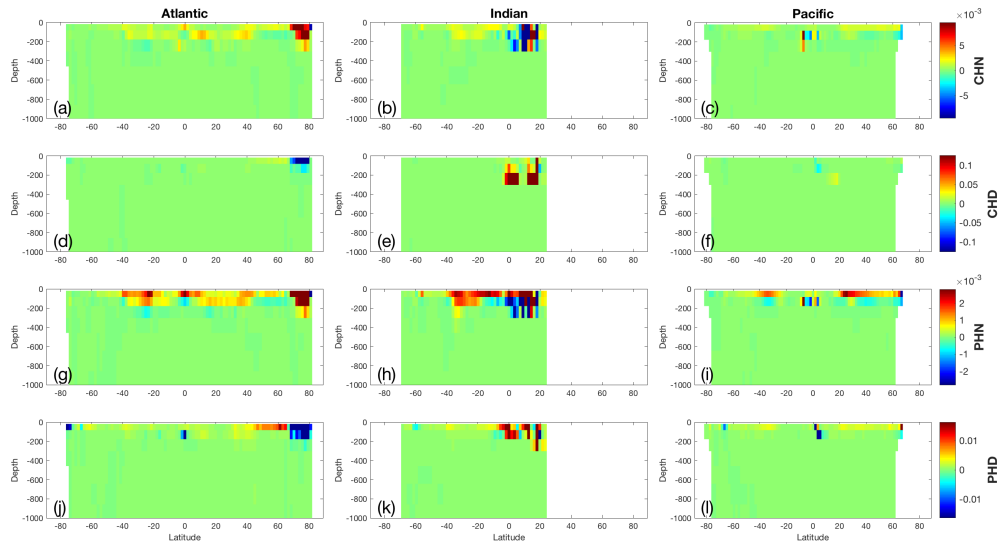


Figure 166: Change in volume-weighted zonally averaged (a-c) CHN, (d-f) CHD, (g-i) PHN, and (j-l) PHD after a +10% perturbation in $xsld$, the diatom silicon nutrient uptake half-saturation constant, for the (left) Atlantic, (middle) Indian, and (right) Pacific Oceans.

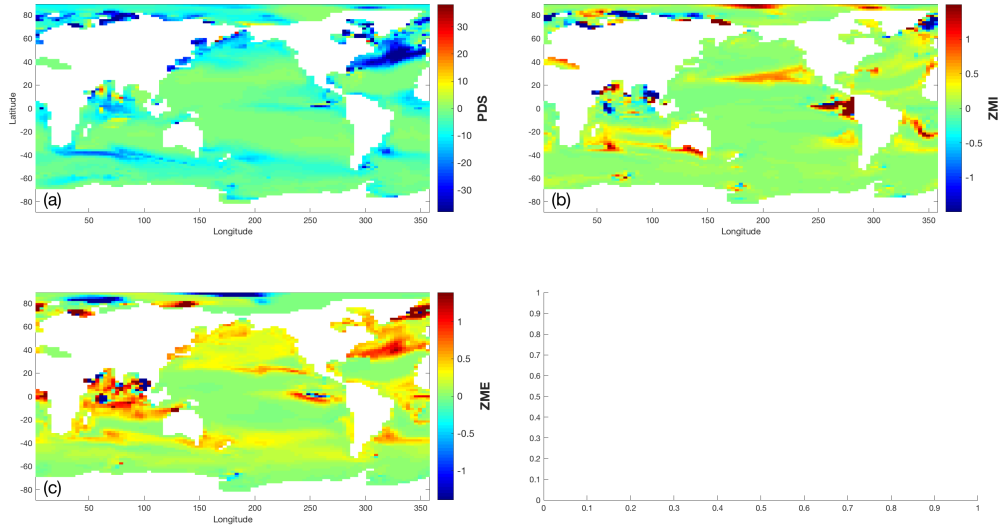


Figure 167: Change in column inventory of (a) PDS, (b) ZMI, and (c) ZME, after a +10% perturbation in x_{sld} , the diatom silicon nutrient uptake half-saturation constant.

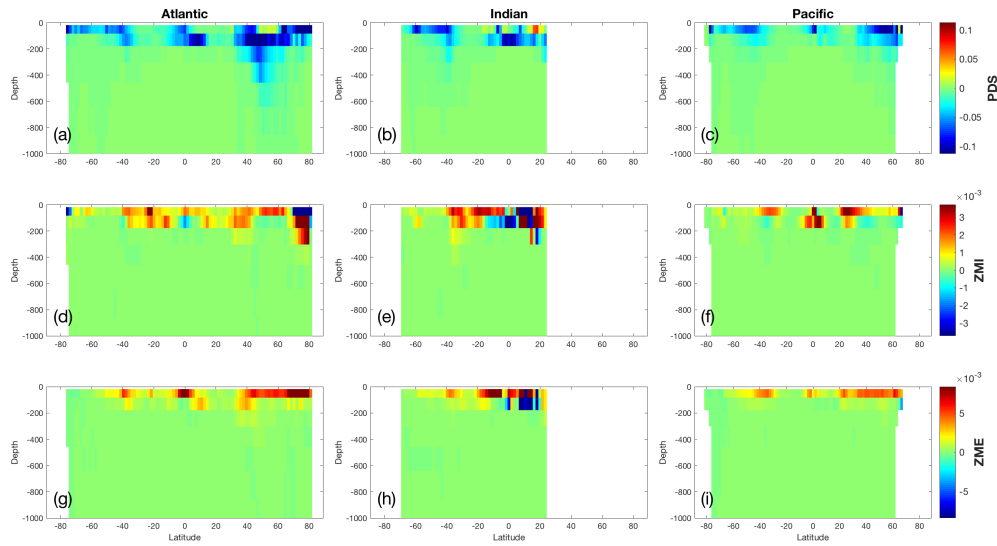


Figure 168: Change in volume-weighted zonally averaged (a-c) PDS, (d-f) ZMI, and (g-i) ZME after a +10% perturbation in x_{sld} , the diatom silicon nutrient uptake half-saturation constant, for the (left) Atlantic, (middle) Indian, and (right) Pacific Oceans.

23 Parameter xthetanit: the oxygen consumption by nitrogen remineralisation.

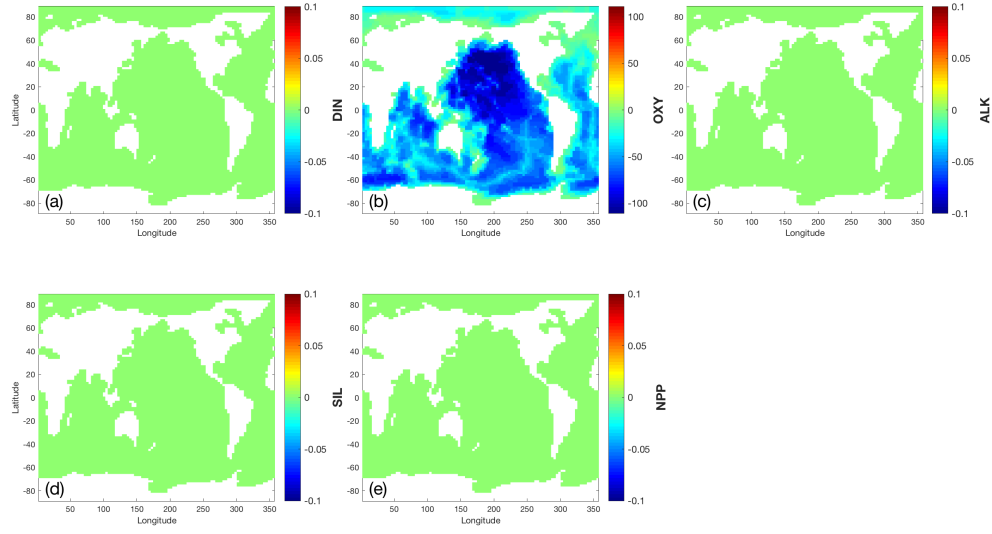


Figure 169: Change in column inventory of (a) DIN, (b) OXY, (c) ALK, (d) SIL, and (e) NPP after a +10% perturbation in xthetanit, the oxygen consumption by nitrogen remineralisation.

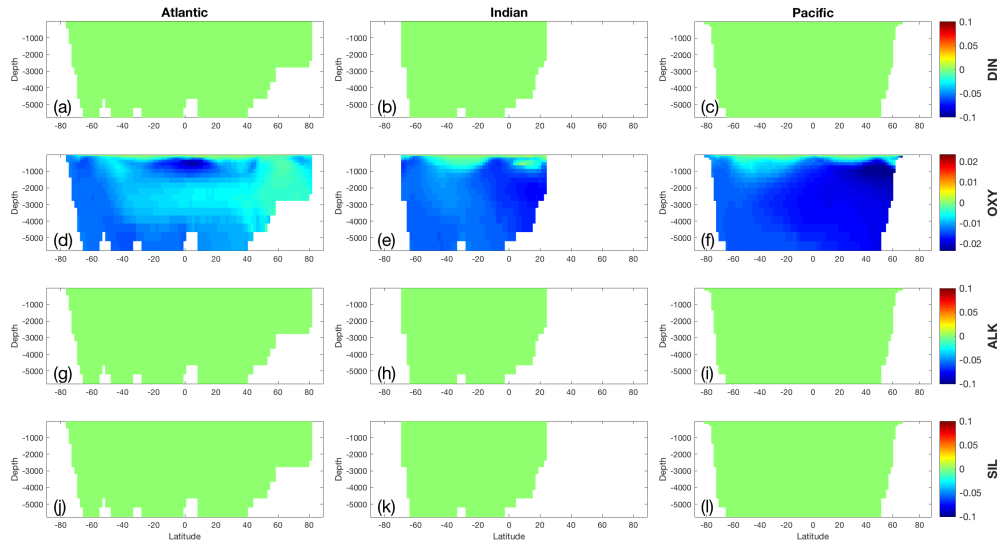


Figure 170: Change in volume-weighted zonally averaged (a-c) DIN, (d-f) OXY, (g-i) ALK, and (j-l) SIL after a +10% perturbation in xthetanit, the oxygen consumption by nitrogen remineralisation, for the (left) Atlantic, (middle) Indian, and (right) Pacific Oceans.

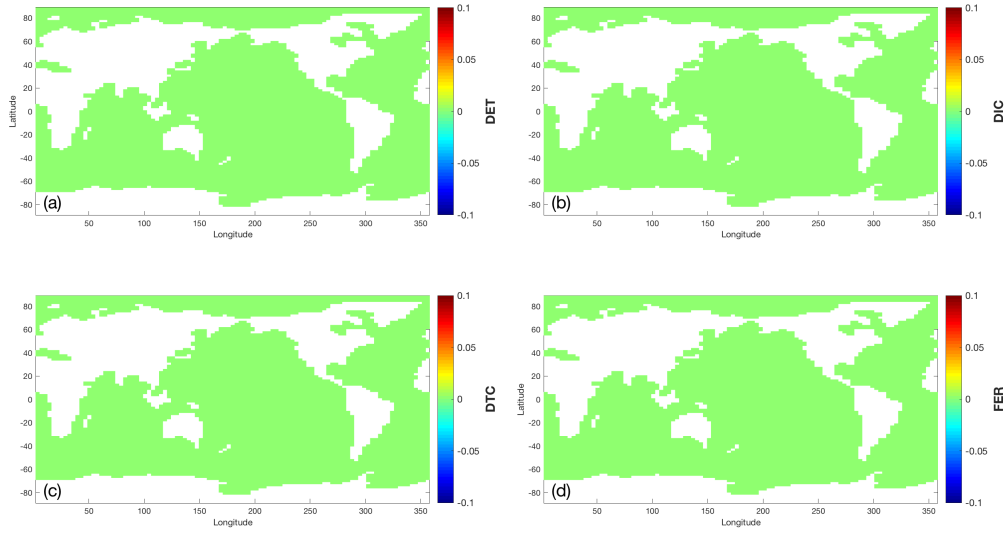


Figure 171: Change in column inventory of (a) DET, (b) DIC, (c) DTC, and (d) FER after a +10% perturbation in x_{thetanit} , the oxygen consumption by nitrogen remineralisation.

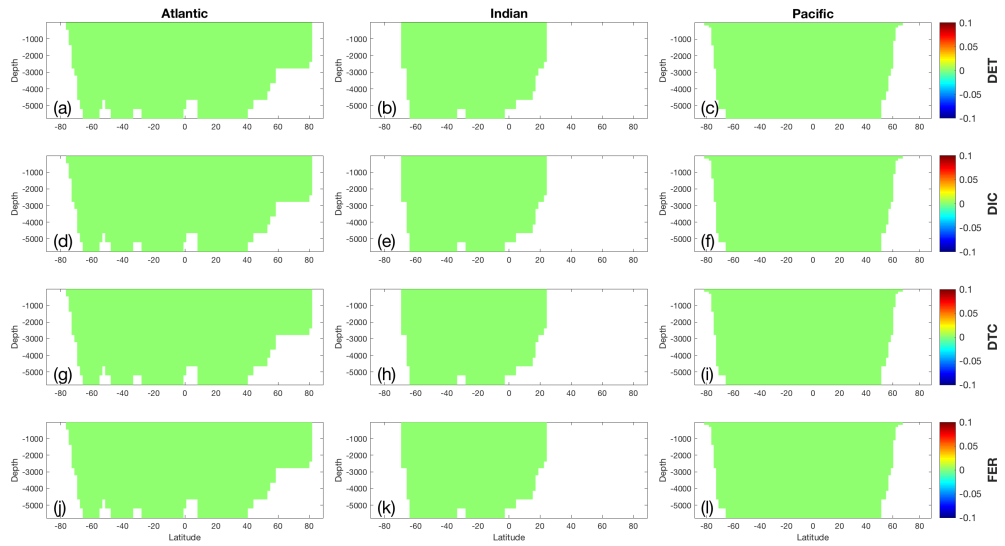


Figure 172: Change in volume-weighted zonally averaged (a-c) DET, (d-f) DIC, (g-i) DTC, and (j-l) FER after a +10% perturbation in x_{thetanit} , the oxygen consumption by nitrogen remineralisation, for the (left) Atlantic, (middle) Indian, and (right) Pacific Oceans.

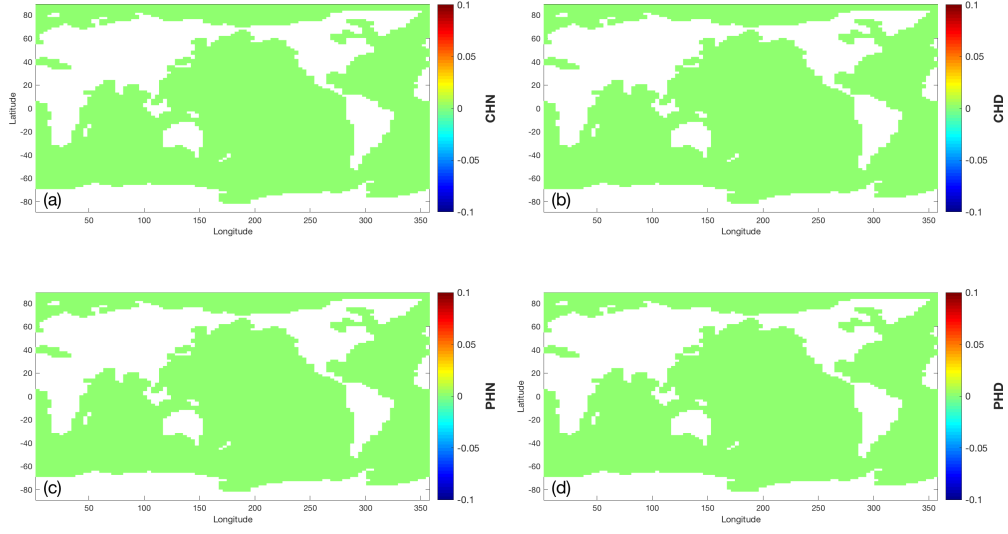


Figure 173: Change in column inventory of (a) CHN, (b) CHD, (c) PHN, and (d) PHD. after a +10% perturbation in x_{thetanit} , the oxygen consumption by nitrogen remineralisation.

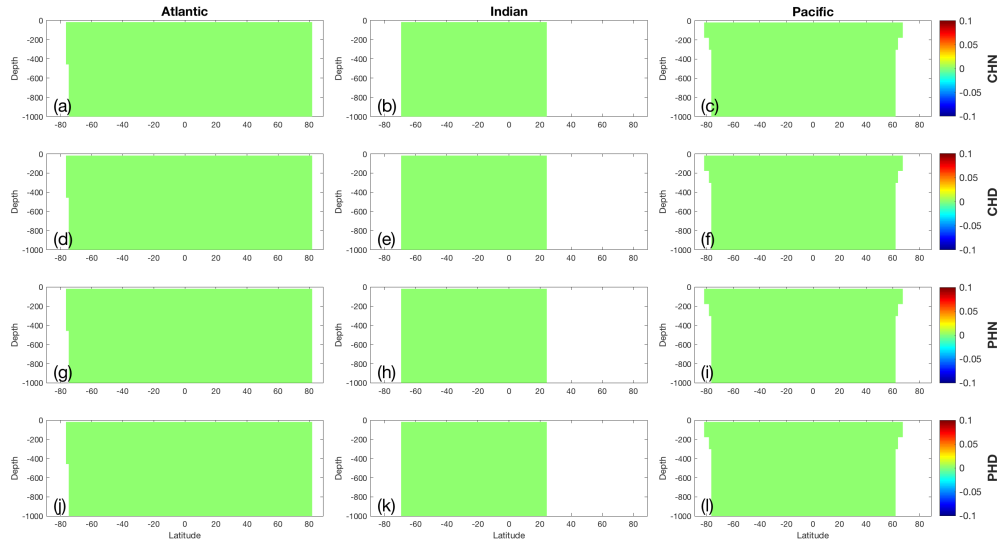


Figure 174: Change in volume-weighted zonally averaged (a-c) CHN, (d-f) CHD, (g-i) PHN, and (j-l) PHD after a +10% perturbation in x_{thetanit} , the oxygen consumption by nitrogen remineralisation, for the (left) Atlantic, (middle) Indian, and (right) Pacific Oceans.

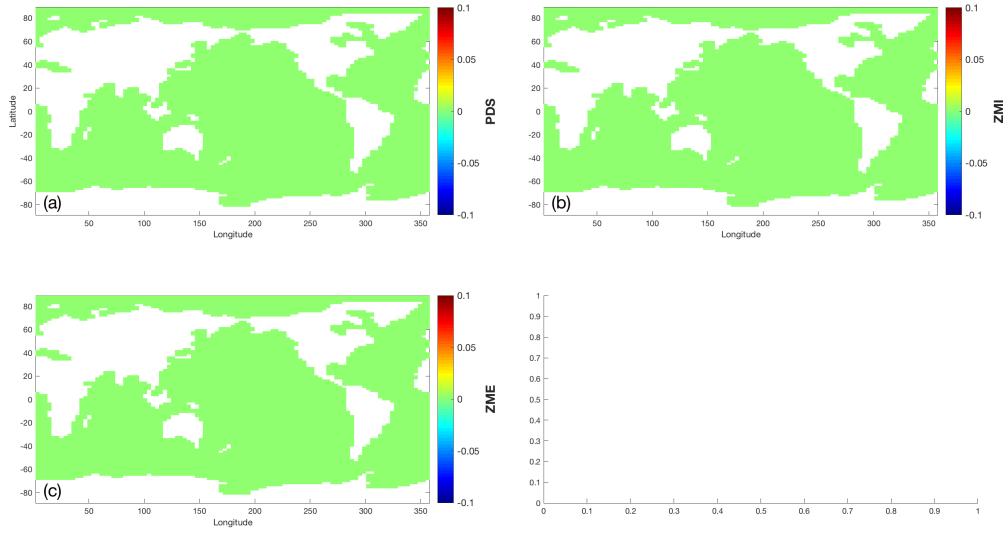


Figure 175: Change in column inventory of (a) PDS, (b) ZMI, and (c) ZME, after a +10% perturbation in xthetanit, the oxygen consumption by nitrogen remineralisation.

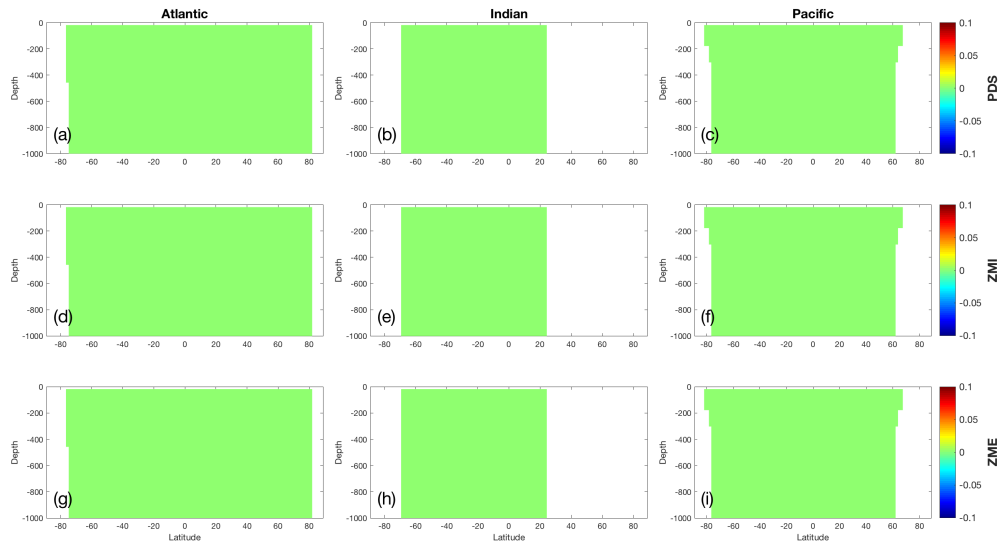


Figure 176: Change in volume-weighted zonally averaged (a-c) PDS, (d-f) ZMI, and (g-i) ZME after a +10% perturbation in xthetanit, the oxygen consumption by nitrogen remineralisation, for the (left) Atlantic, (middle) Indian, and (right) Pacific Oceans.

- 24 Parameter x_{thetarem} : the oxygen consumption by carbon remineralisation.

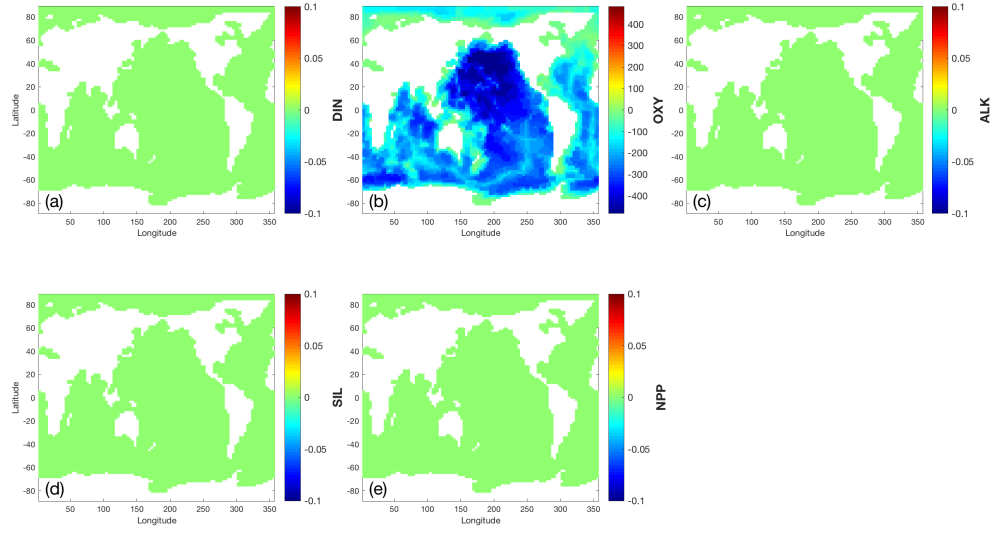


Figure 177: Change in column inventory of (a) DIN, (b) OXY, (c) ALK, (d) SIL, and (e) NPP after a +10% perturbation in $x_{thetarem}$, the oxygen consumption by carbon remineralisation.

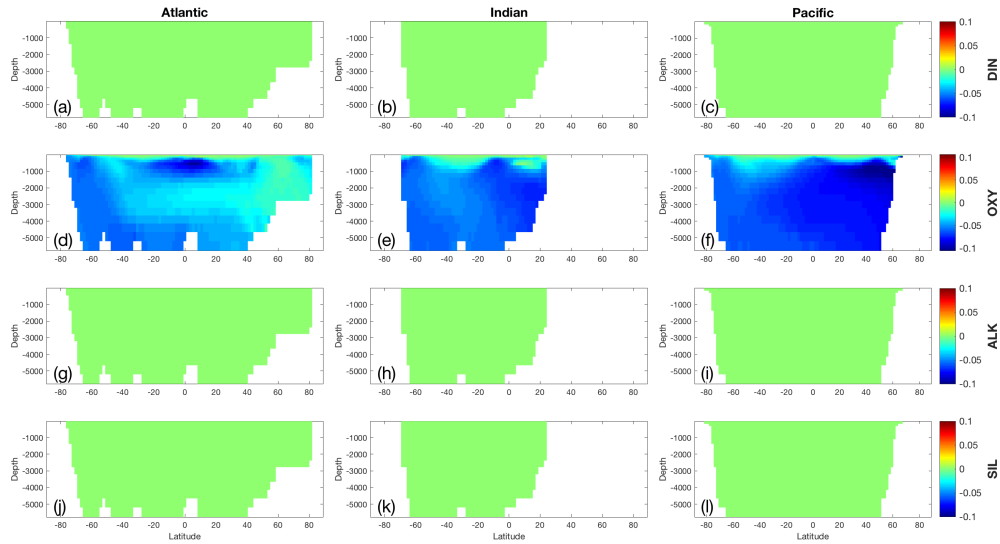


Figure 178: Change in volume-weighted zonally averaged (a-c) DIN, (d-f) OXY, (g-i) ALK, and (j-l) SIL after a +10% perturbation in $x_{thetarem}$, the oxygen consumption by carbon remineralisation, for the (left) Atlantic, (middle) Indian, and (right) Pacific Oceans.

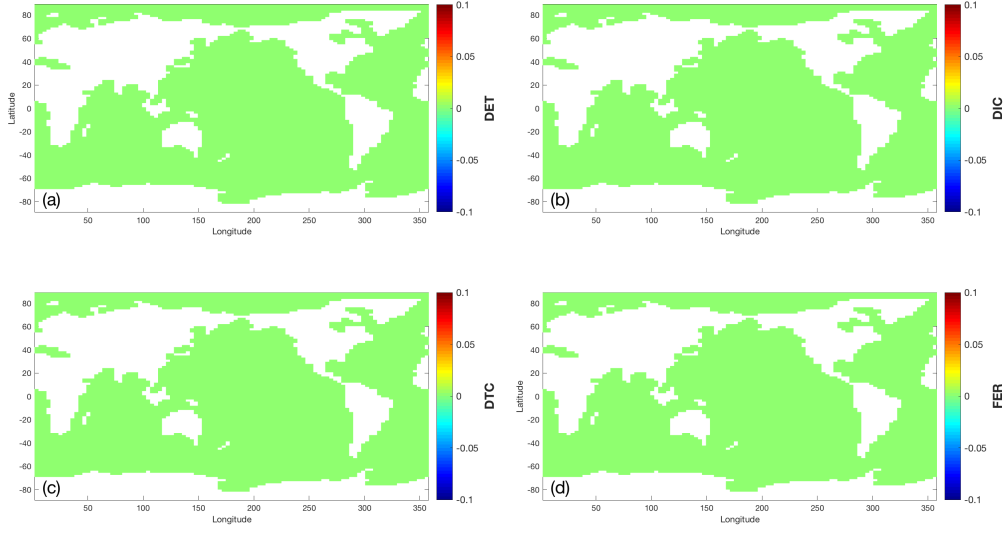


Figure 179: Change in column inventory of (a) DET, (b) DIC, (c) DTC, and (d) FER after a +10% perturbation in $x_{thetarem}$, the oxygen consumption by carbon remineralisation.

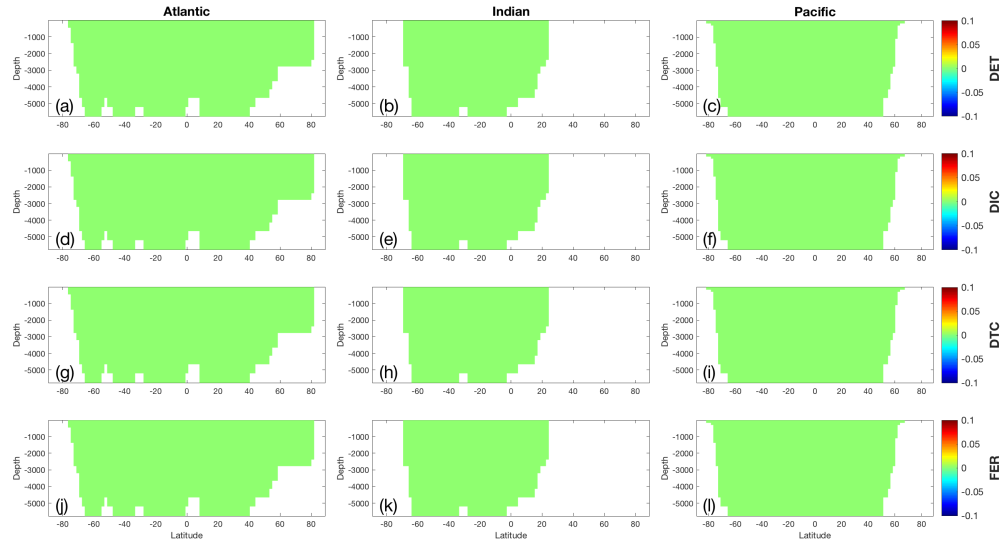


Figure 180: Change in volume-weighted zonally averaged (a-c) DET, (d-f) DIC, (g-i) DTC, and (j-l) FER after a +10% perturbation in $x_{thetarem}$, the oxygen consumption by carbon remineralisation, for the (left) Atlantic, (middle) Indian, and (right) Pacific Oceans.

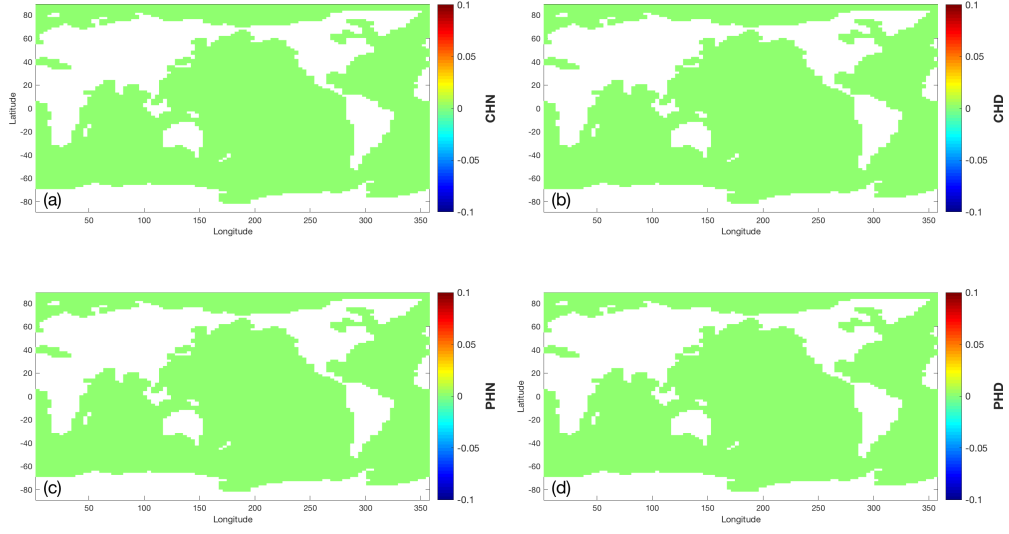


Figure 181: Change in column inventory of (a) CHN, (b) CHD, (c) PHN, and (d) PHD. after a +10% perturbation in x_{thetarem} , the oxygen consumption by carbon remineralisation.

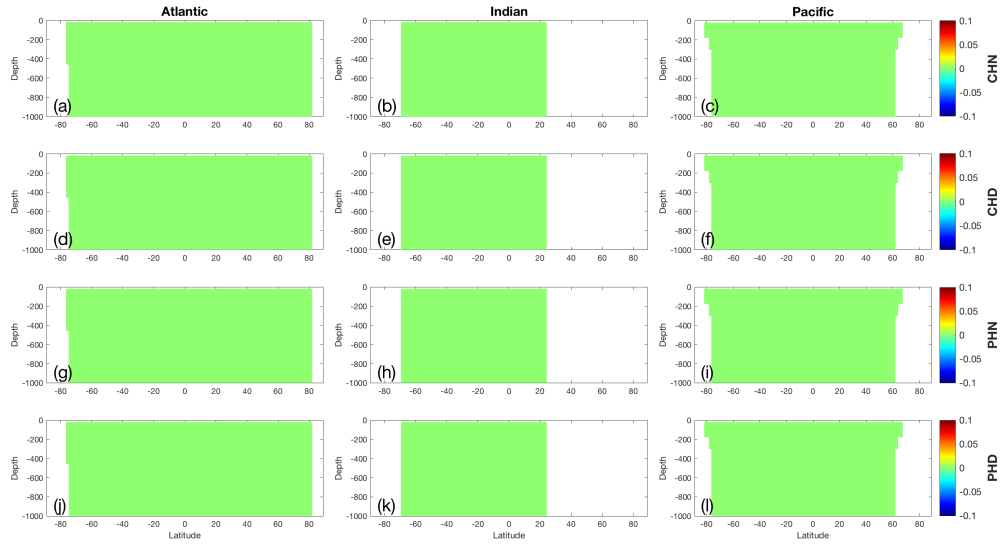


Figure 182: Change in volume-weighted zonally averaged (a-c) CHN, (d-f) CHD, (g-i) PHN, and (j-l) PHD after a +10% perturbation in x_{thetarem} , the oxygen consumption by carbon remineralisation, for the (left) Atlantic, (middle) Indian, and (right) Pacific Oceans.

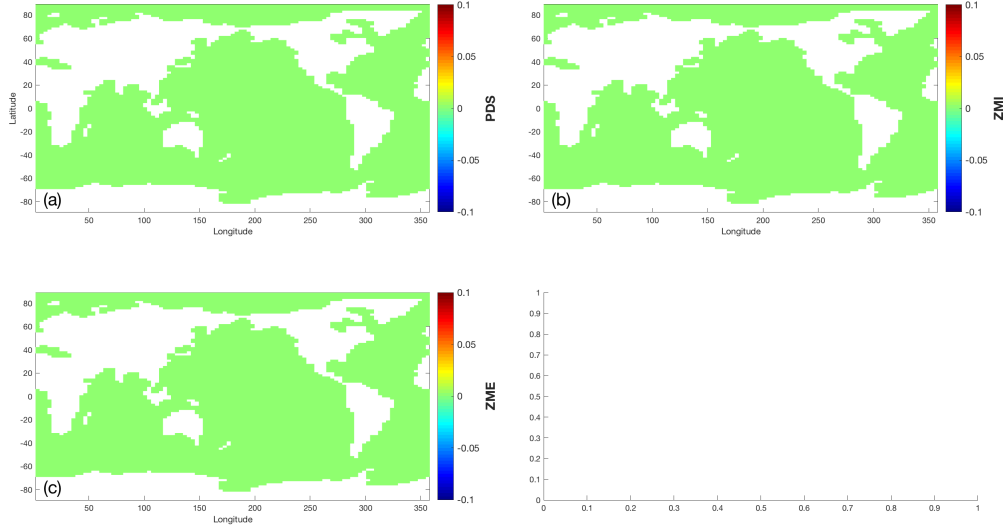


Figure 183: Change in column inventory of (a) PDS, (b) ZMI, and (c) ZME, after a +10% perturbation in x_{thetarem} , the oxygen consumption by carbon remineralisation.

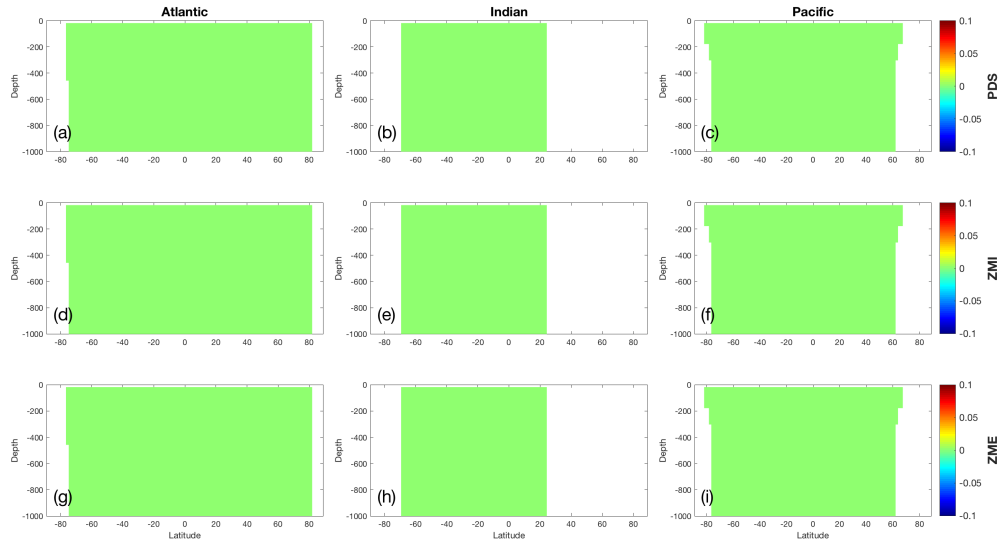


Figure 184: Change in volume-weighted zonally averaged (a-c) PDS, (d-f) ZMI, and (g-i) ZME after a +10% perturbation in x_{thetarem} , the oxygen consumption by carbon remineralisation, for the (left) Atlantic, (middle) Indian, and (right) Pacific Oceans.

25 Parameter `xvpd`: the maximum growth rate for diatoms.

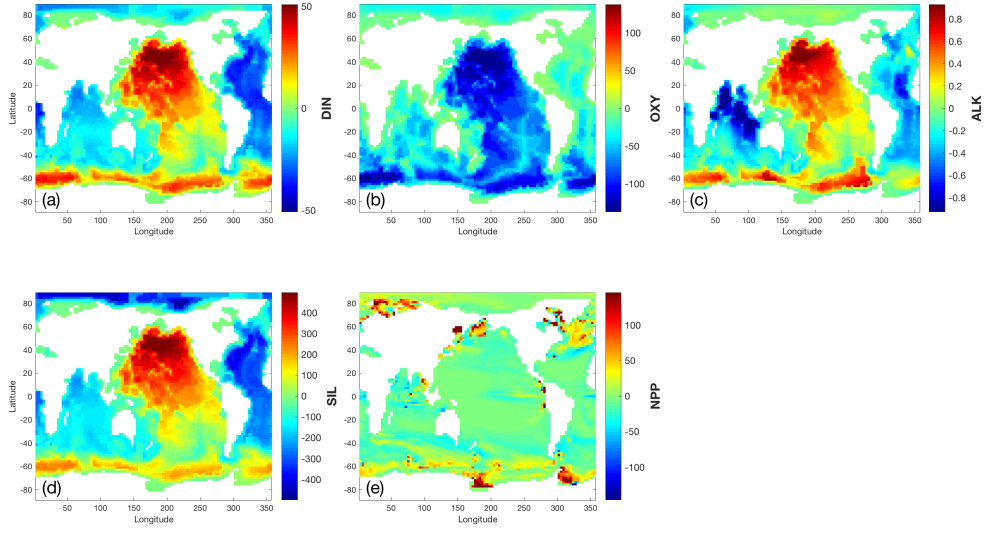


Figure 185: Change in column inventory of (a) DIN, (b) OXY, (c) ALK, (d) SIL, and (e) NPP after a +10% perturbation in x_{vpd} , the maximum growth rate for diatoms.

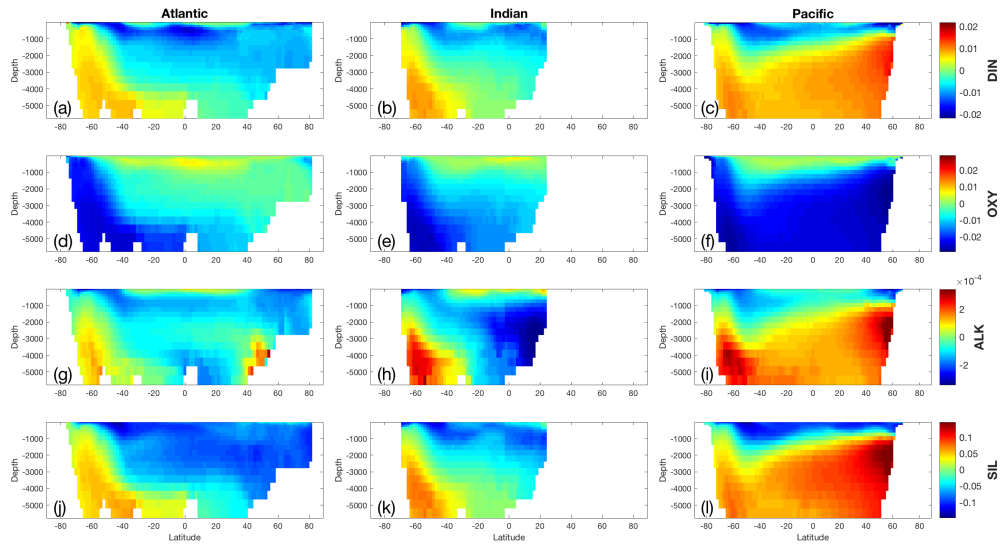


Figure 186: Change in volume-weighted zonally averaged (a-c) DIN, (d-f) OXY, (g-i) ALK, and (j-l) SIL after a +10% perturbation in x_{vpd} , the maximum growth rate for diatoms, for the (left) Atlantic, (middle) Indian, and (right) Pacific Oceans.

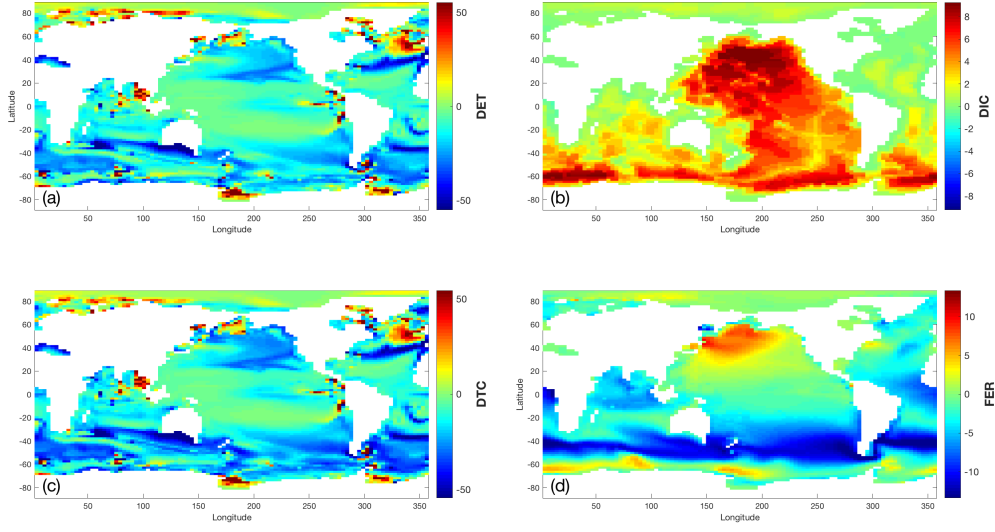


Figure 187: Change in column inventory of (a) DET, (b) DIC, (c) DTC, and (d) FER after a +10% perturbation in xvpd, the maximum growth rate for diatoms.

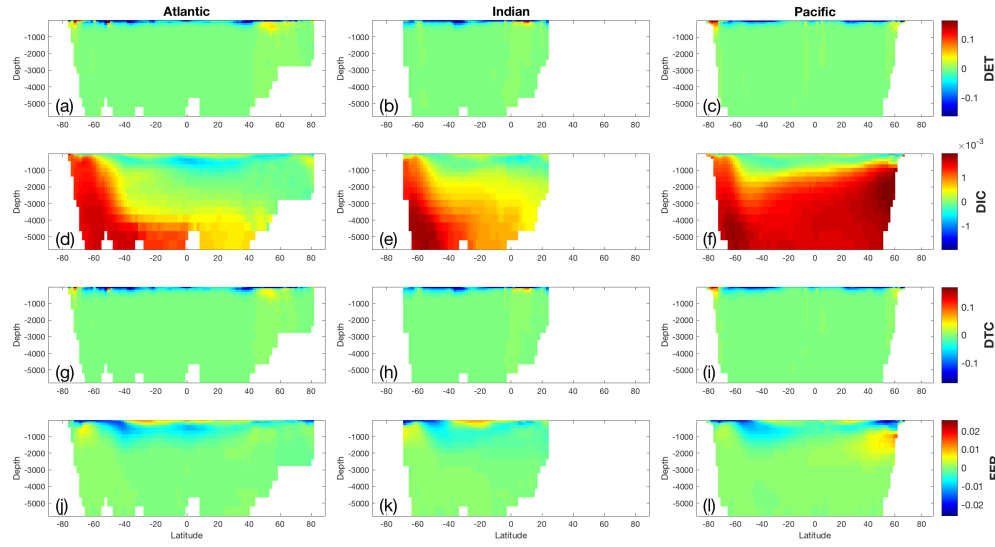


Figure 188: Change in volume-weighted zonally averaged (a-c) DET, (d-f) DIC, (g-i) DTC, and (j-l) FER after a +10% perturbation in xvpd, the maximum growth rate for diatoms, for the (left) Atlantic, (middle) Indian, and (right) Pacific Oceans.

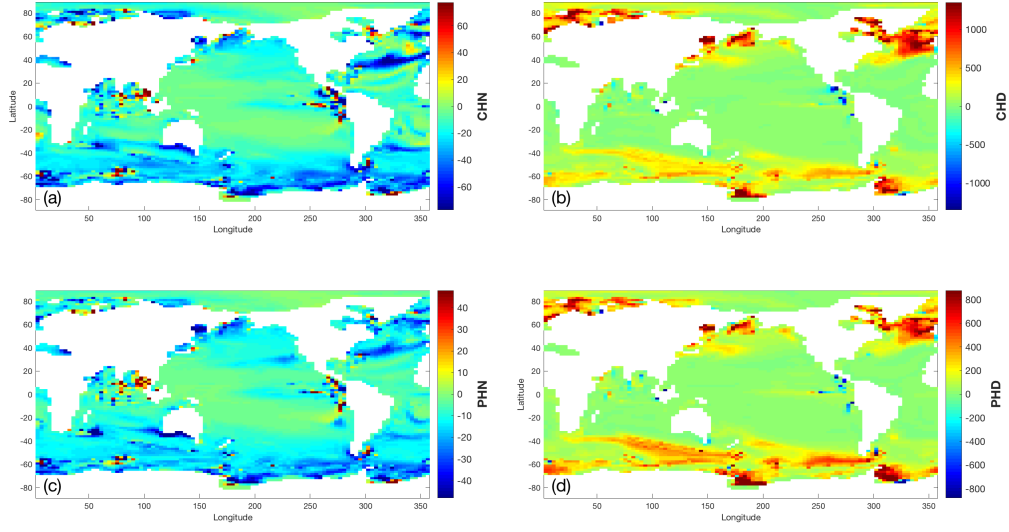


Figure 189: Change in column inventory of (a) CHN, (b) CHD, (c) PHN, and (d) PHD. after a +10% perturbation in x_{vpd} , the maximum growth rate for diatoms.

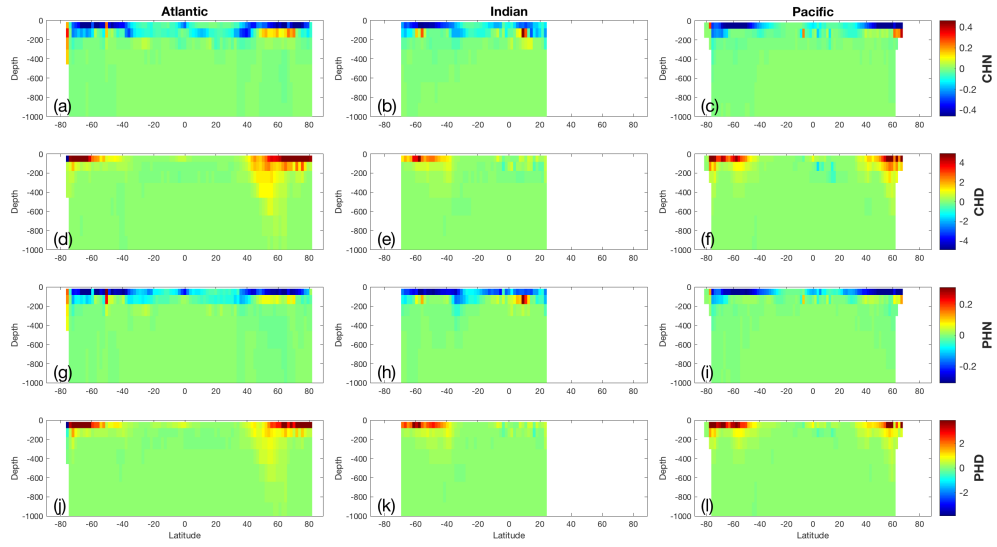


Figure 190: Change in volume-weighted zonally averaged (a-c) CHN, (d-f) CHD, (g-i) PHN, and (j-l) PHD after a +10% perturbation in x_{vpd} , the maximum growth rate for diatoms, for the (left) Atlantic, (middle) Indian, and (right) Pacific Oceans.

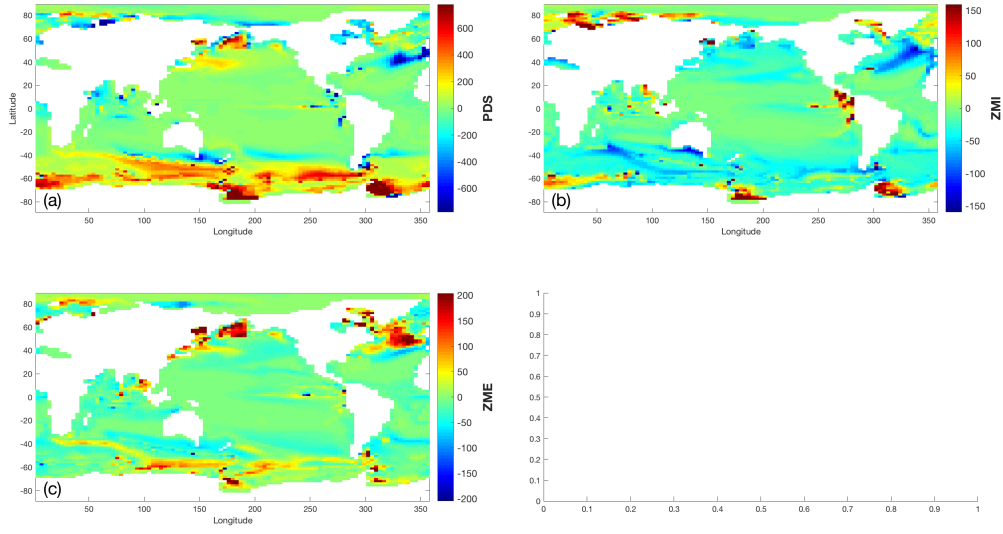


Figure 191: Change in column inventory of (a) PDS, (b) ZMI, and (c) ZME, after a +10% perturbation in $xvpd$, the maximum growth rate for diatoms.

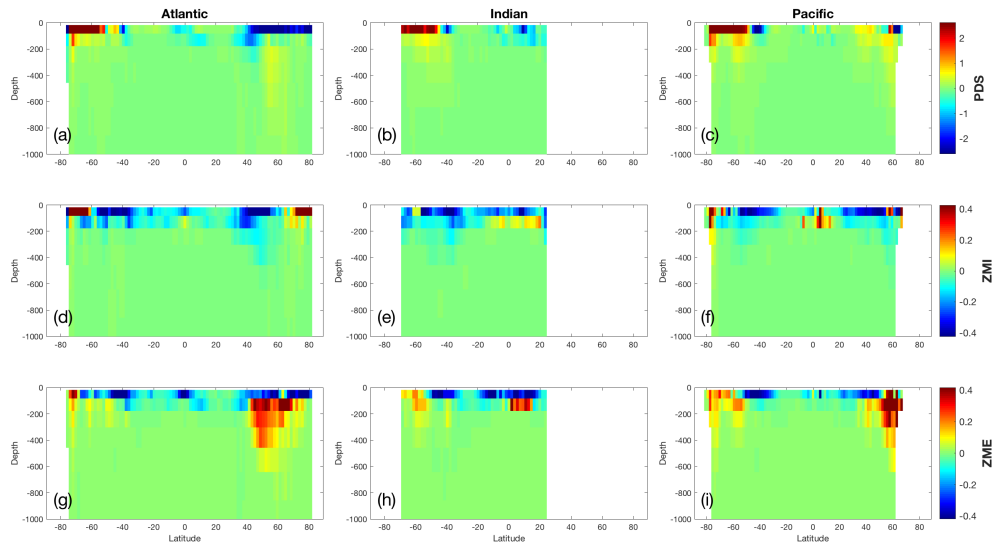


Figure 192: Change in volume-weighted zonally averaged (a-c) PDS, (d-f) ZMI, and (g-i) ZME after a +10% perturbation in $xvpd$, the maximum growth rate for diatoms, for the (left) Atlantic, (middle) Indian, and (right) Pacific Oceans.

- 26 Parameter xvpn: the maximum growth rate for non-diatoms.

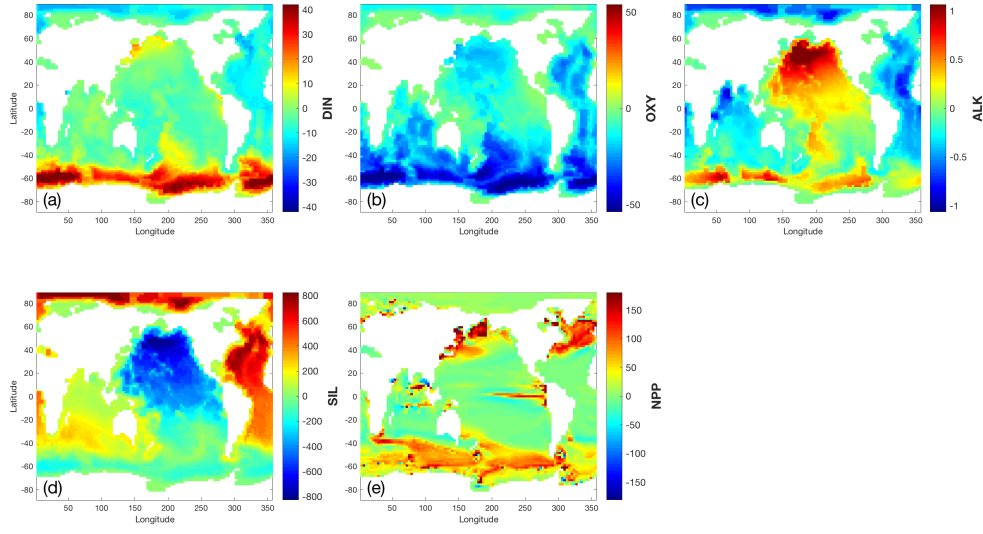


Figure 193: Change in column inventory of (a) DIN, (b) OXY, (c) ALK, (d) SIL, and (e) NPP after a +10% perturbation in x_{vpn} , the maximum growth rate for non-diatoms.

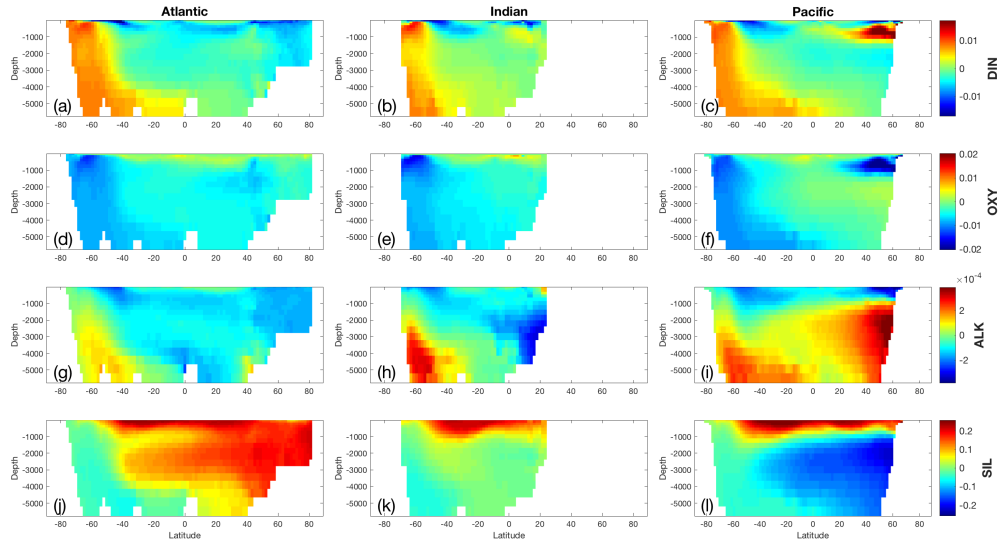


Figure 194: Change in volume-weighted zonally averaged (a-c) DIN, (d-f) OXY, (g-i) ALK, and (j-l) SIL after a +10% perturbation in x_{vpn} , the maximum growth rate for non-diatoms, for the (left) Atlantic, (middle) Indian, and (right) Pacific Oceans.

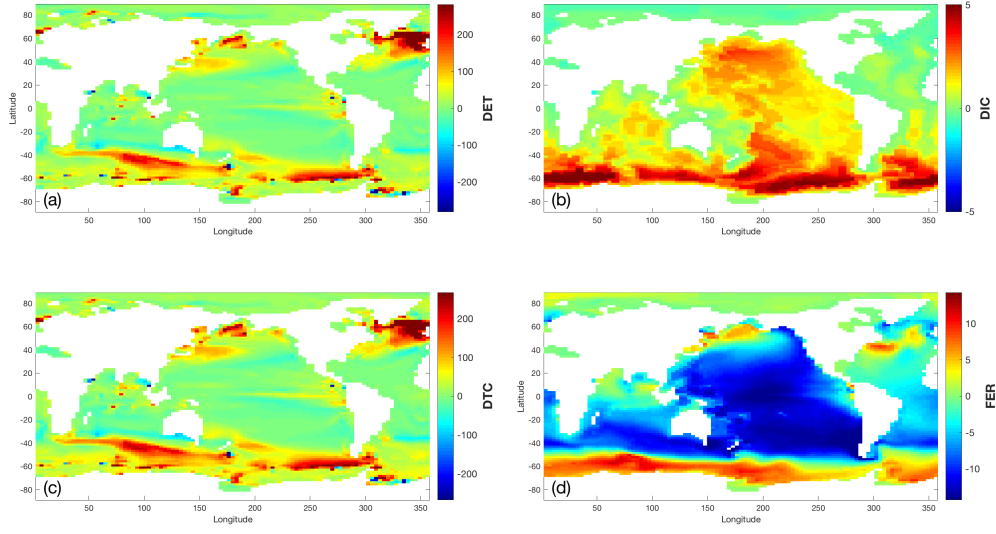


Figure 195: Change in column inventory of (a) DET, (b) DIC, (c) DTC, and (d) FER after a +10% perturbation in x_{vpn} , the maximum growth rate for non-diatoms.

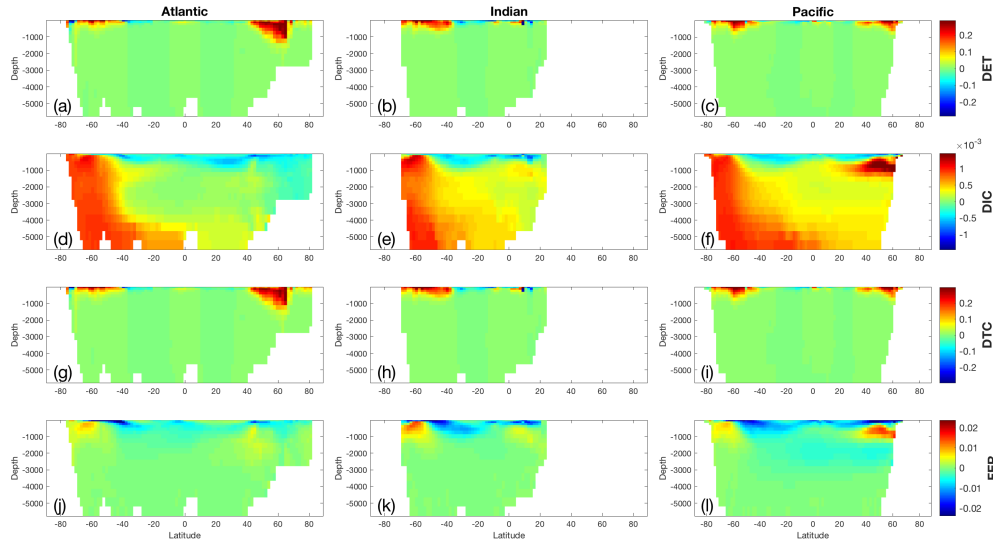


Figure 196: Change in volume-weighted zonally averaged (a-c) DET, (d-f) DIC, (g-i) DTC, and (j-l) FER after a +10% perturbation in x_{vpn} , the maximum growth rate for non-diatoms, for the (left) Atlantic, (middle) Indian, and (right) Pacific Oceans.

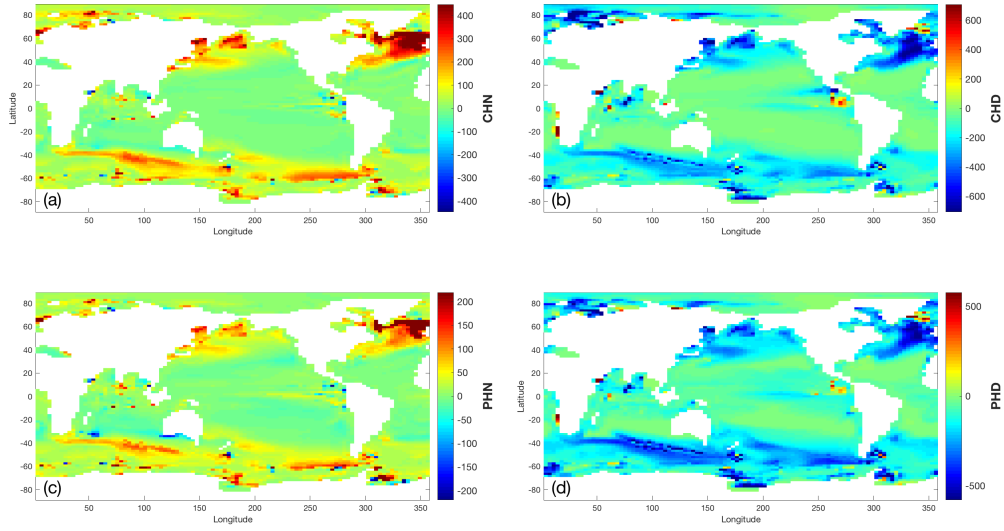


Figure 197: Change in column inventory of (a) CHN, (b) CHD, (c) PHN, and (d) PHD. after a +10% perturbation in xvpn, the maximum growth rate for non-diatoms.

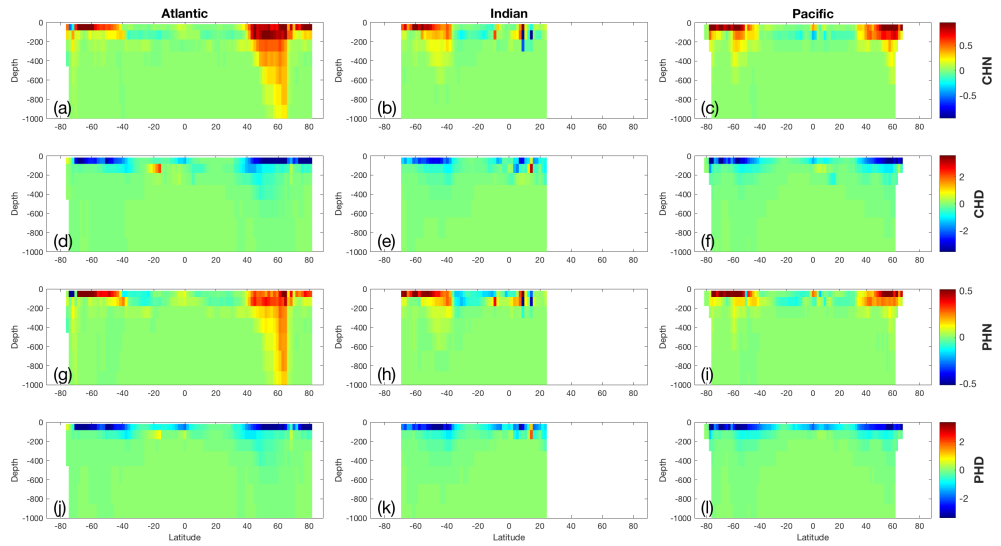


Figure 198: Change in volume-weighted zonally averaged (a-c) CHN, (d-f) CHD, (g-i) PHN, and (j-l) PHD after a +10% perturbation in xvpn, the maximum growth rate for non-diatoms, for the (left) Atlantic, (middle) Indian, and (right) Pacific Oceans.

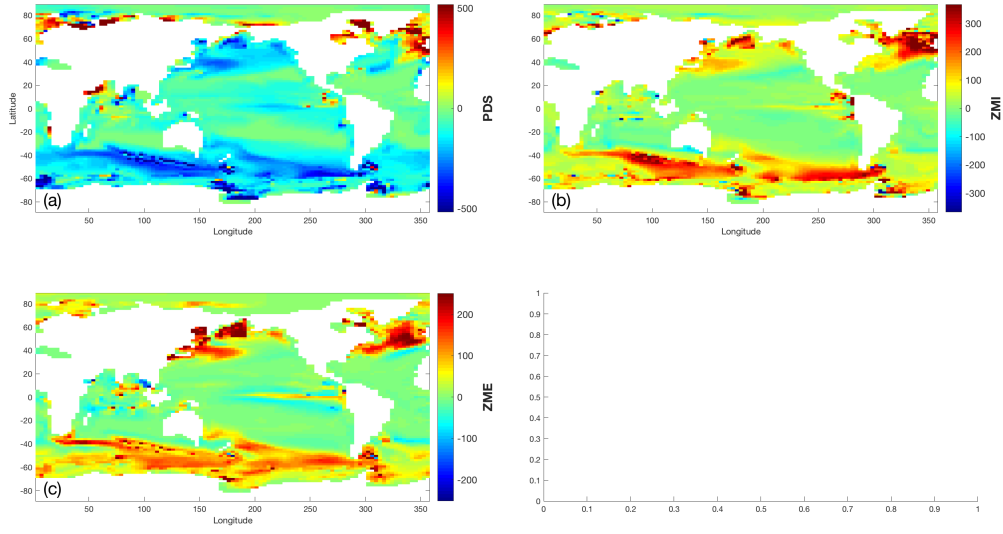


Figure 199: Change in column inventory of (a) PDS, (b) ZMI, and (c) ZME, after a +10% perturbation in x_{vnp} , the maximum growth rate for non-diatoms.

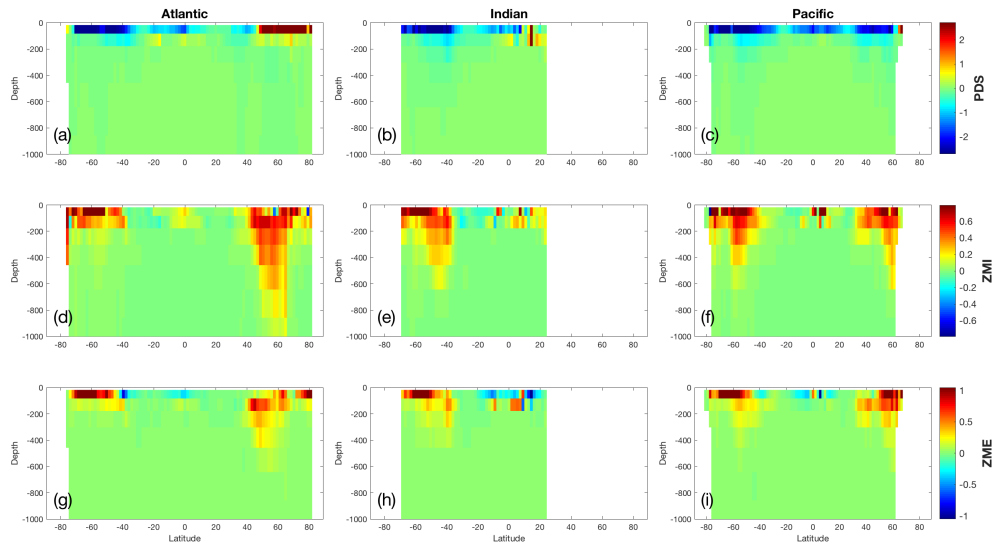


Figure 200: Change in volume-weighted zonally averaged (a-c) PDS, (d-f) ZMI, and (g-i) ZME after a +10% perturbation in x_{vnp} , the maximum growth rate for non-diatoms, for the (left) Atlantic, (middle) Indian, and (right) Pacific Oceans.